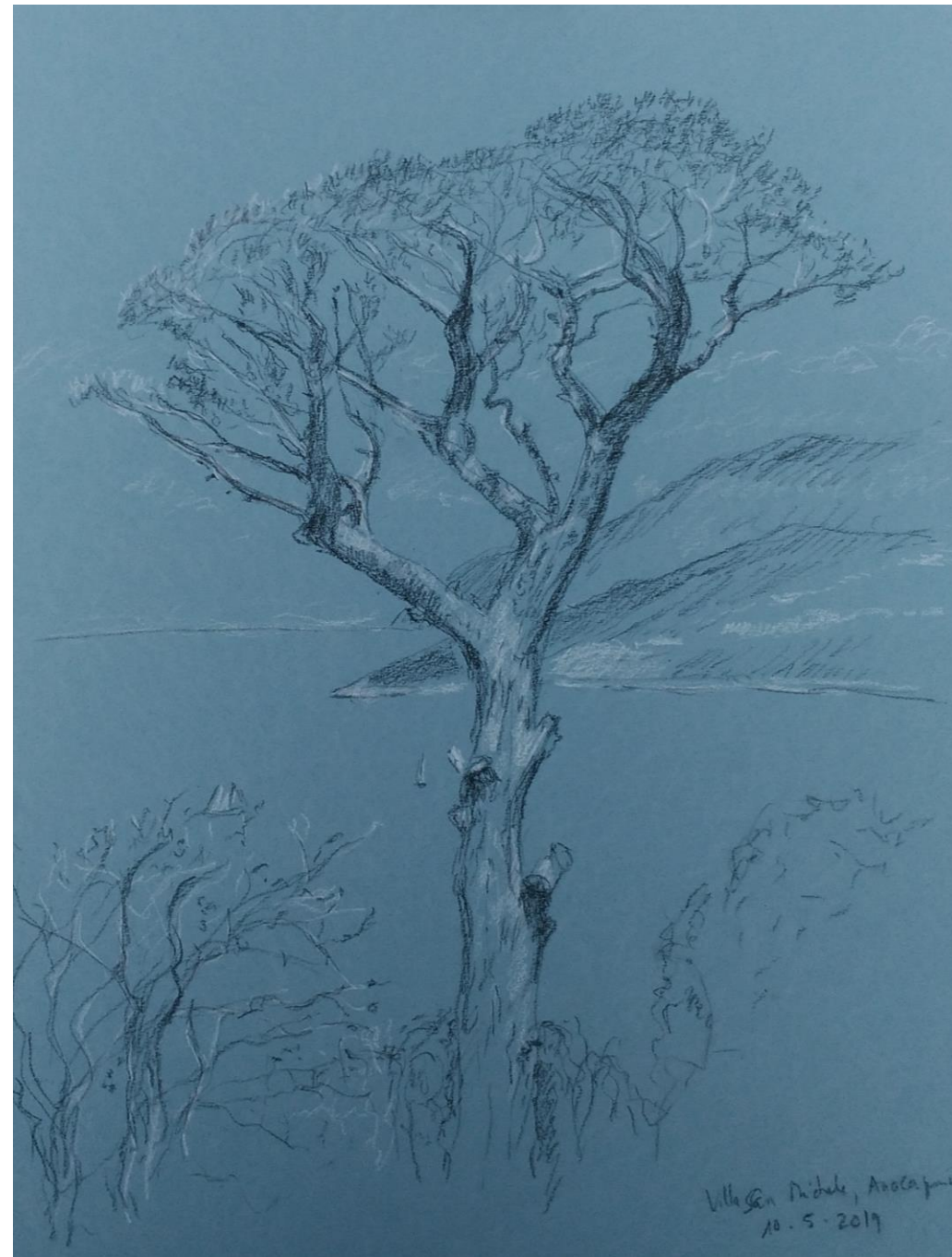


Sophie Guéron

Capri Spring  
School on  
Transport  
in  
Nanostructures  
2019

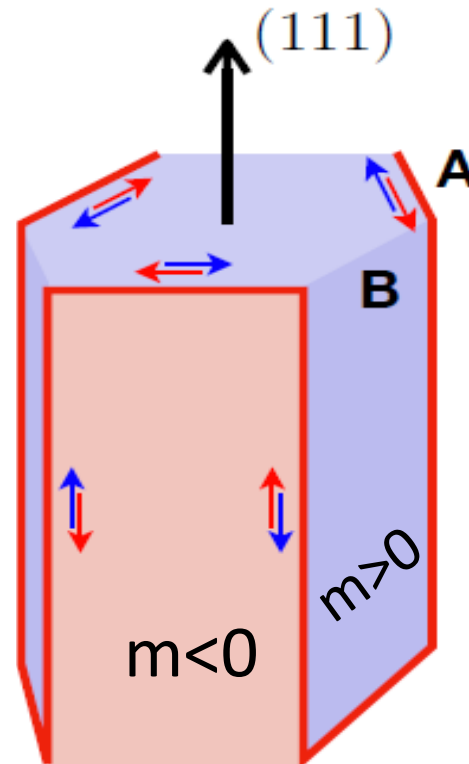
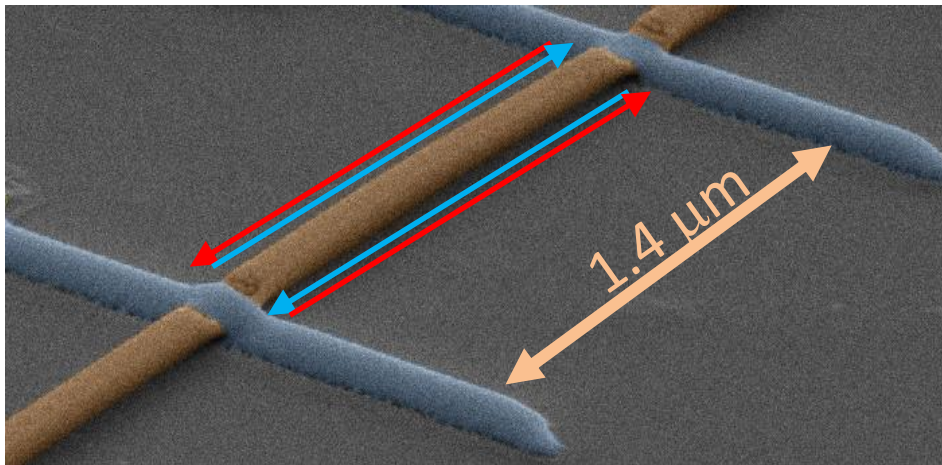


Village de Nidale, Anacapri  
10.5.2019

# Bismuth, a “real life” Second Order Topological Insulator ?

## Mesoscopic physics lends a helping hand to topological quantum chemistry

Anil Murani, B. Dassonneville, A. Kasumov, R. Delagrangé, S. Sengupta, C. Li, F. Brisset, F. Fortuna, A. Chepelianskii, R. Deblock, M. Ferrier, H. Bouchiat, S. Guéron (Orsay, France)  
K. Napolskii, D. Koshkodaev, G. Tsirlina, Y. Kasumov, I. Khodos (Moscow and Chernogolovka)  
F. Schindler, Z. Wang, M. Vergniory, A., B. A. Bernevig, T. Neupert (Zurich, San Sebastian, Princeton)



Murani et al, Phys. Rev. Lett (2019)  
Schindler et al, Nature Physics (2018)  
Murani et al, Nature Comm. (2017)  
Murani et al, Phys.Rev. B **96**, 165415 (2017)





ERC advanced grant, H       Bouchiat,  
         1D ballistic charge and spin currents in second order topological insulators  ,  
April 2020-April 2025

Mesoscopic Physics  
group, Orsay

Richard Deblock

H       Bouchiat



Sophie Gu       Alik Kasumov



Meydi Ferrier



Sandrine  
Autier-Laurent



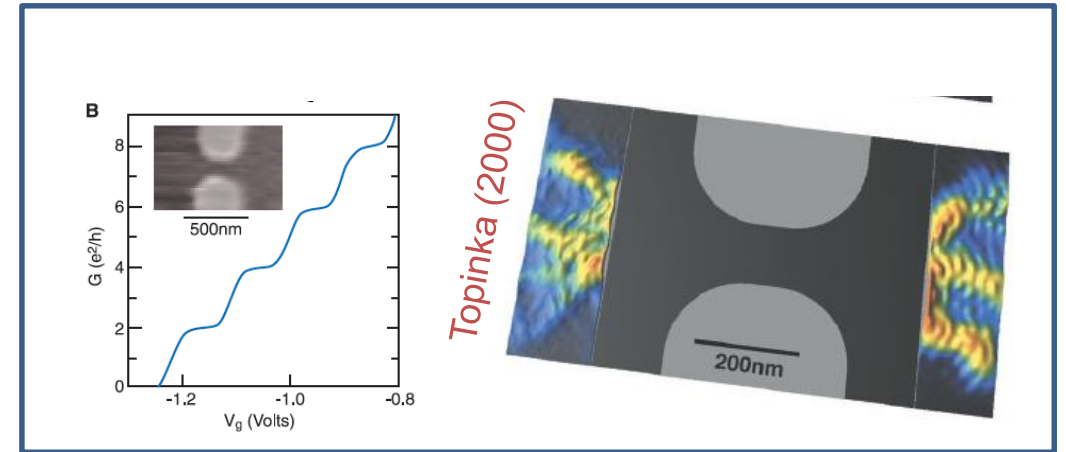
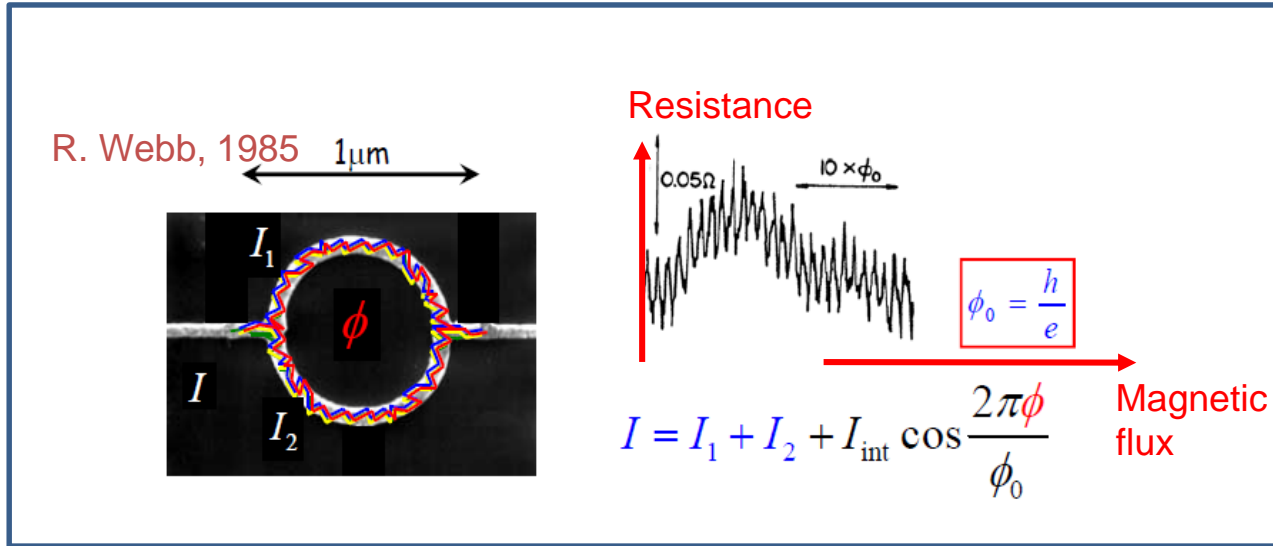
PhD students and Post-docs  
welcome!



Alexei Chepelianskii

# Motivation: Mesoscopic physics to explore topology

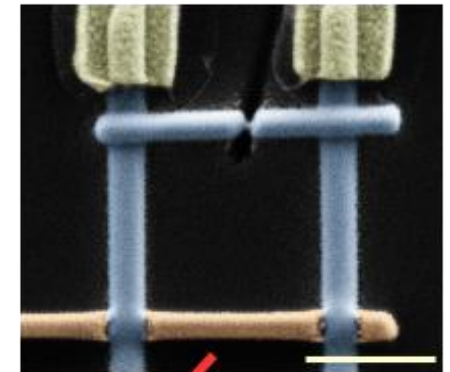
- Previously: Mesoscopic physics to explore quantum mechanics in condensed matter



- More recently: Mesoscopic physics to explore different phases/order/coupling in condensed matter: pairing, spin order, spin-orbit...

- What characterizes mesoscopic physics?:

- individual objects
- small (micron): phase coherent!
- contacts! Invasive/tunnel/no contacts, superconducting, magnetic





# Bismuth, a “real life” Second Order Topological Insulator ?

Mesoscopic physics lends a helping hand to topological quantum chemistry

## 1- Bismuth, a Second Order Topological Insulator?

From bulk to surfaces to nanowires

(or why we chose to work with bismuth).

Different experimental techniques probe different parts/aspects of a crystal

## 2- Induced superconductivity through a Bi nanowire to probe possible SOTI character

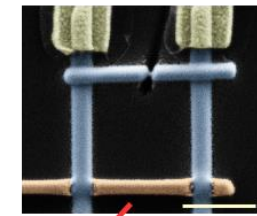
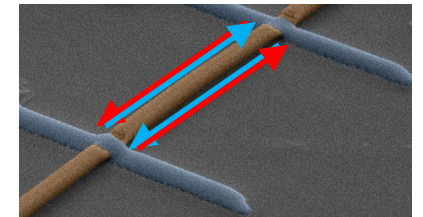
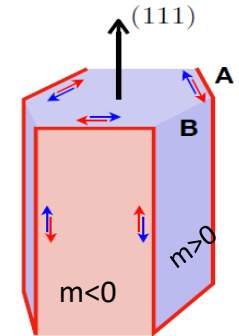
a- What is the superconducting proximity effect

b- Critical current displays interference : edge states

c- (dc) Supercurrent versus Phase relation (CPR) to probe transport regime. Also detects effect of spin-orbit.

d- Dynamic response of the system: (ac) susceptibility  $\chi = dI/d\phi$  : topologically protected !

## 4- Summary of open questions. Other (mesoscopic) probes? Persistent charge/spin currents?

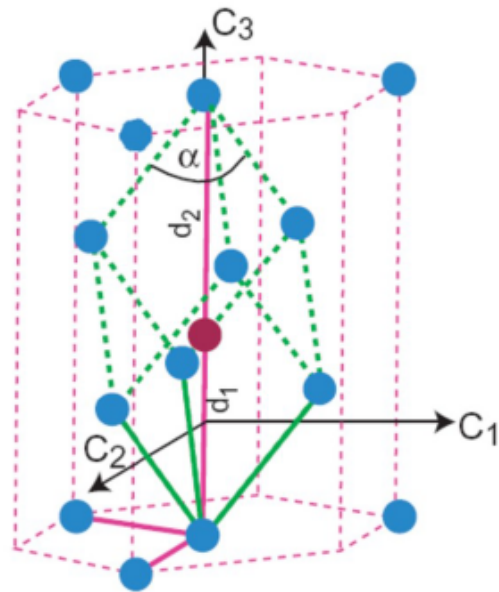


# What is bismuth?

The heaviest non radioactive element

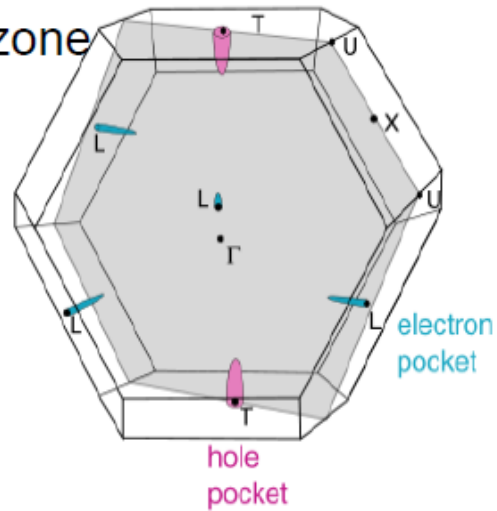
→ Strong spin-orbit interaction

Lattice structure



Semimetal

Bulk Brillouin zone

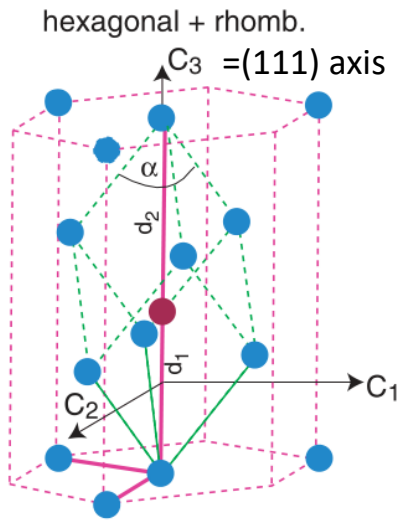


Periodic Table of the Elements

Periodic Table of the Elements																	
1 H Hydrogen 1.01																	2 He Helium 4.00
3 Li Lithium 6.94	4 Be Beryllium 9.01											5 B Boron 10.81	6 C Carbon 12.01	7 N Nitrogen 14.01	8 O Oxygen 16.00	9 F Fluorine 19.00	10 Ne Neon 20.18
11 Na Sodium 22.99	12 Mg Magnesium 24.31											13 Al Aluminum 26.98	14 Si Silicon 28.09	15 P Phosphorus 30.97	16 S Sulfur 32.06	17 Cl Chlorine 35.45	18 Ar Argon 39.95
19 K Potassium 39.10	20 Ca Calcium 40.08	21 Sc Scandium 44.96	22 Ti Titanium 47.88	23 V Vanadium 50.94	24 Cr Chromium 51.99	25 Mn Manganese 54.94	26 Fe Iron 55.85	27 Co Cobalt 58.93	28 Ni Nickel 58.69	29 Cu Copper 63.55	30 Zn Zinc 65.38	31 Ga Gallium 69.72	32 Ge Germanium 72.63	33 As Arsenic 74.92	34 Se Selenium 78.97	35 Br Bromine 79.90	36 Kr Krypton 84.80
37 Rb Rubidium 85.47	38 Sr Strontium 87.62	39 Y Yttrium 88.91	40 Zr Zirconium 91.22	41 Nb Niobium 92.91	42 Mo Molybdenum 95.95	43 Tc Technetium 98.91	44 Ru Ruthenium 101.07	45 Rh Rhodium 102.91	46 Pd Palladium 106.42	47 Ag Silver 107.87	48 Cd Cadmium 112.41	49 In Indium 114.82	50 Sn Tin 118.71	51 Sb Antimony 121.76	52 Te Tellurium 127.6	53 I Iodine 126.90	54 Xe Xenon 131.29
55 Cs Cesium 132.91	56 Ba Barium 137.33	57-71 Lanthanides	72 Hf Hafnium 178.49	73 Ta Tantalum 180.95	74 W Tungsten 183.85	75 Re Rhenium 186.21	76 Os Osmium 190.23	77 Ir Iridium 192.22	78 Pt Platinum 195.08	79 Au Gold 196.97	80 Hg Mercury 200.59	81 Tl Thallium 204.38	82 Pb Lead 207.2	83 Bi Bismuth 208.98	84 Po Polonium [209]	85 At Astatine [210]	86 Rn Radon [222]
87 Fr Francium 223.02	88 Ra Radium 226.03	89-103 Actinides	104 Rf Rutherfordium [261]	105 Db Dubnium [262]	106 Sg Seaborgium [266]	107 Bh Bohrium [264]	108 Hs Hassium [269]	109 Mt Meitnerium [278]	110 Ds Darmstadtium [281]	111 Rg Roentgenium [280]	112 Cn Copernicium [285]	113 Nh Nihonium [286]	114 Fl Flerovium [289]	115 Mc Moscovium [289]	116 Lv Livermorium [293]	117 Ts Tennessine [294]	118 Og Oganesson [294]
57 La Lanthanum 138.91	58 Ce Cerium 140.12	59 Pr Praseodymium 140.91	60 Nd Neodymium 144.24	61 Pm Promethium 144.91	62 Sm Samarium 150.36	63 Eu Europium 151.96	64 Gd Gadolinium 157.25	65 Tb Terbium 158.93	66 Dy Dysprosium 162.50	67 Ho Holmium 164.93	68 Er Erbium 167.26	69 Tm Thulium 168.93	70 Yb Ytterbium 173.05	71 Lu Lutetium 174.97			
89 Ac Actinium 227.03	90 Th Thorium 232.04	91 Pa Protactinium 231.04	92 U Uranium 238.03	93 Np Neptunium 237.05	94 Pu Plutonium 244.06	95 Am Americium 243.06	96 Cm Curium 247.07	97 Bk Berkelium 247.07	98 Cf Californium 251.08	99 Es Einsteinium [254]	100 Fm Fermium 257.10	101 Md Mendelevium 258.10	102 No Nobelium 259.10	103 Lr Lawrencium [262]			
Alkali Metal	Alkaline Earth	Transition Metal	Basic Metal	Metalloid	Nonmetal	Halogen	Noble Gas	Lanthanide	Actinide								

Ph. Hofmann, Prog. Sci. Surf. **81**, 191 (2006).

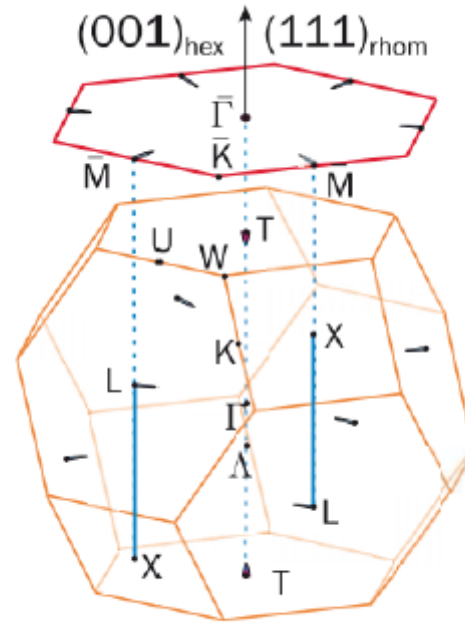
# Bismuth as it was known one year ago: bulk and surfaces



Hofmann 2006 review

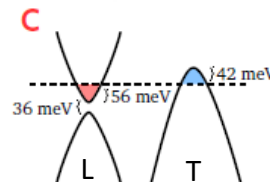
Z=83: huge spin-orbit

**Bulk** Brillouin zone



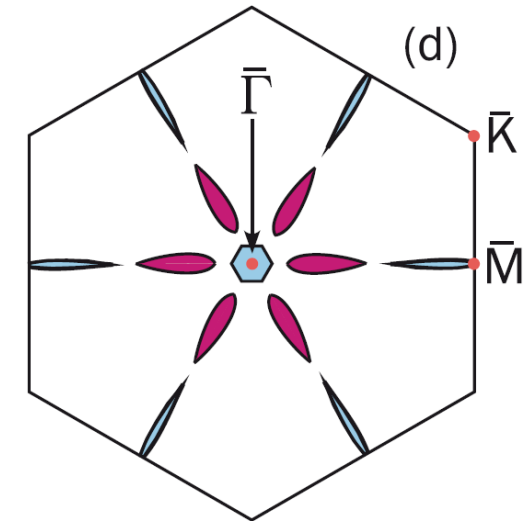
**Bulk**  
 semi-metal  
 $\lambda_F \approx 50$  nm

→ No bulk states  
 left in structures  
 smaller than 50 nm



Light electrons, heavy holes  
 $\lambda_F \sim 50$  nm,  $g \sim$  up to 1000

**Surface** Brillouin zone

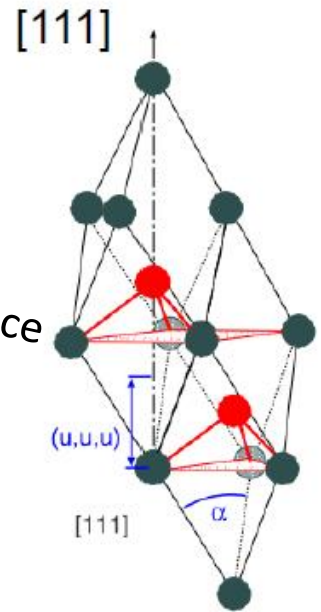
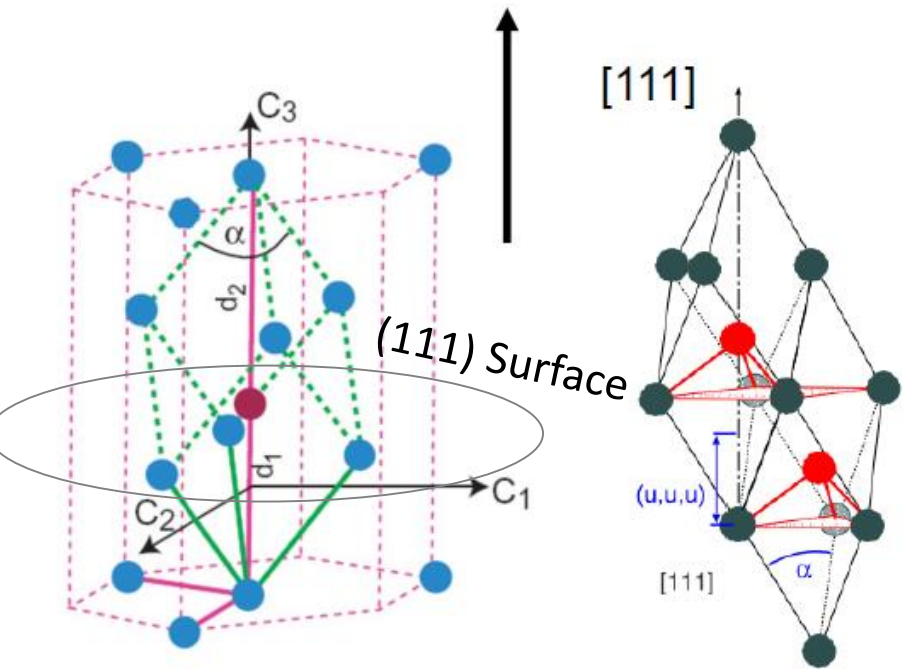


**Surfaces**  
 $\lambda_F \approx 1$  nm,  
 spin-split,  
 $E_{SO} \sim E_F \sim 100$  meV,  $g_{eff}: 1 \sim 100$

Topological properties?



# (111) Bi bilayers predicted to be 2D topological insulators in 2006

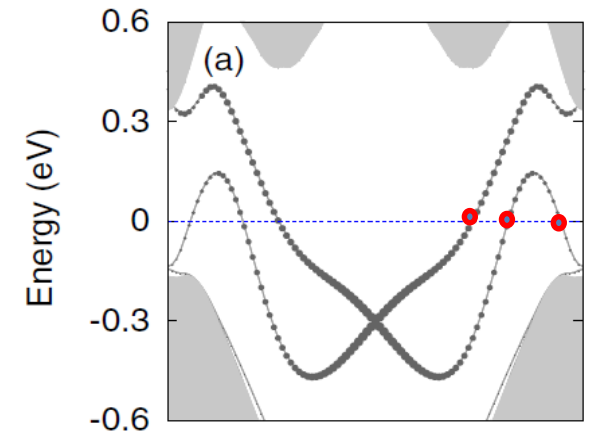


} Bilayer

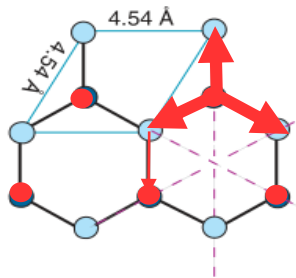
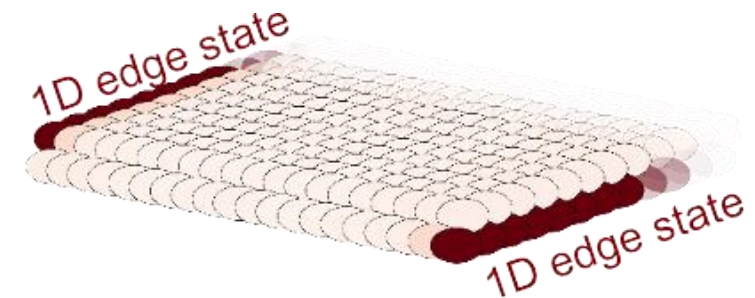
(111) Surface= buckled honeycomb  
 $\approx$  graphene with huge spin-orbit!  
 $\Rightarrow$  freestanding bilayer is predicted  
2D topological insulator  
With 3 Quantum Spin Hall (helical)  
edge states

Murakami, 2006

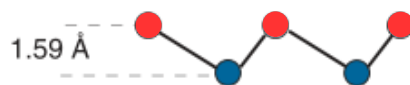
Liu & Allen, 1991



Free standing (111 bilayer)  
Spin-polarized 1D edge states



(b) Side view (parallel to mirror plane)



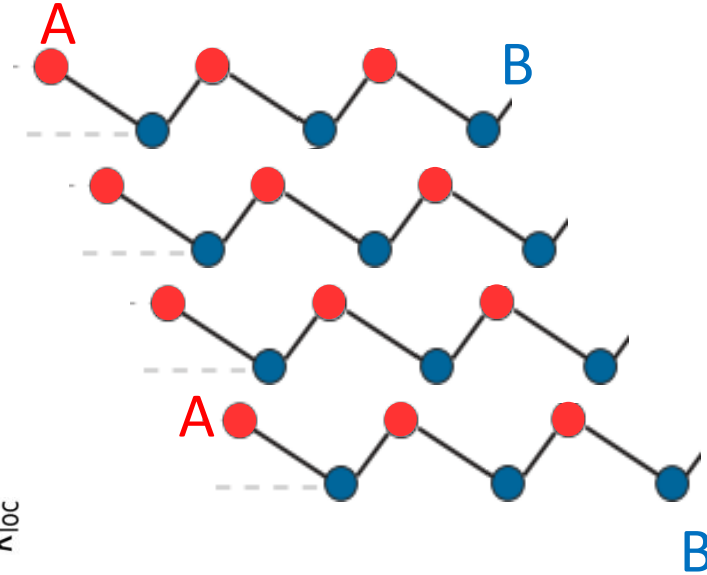
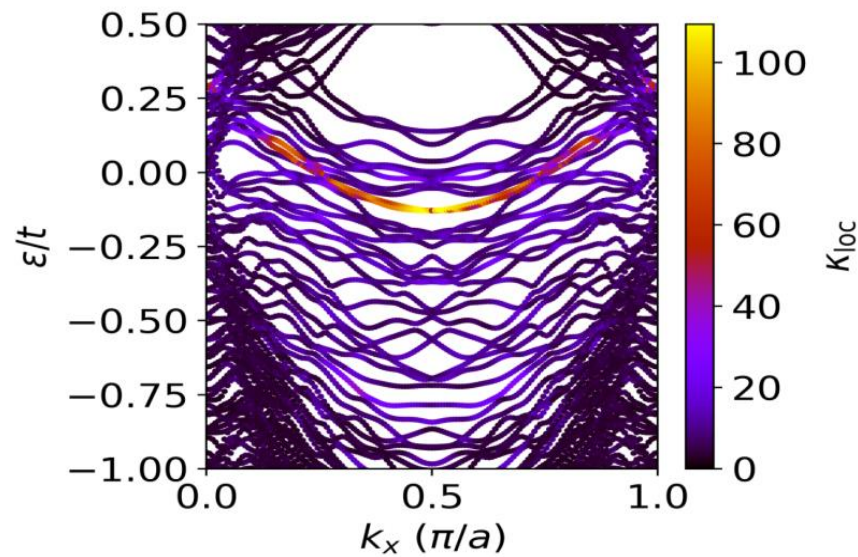
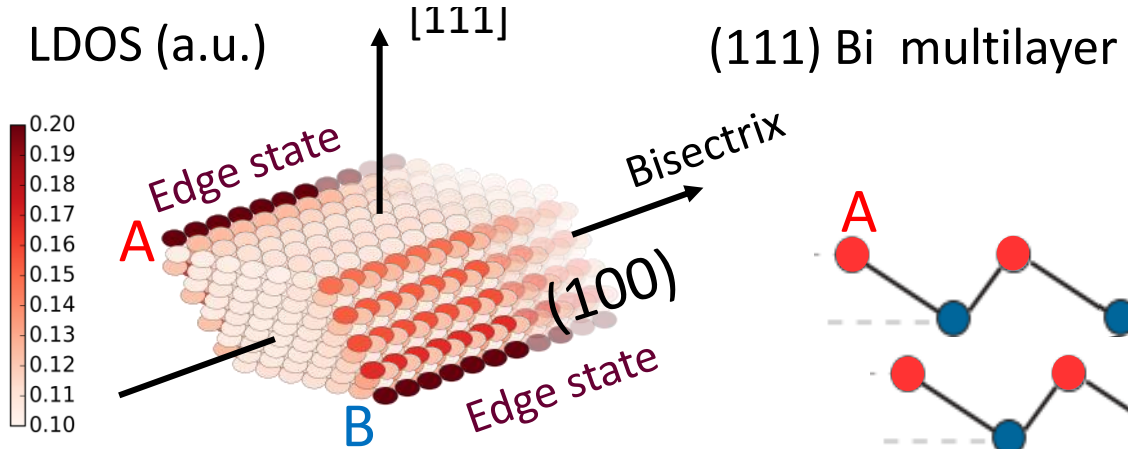
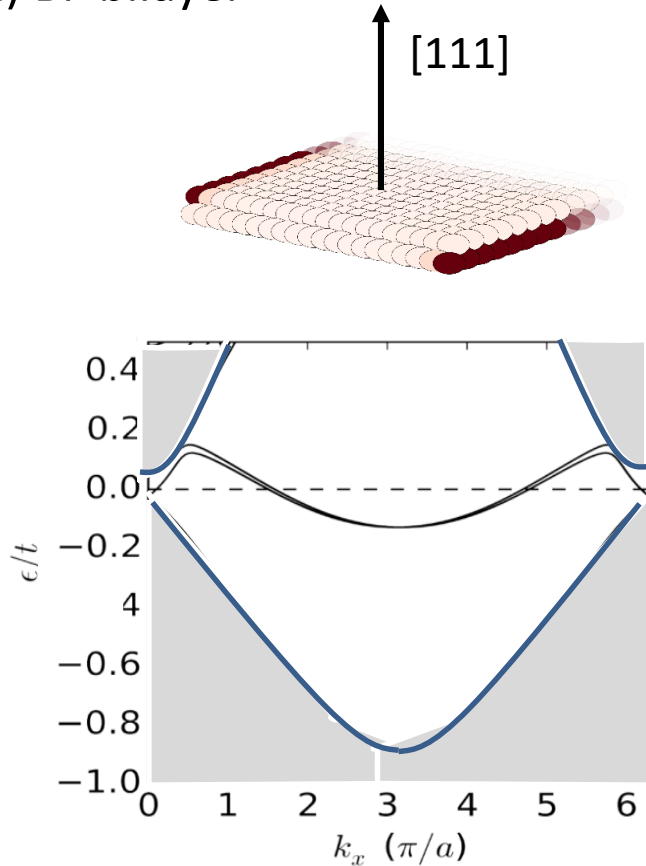
Hofmann 2006 review

We chose to work with monocrystalline nanowires with (111) surfaces

# What about a stack of (111) bilayers?

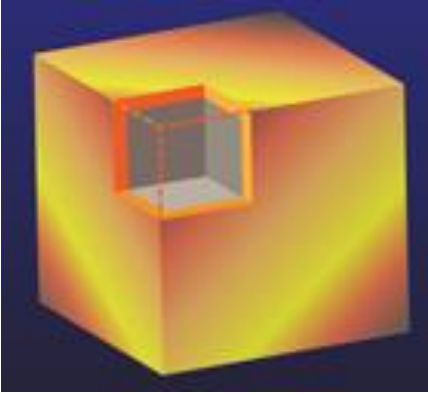
## Tight binding simulation of bilayer and (small) nanowire (Anil Murani)

(111) Bi bilayer



1D edge states seem to persist in 3D wires (at sharp angles of nanowires), but many other states as well...  
Does theory confirm this? Does experiment confirm this?

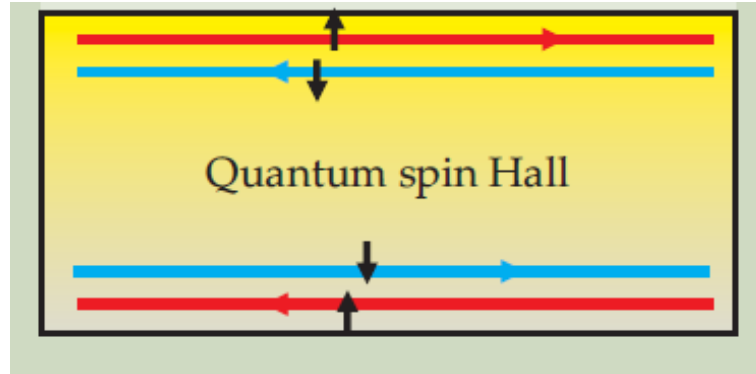
# Higher order Topological Insulators



3D topological insulator

**3D** insulating bulk

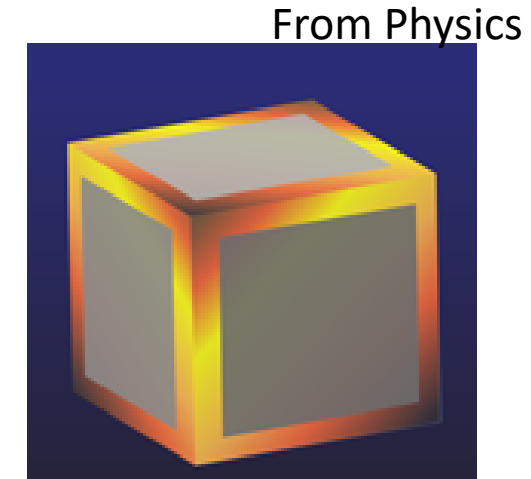
2D Conducting surfaces



2D topological insulator

**2D** insulating bulk

1D conducting « helical » edges



Second Order Topological Insulator

**3D** insulating bulk

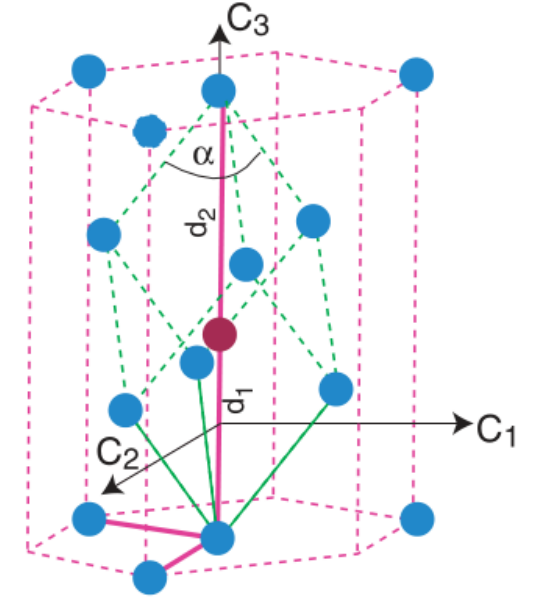
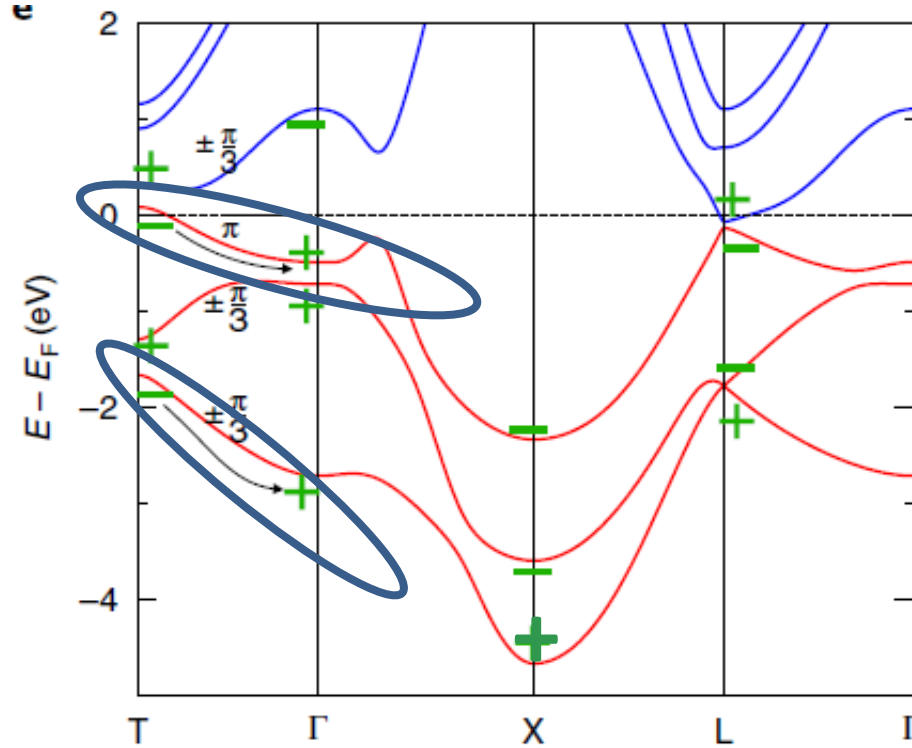
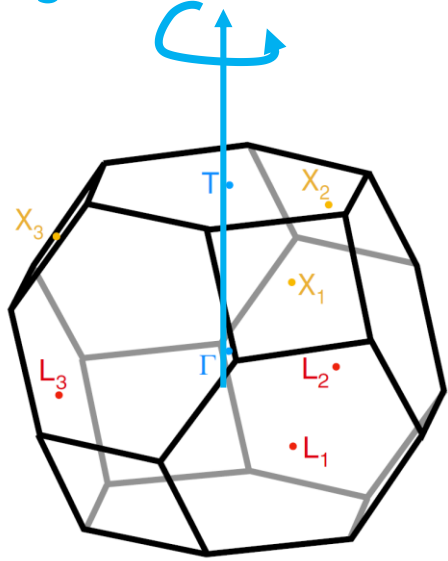
2D insulating surfaces

**1D** conducting helical « hinges »



Last year: Bulk Bismuth may not be topologically trivial!

$$C_3 = [111]$$



Symmetries of Bi:

-Time Reversal

-Inversion

- $C_3$  rotation: defines two subspaces with eigenvalues  $e^{i\pi}$ ,  $e^{\pm i\pi/3}$

Fu-Kane topological index:  $\nu=1$  (trivial) or  $-1$  (topological)

$\nu = \nu_T \nu_\Gamma \nu_X \nu_L = 1$ : bulk Bi is not a 3DTI

$\nu^{(\pi)} = -1 = \nu^{(\pm i\pi/3)}$ : each subspace is a topological insulator (“ $C_3$ -graded double band inversion at  $T$  point”)

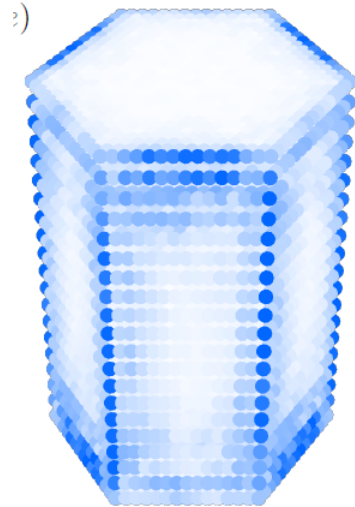
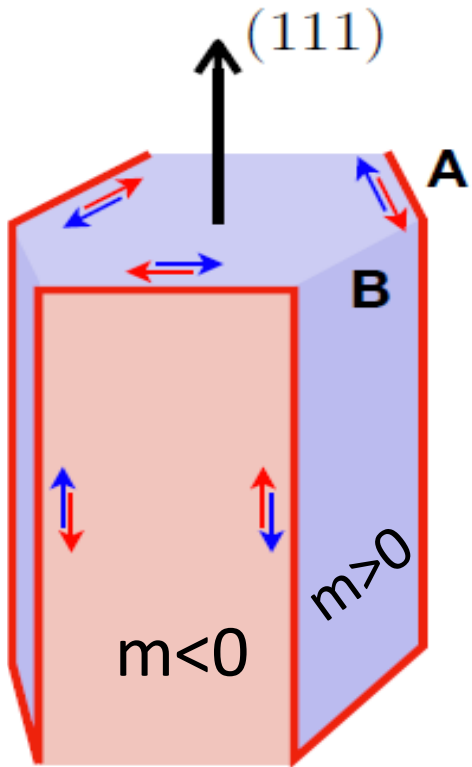
Bi is a superposition of two TI

Bulk Bismuth is a Second Order TI (Schindler et al, Nat. Phys. 2018)

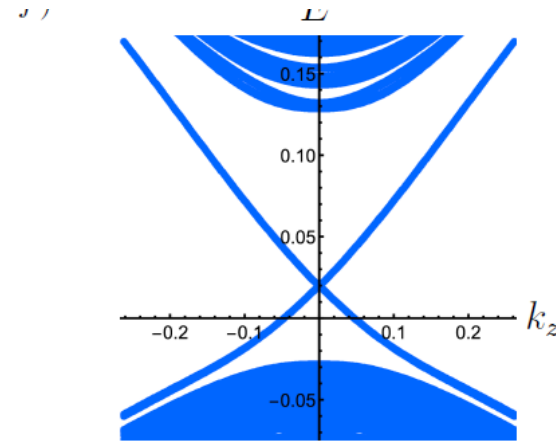
# Bismuth, a Second Order Topological Insulator?

Bi  $\sim$  superposition of two topological insulators in 2 independent subspaces

$\Rightarrow$  Topologically protected Kramers pairs of gapless modes at “hinges”



Helical edge state that winds around the crystal

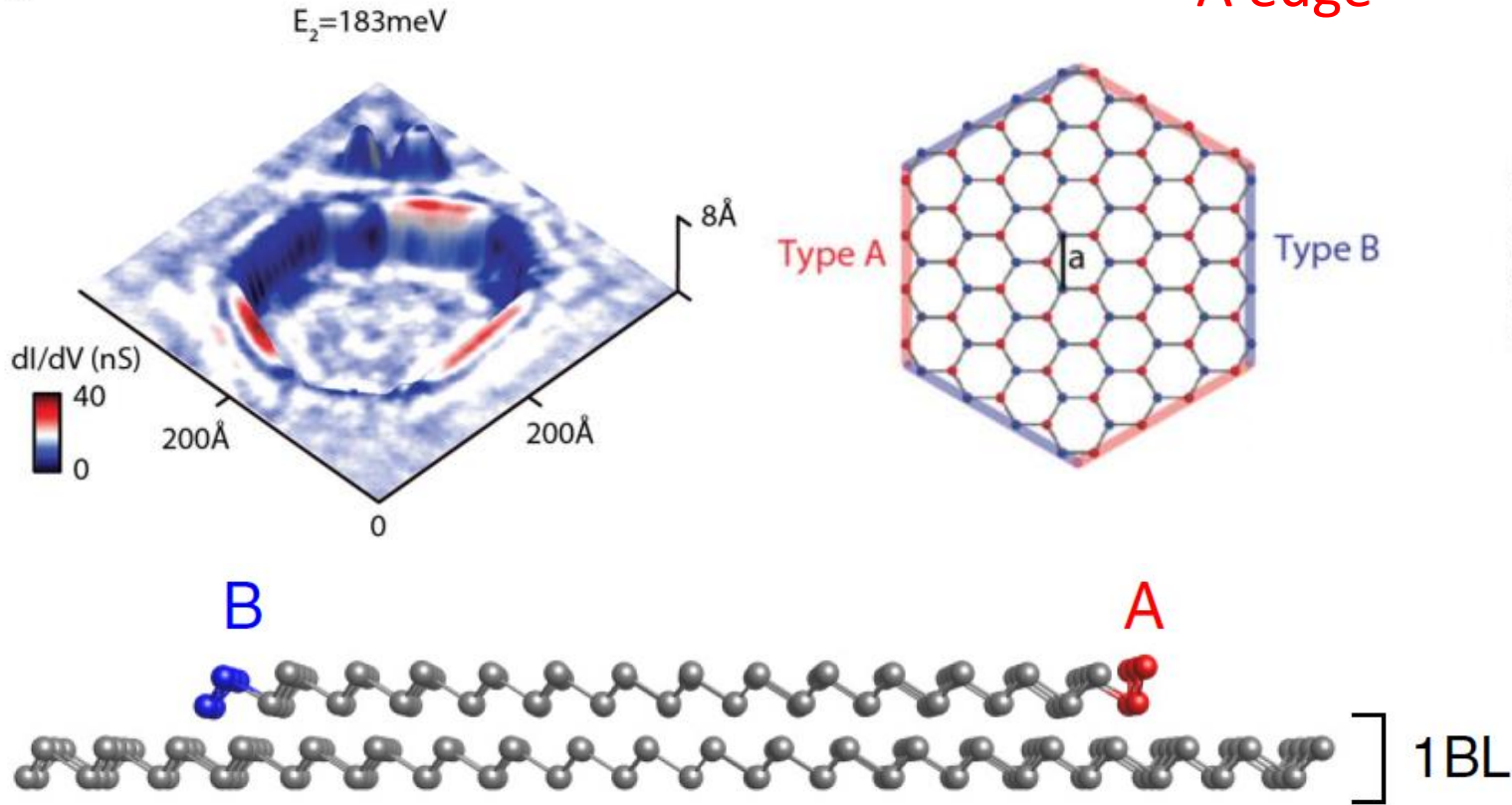


Is bismuth really like that?

(Schindler et al, Nat. Phys. 2018)

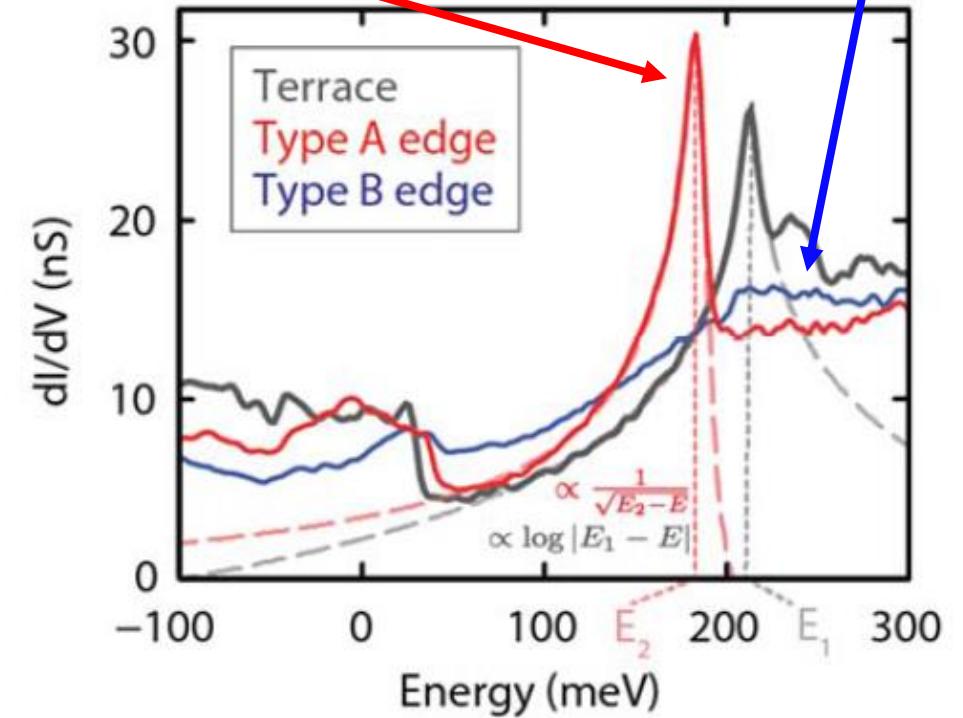
# 1D edge states observed by STM! (decoupled from bulk Bi)

Bilayer pits in (111) bulk Bi crystals  
Drozdov Yazdani (2014)



1D-like Van Hove singularity on type A edge

No van Hove on type B edge

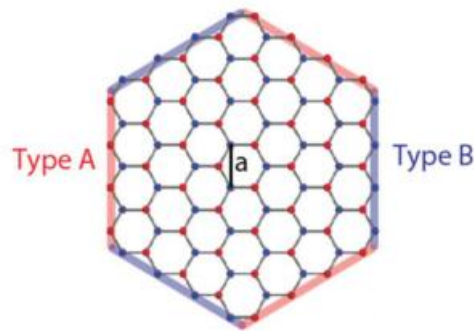
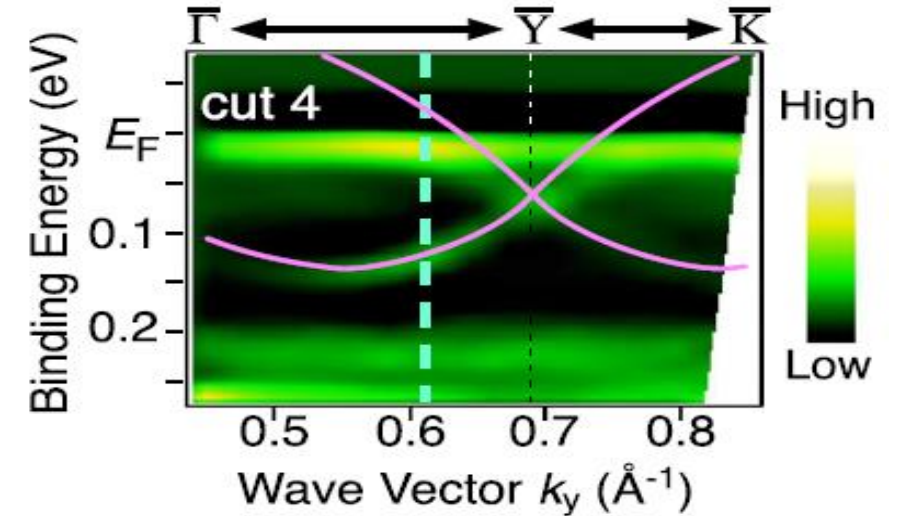
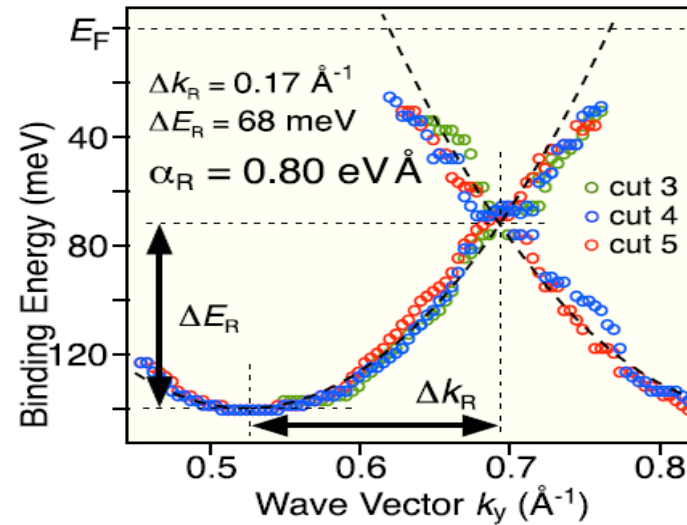
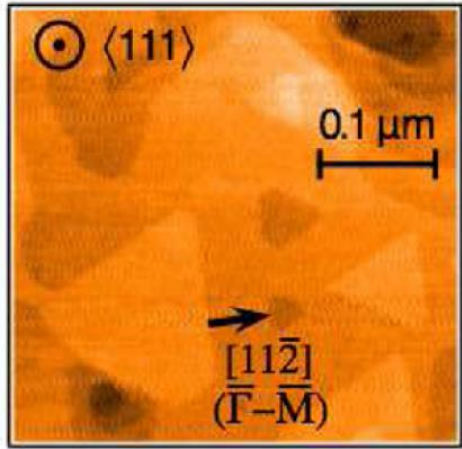


- Only A-type edges show 1D features
  - Suppressed backscattering



# Photoemission on many (111) few layer Bi

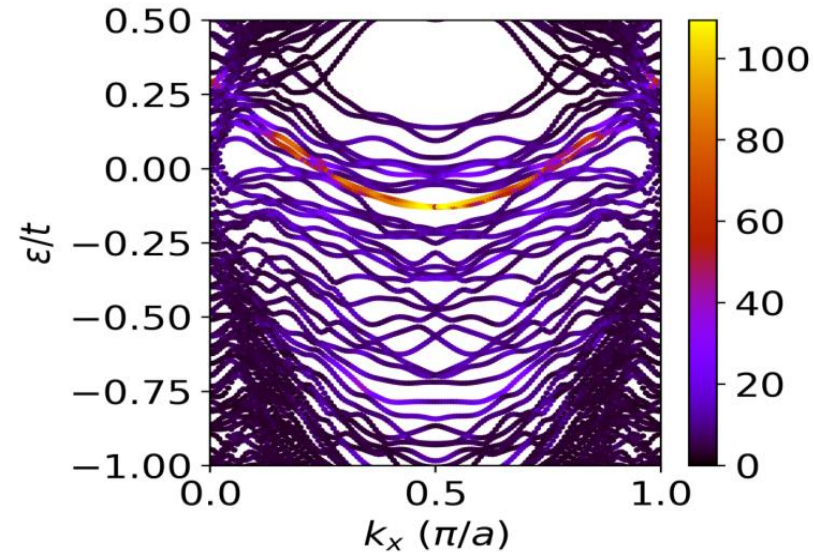
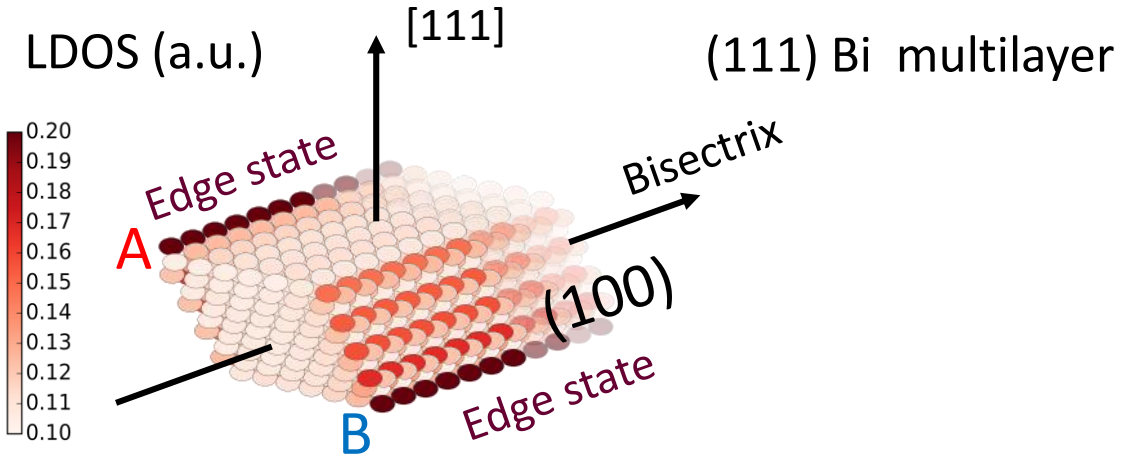
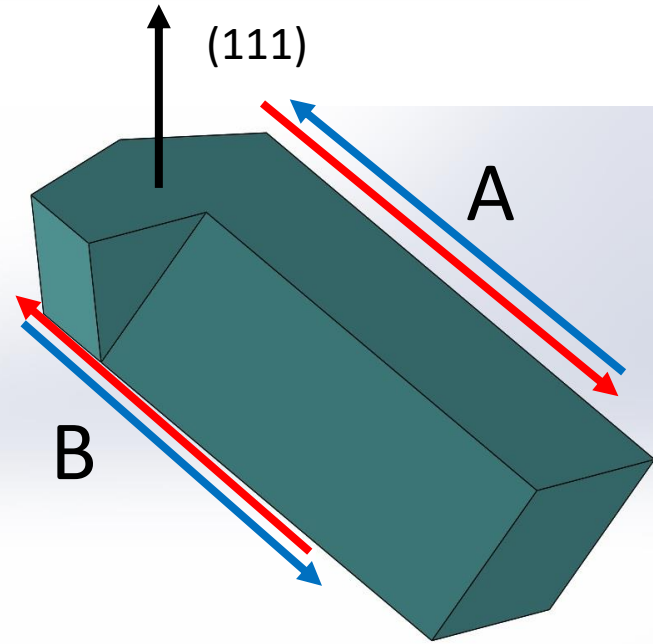
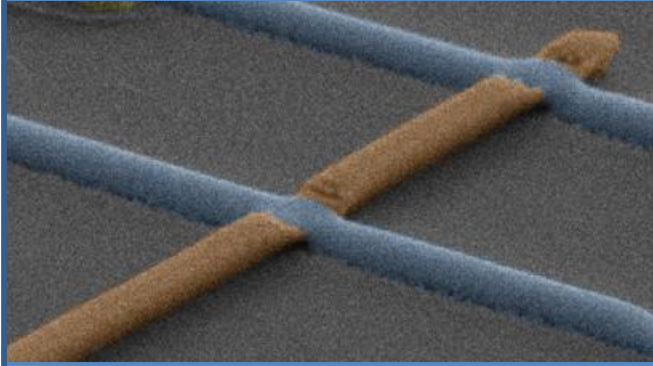
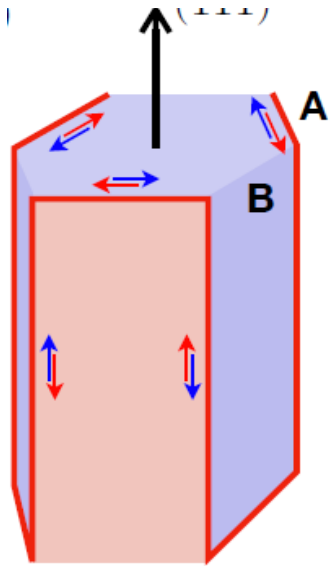
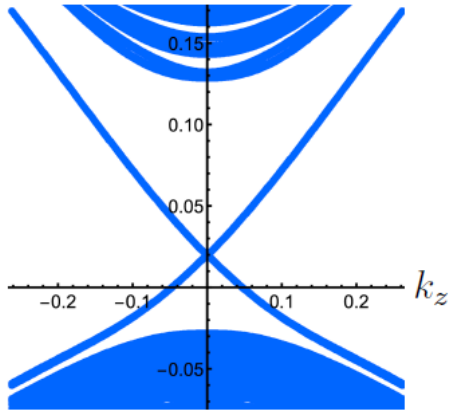
Takayama PRL 2015: mostly triangular crystals, less than 15 nm thick



Photoemission detects spin-split surfaces and 1D edge states  
... but maybe not topological

# Bismuth Nanowires IRL (in real life): bulk surfaces and edges?

## Theory



Hinge states plus a lot of other states!

Can the ballisticity of the few topological hinge states emerge?  
Mesoscopic physics!



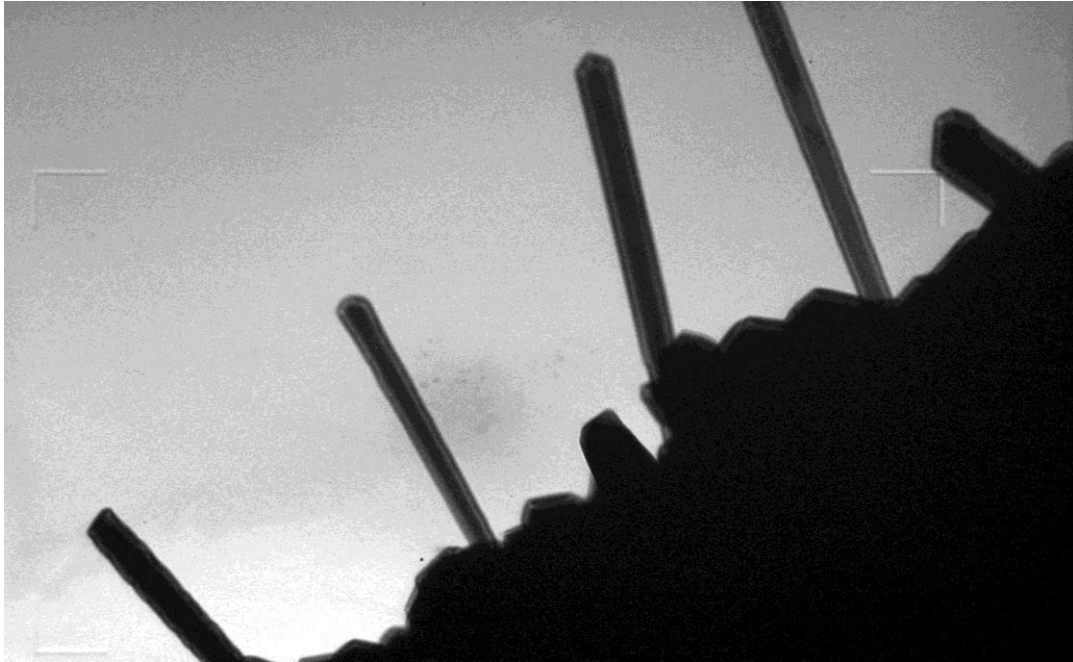
## Our samples Monocrystalline Bismuth nanowires

High quality single crystals

Sputtering, buffer layer of Fe or V

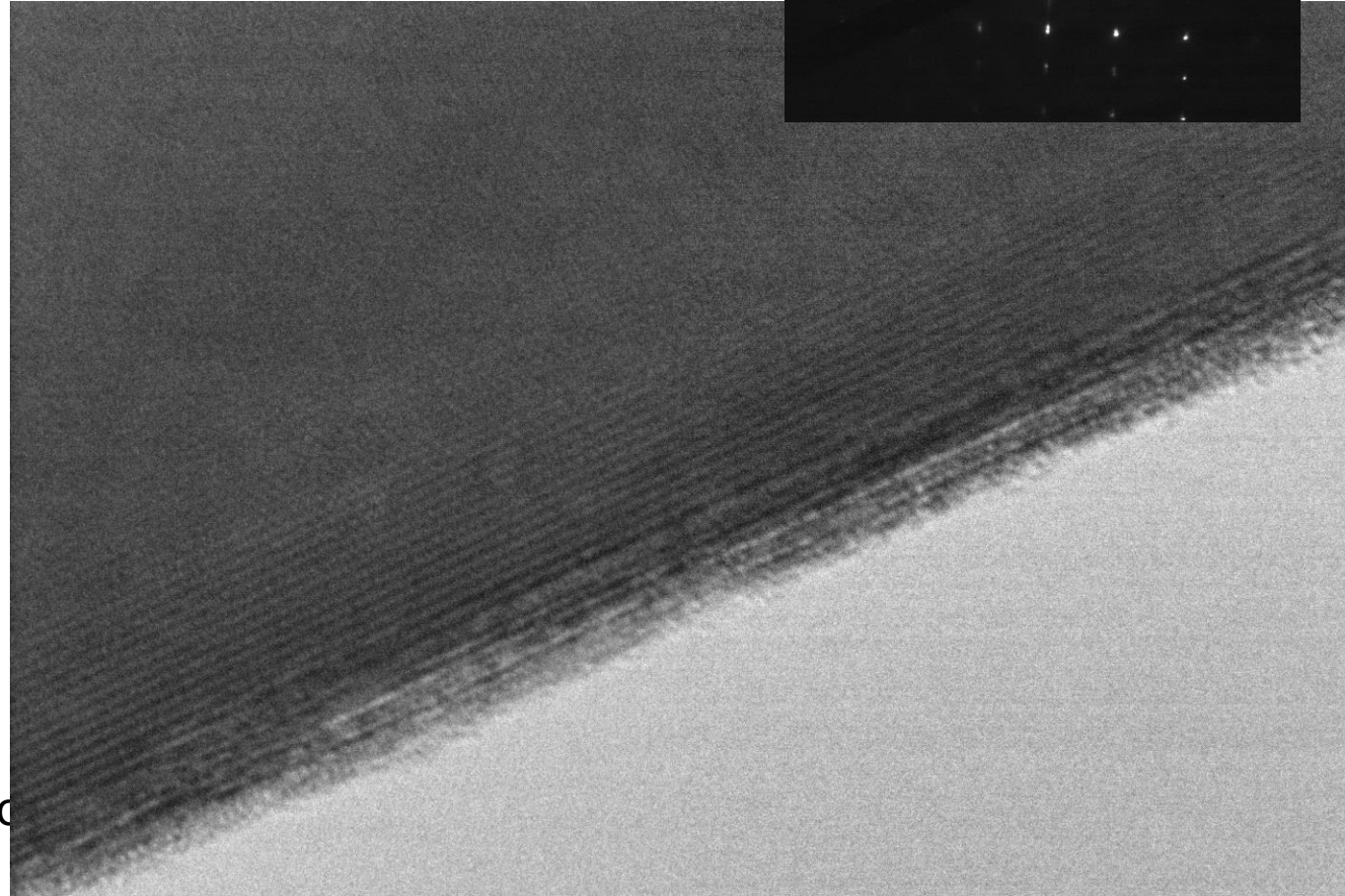
(A. Kasumov)

Diameter ~100 nm



Low magnification, Transmission Electron Microscopy

High resolution TEM

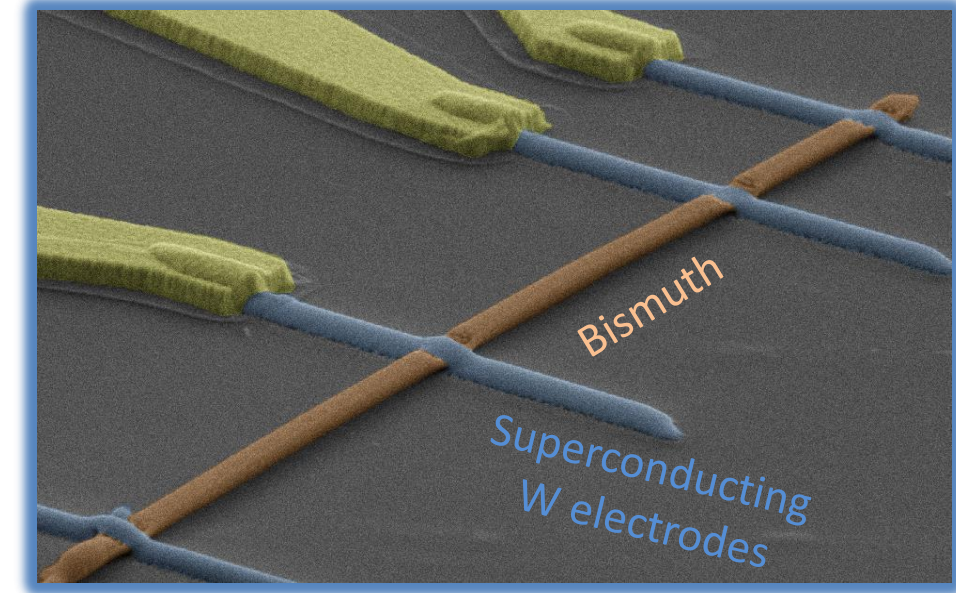
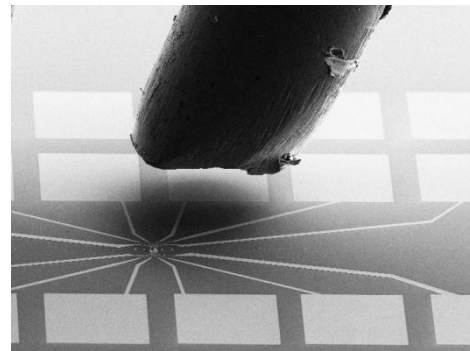
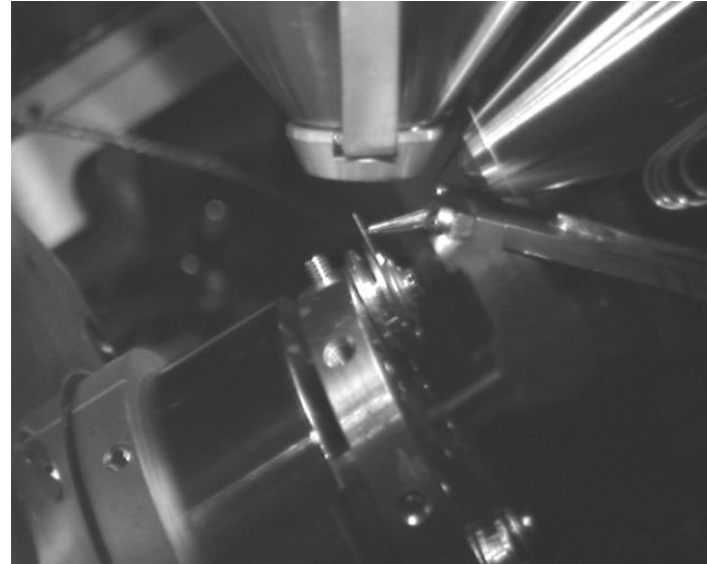
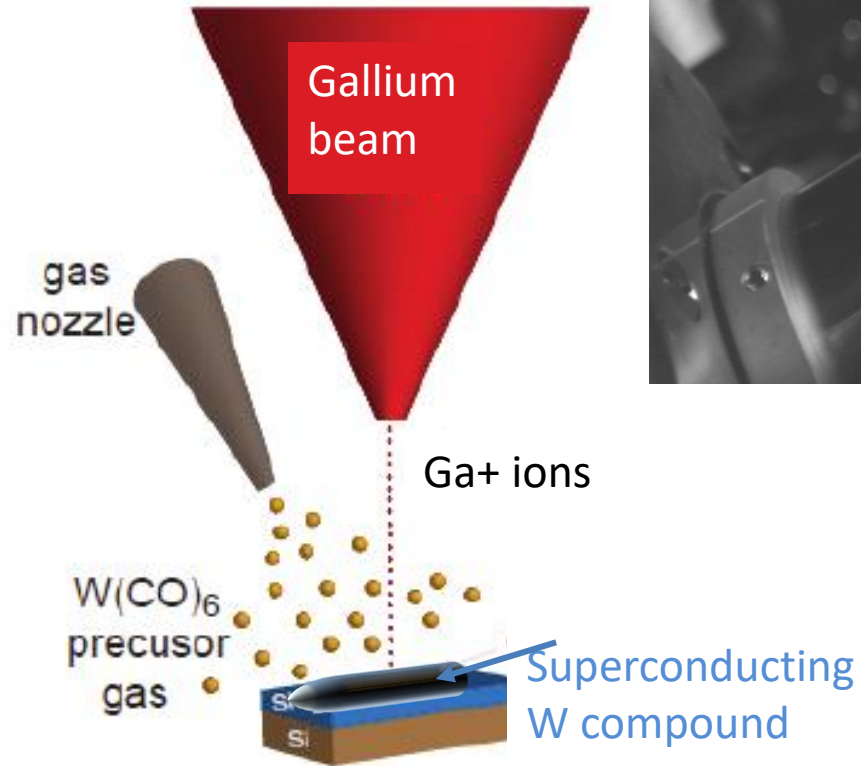


High quality monocrystals



# Connect selected nanowires with Superconducting contacts by focused-ion-beam-assisted deposition

Kasumov 2005



Superconducting electrodes:

C and Ga-doped amorphous tungsten  
200 nm thick and wide

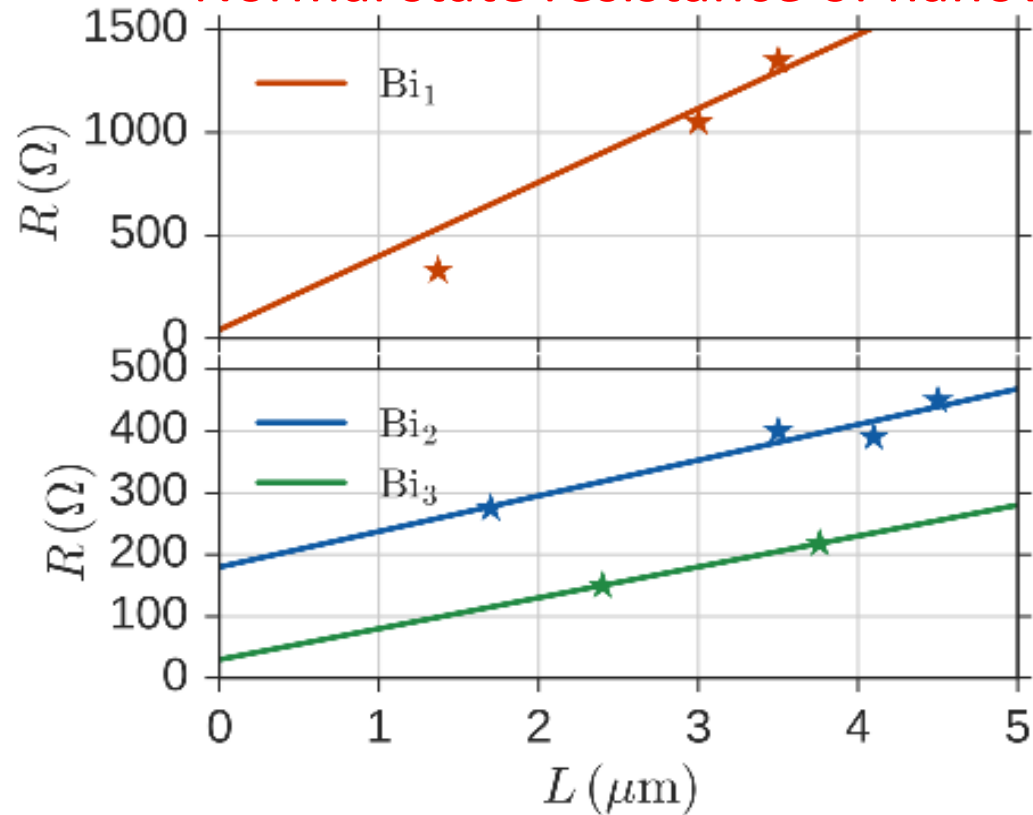
Great superconducting properties:  $T_c \sim 4$  K,  $\Delta \sim 0.8$  meV,  $H_c \sim 12$  Tesla!

# Normal transport doesn't show any ballistic states

**Diffusive Surface states carry most of the normal current**

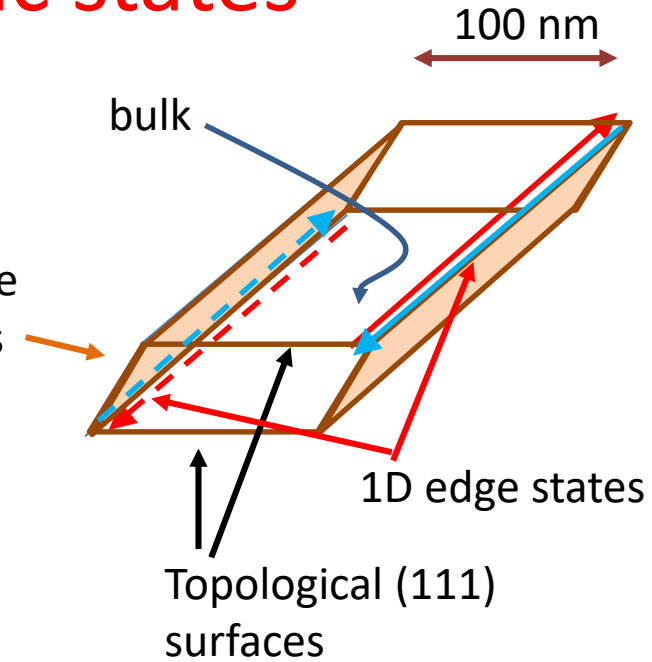
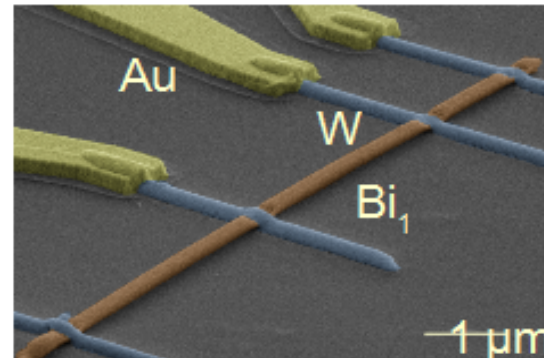
Bulk  $\lambda_F \simeq 50 \text{ nm}$   
Surface  $\lambda_F \simeq 5 \text{ nm}$  } Roughly 50 times more surface states than bulk states  
~ 100 diffusive Surface states

**Normal state resistance of nanowire**



$$R(L) = R_c + \frac{R_Q}{M} \frac{L}{l_e}$$

Thus  $l_e \lesssim 200 \text{ nm}$

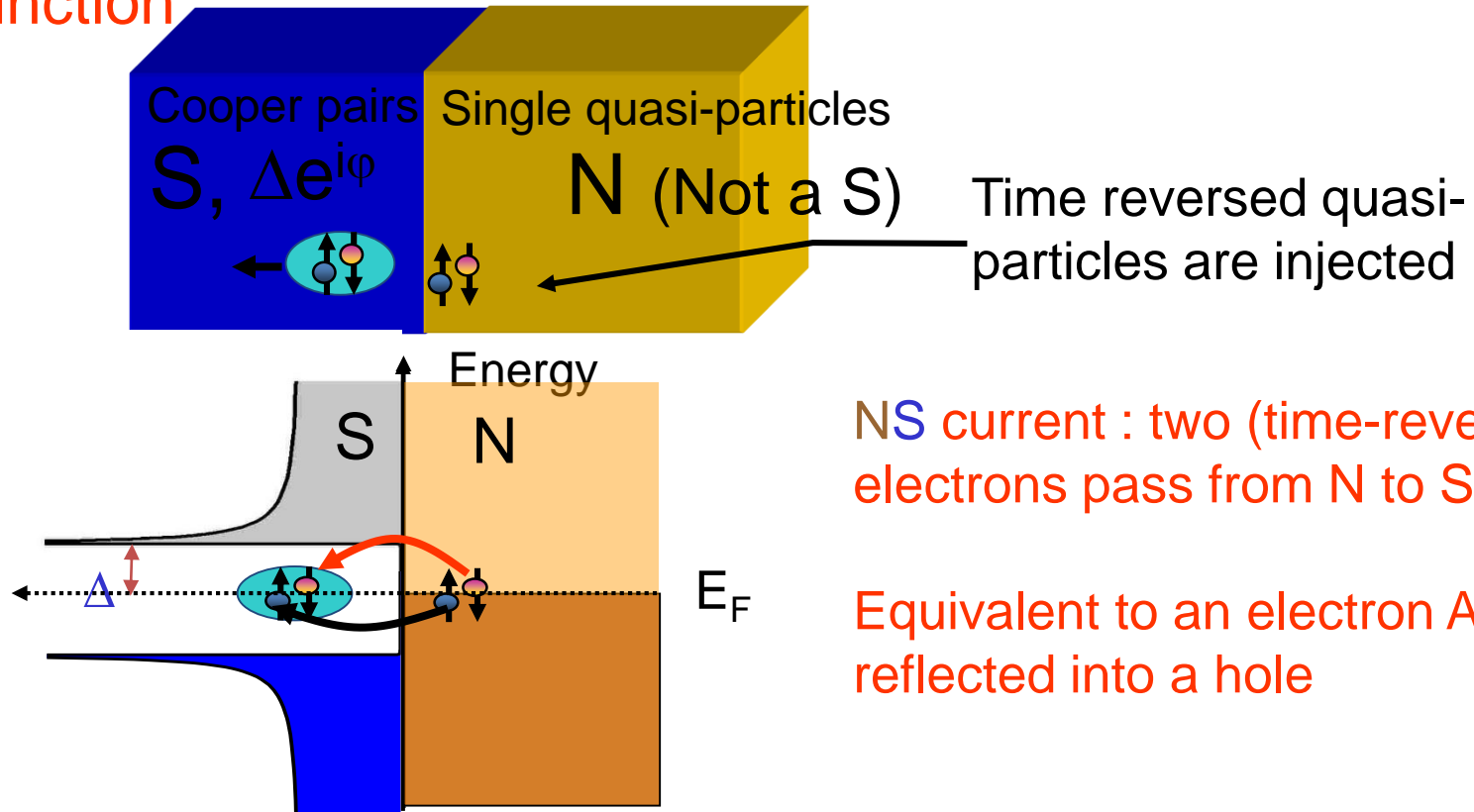


**Diffusive surface states carry almost all the normal current**  
**⇒ Turn to supercurrent to enhance visibility of ballistic states**

How does the superconducting proximity effect help ?

# Induced superconductivity

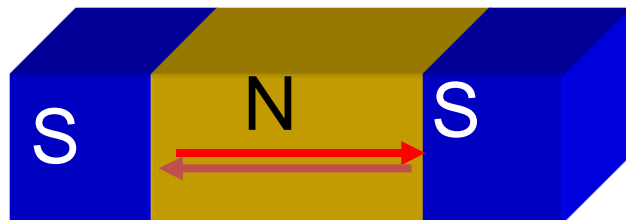
## NS junction



NS current: two (time-reversed) electrons pass from N to S

Equivalent to an electron Andreev reflected into a hole

## SNS junction

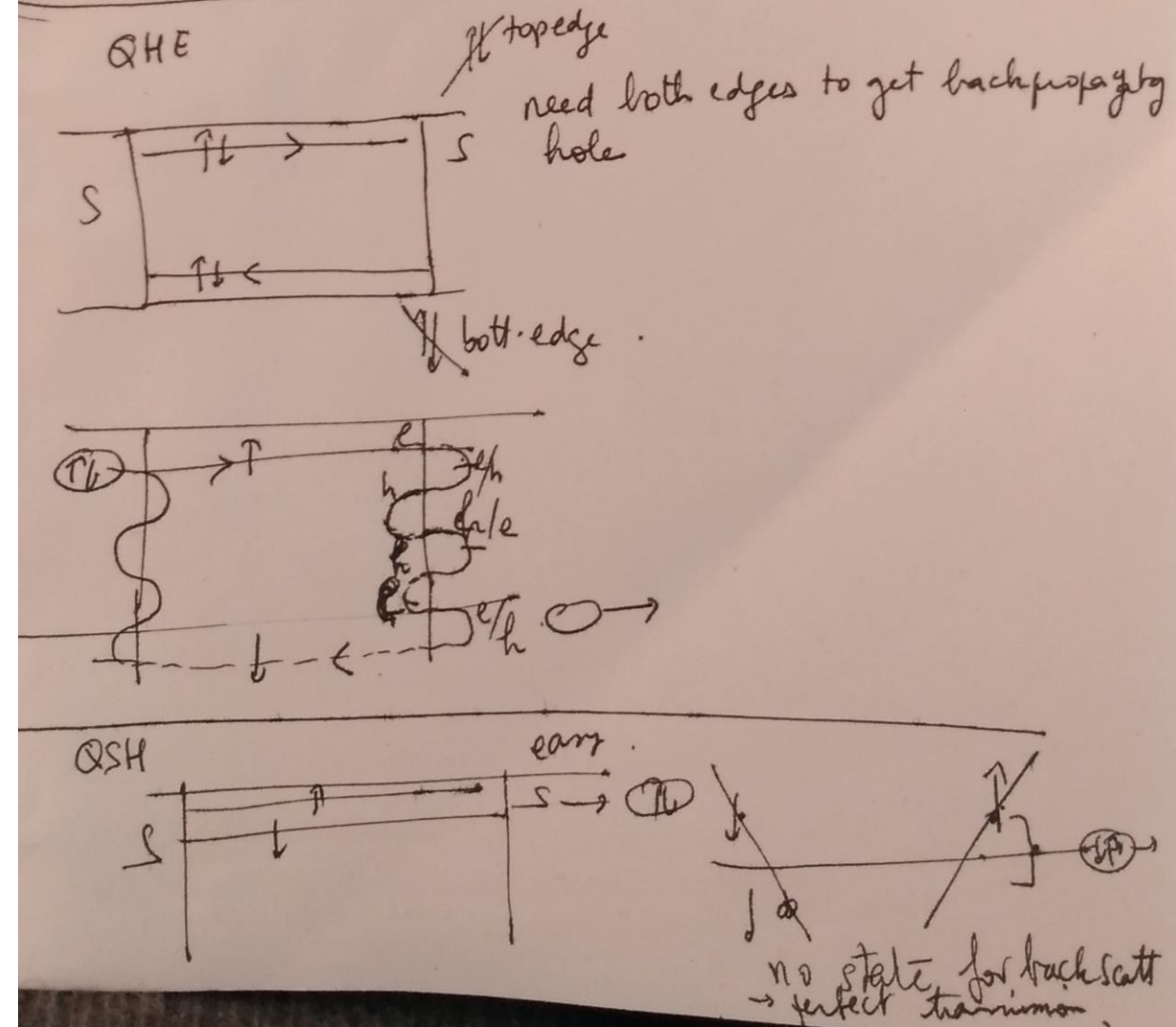
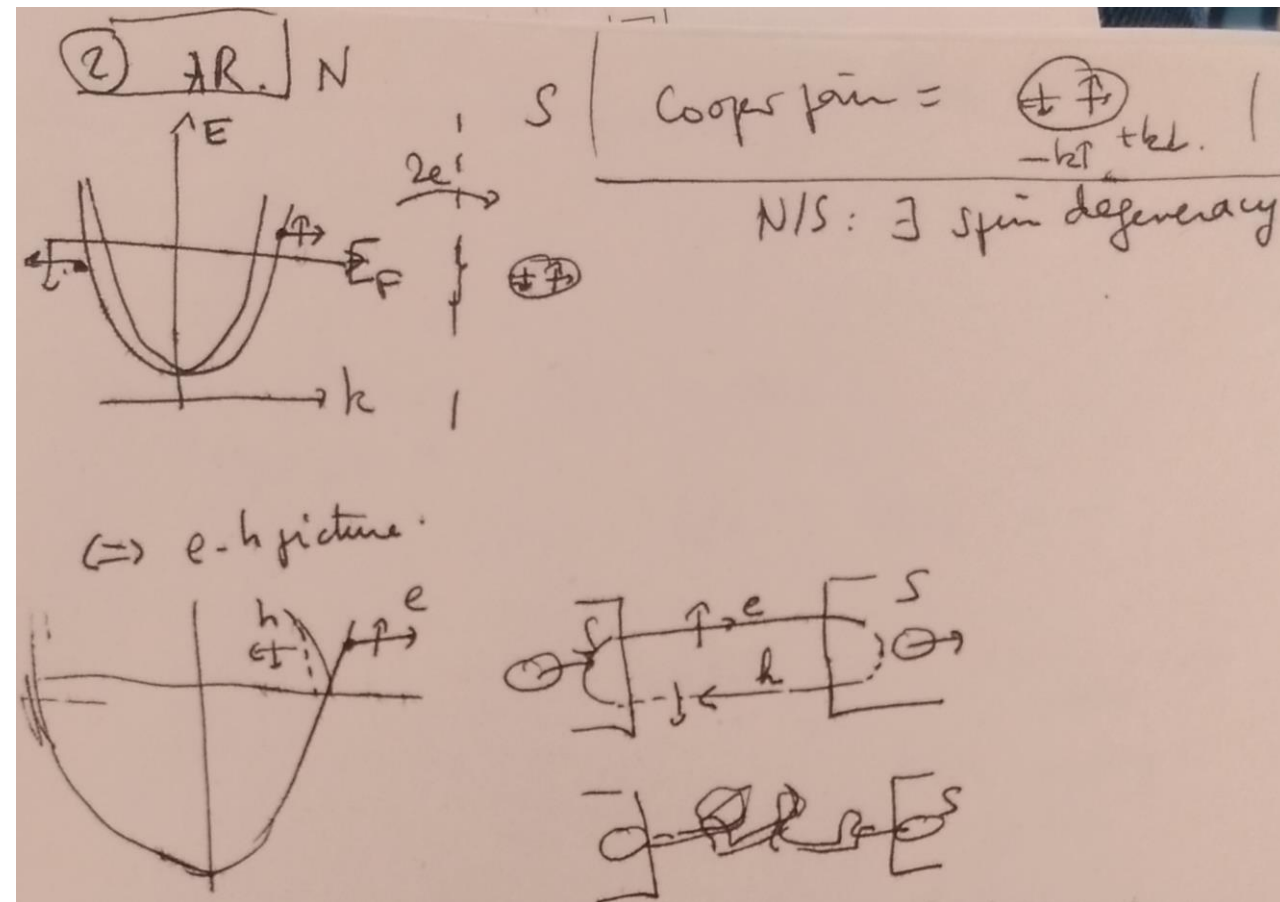


A supercurrent flows (zero resistance!) if N is quantum coherent ( $L < L_\phi$ ).

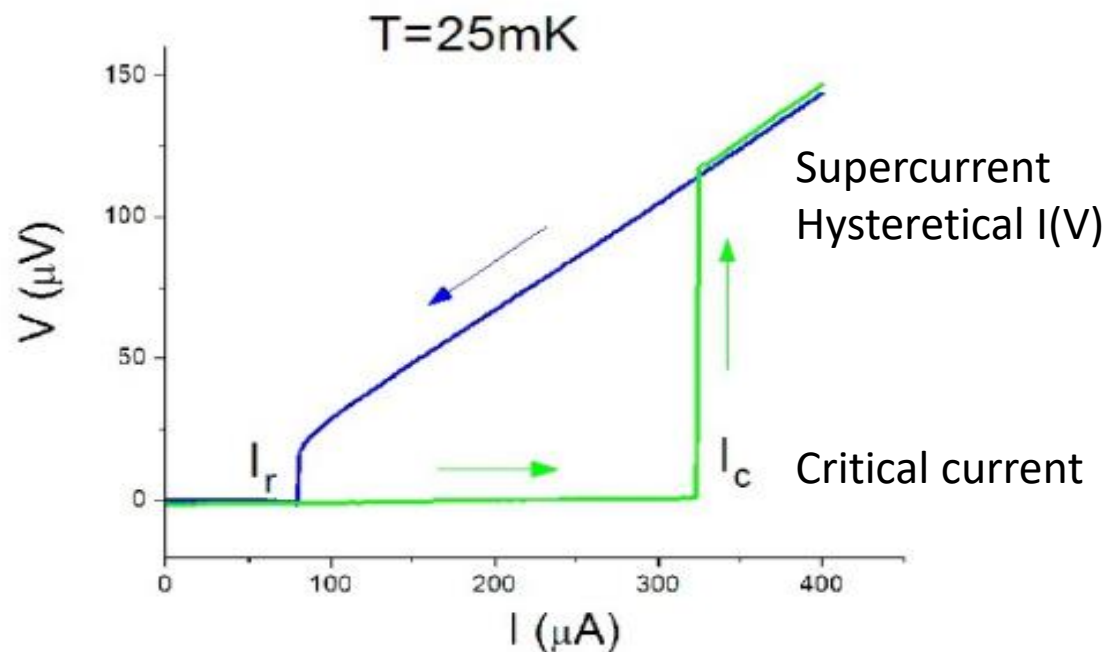
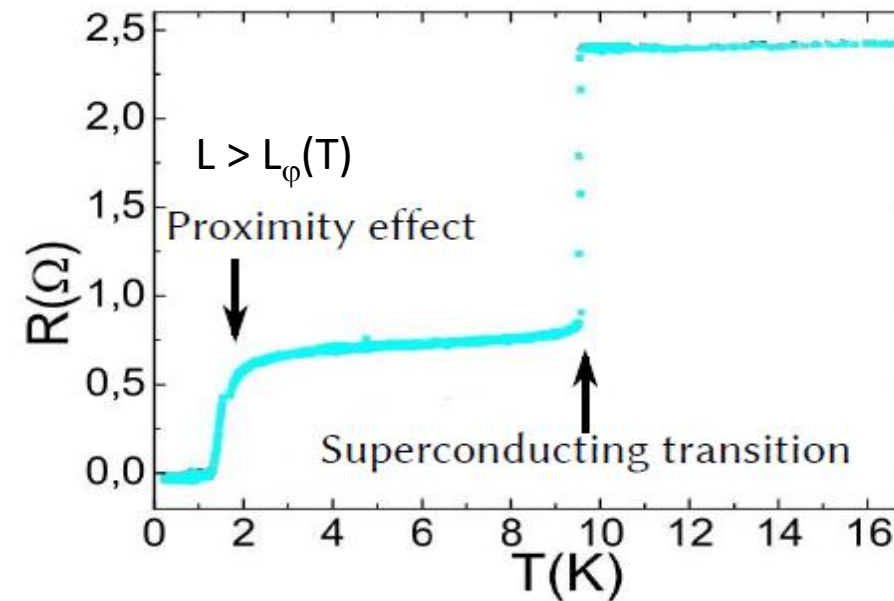
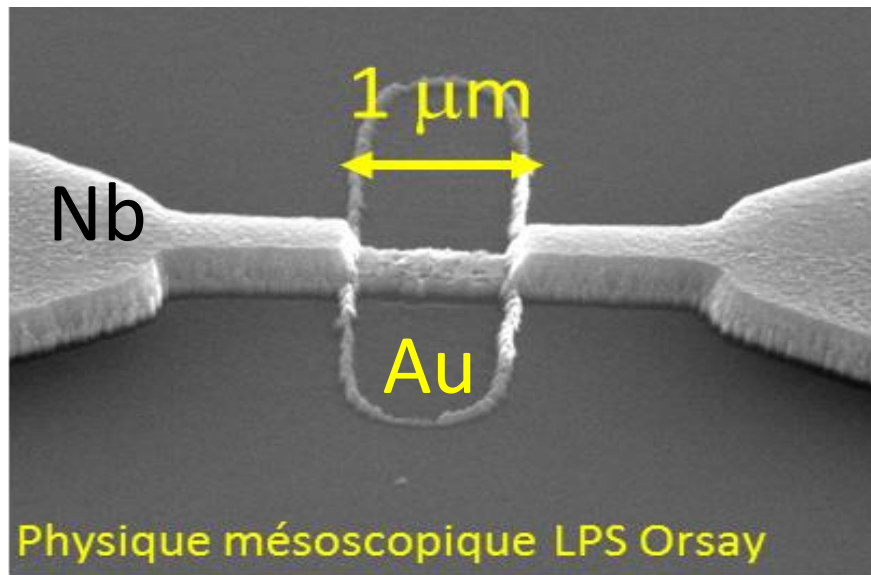
No change of the quantum state of electrons during propagation



## Interesting AR situations



## Conventional superconducting proximity effect



How much supercurrent can flow?

Where does it flow?

# Maximum supercurrent depends on junction length

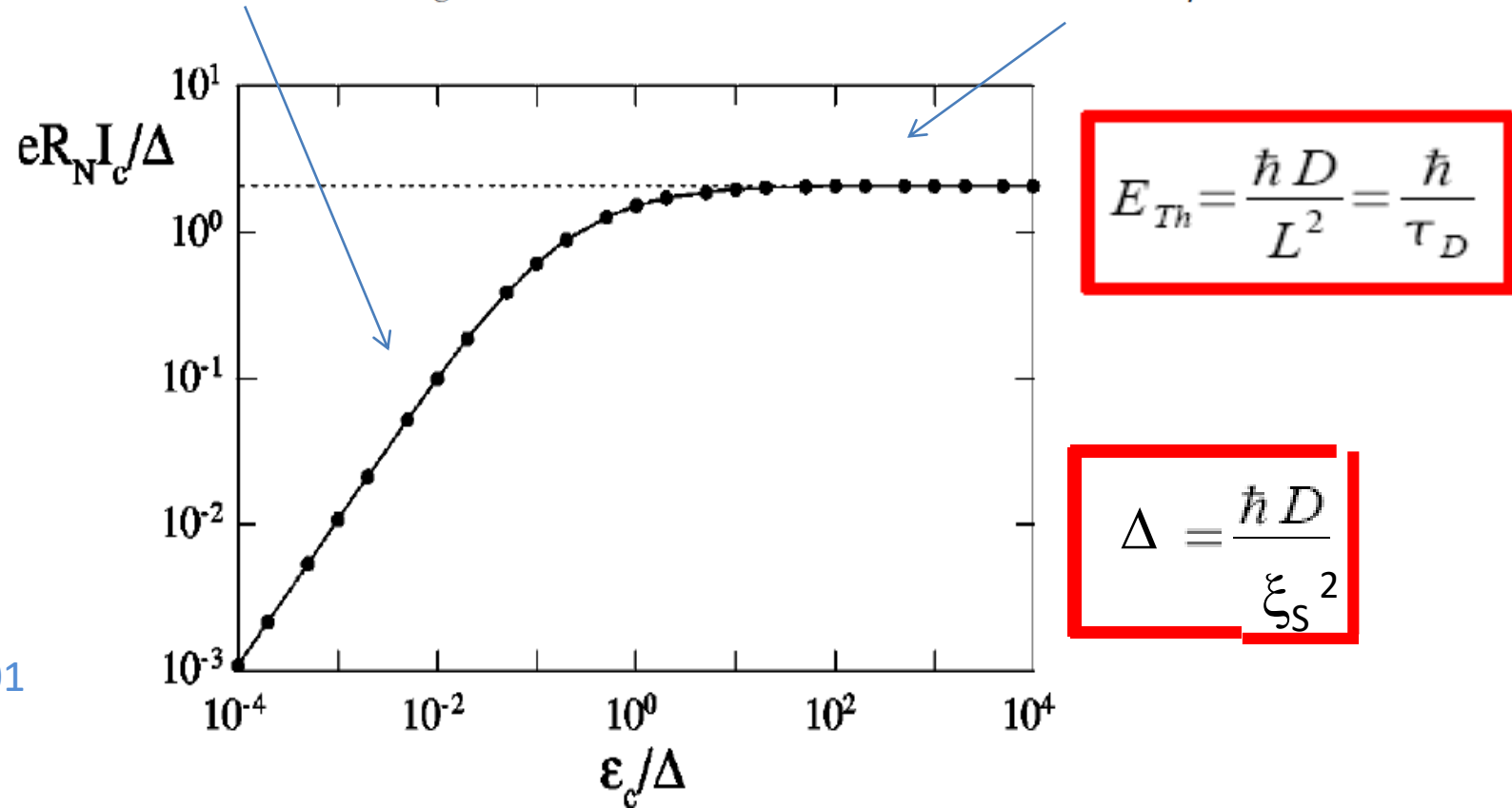
$$R_N I_c = \min(\Delta, E_{\text{Thouless}})$$

Long junction limit  $L \gg \xi_S$

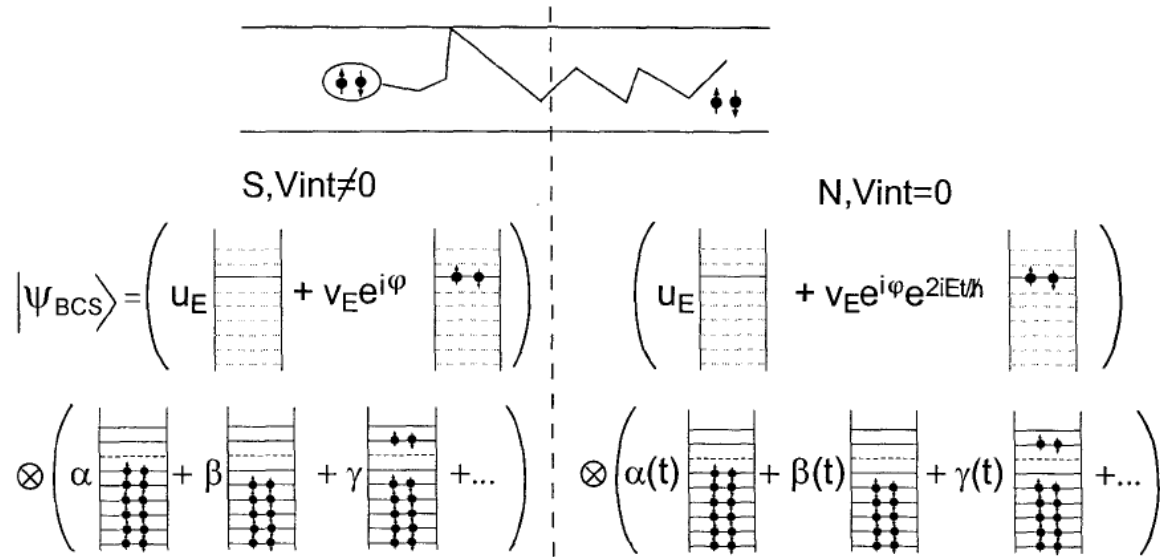
$$e R_N I_c(T = 0) = 10.82 E_{\text{Th}} = 3.2 \Delta_g.$$

Short junction limit  $L \ll \xi_S$

$$e R_N I_c \simeq 1.326 \pi \Delta / 2 \simeq 2.07 \Delta.$$



# Simplified picture of why diffusion time determines energy scale of proximity effect (in long junctions)



Dephasing  $\exp(-i2Et/\hbar)$  :  $2\pi$  after  $t = \hbar/E \sim \hbar D/L^2$ , with spread.

Pair correlation of energy  $E$  can propagate in  $N$  a distance

$$x \sim \sqrt{\hbar D/E}$$

Induced minigap, critical current of the order of

$$E_{Th} = \frac{\hbar D}{L^2} = \frac{\hbar}{\tau_D}$$



This should help understand why superconductivity helps detect ballistic states, even if many more diffusive states

① [Meso slide]

$e R_N I_c = \min(\Delta, E_{Th})$

$E_{Th} = \frac{\hbar}{\tau_{traversal}}$

Thouless  $\tau_{diff} = \frac{L^2}{D}$ ,  $D = \frac{1}{3} v_F l_e$

$\tau_{bal} = \frac{L}{v_F}$

Short junction  $L < \xi_S = \sqrt{\frac{\hbar D}{\Delta}}$

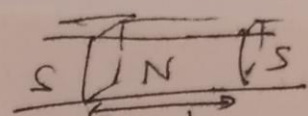
long junction  $L > \xi_S$

Short jxn:  $\Delta$  gives energy scale

$I_c^{short} \approx \frac{\Delta}{e R_N}$

long jxn:  $E_{Th}$

$I_c^{long} \approx \frac{E_{Th}}{e R_N}$



$R_N$ ? Mesoscopic physics

diff.  $R = e \frac{L}{\text{section}} = \frac{\hbar}{e^2} \frac{1}{\pi}$

$R = \frac{1}{\text{dos}} \frac{L}{\text{section}} = \frac{1}{\text{dos}} \frac{L}{\frac{\pi}{2} \frac{L}{l_e}} = \frac{2 l_e}{\pi}$

$R^{diff} = \frac{\hbar}{e^2} \frac{1}{\pi} \frac{L}{l_e}$

$R^{bal} = \frac{\hbar}{e^2} \frac{1}{\pi} \frac{L}{l_e}$

$\tau_{eff} = \tau \times \frac{l_e}{L}$

$\text{dos} = \frac{1}{\# \text{states/cm}^3 \text{vol}} = \frac{1}{\Delta_F^3}$

$\frac{I_c^{short bal}}{I_c^{short diff}} = \frac{R_N^{diff}}{R_N^{bal}} = \frac{M_{eff}}{M} = \frac{L}{l_e}$

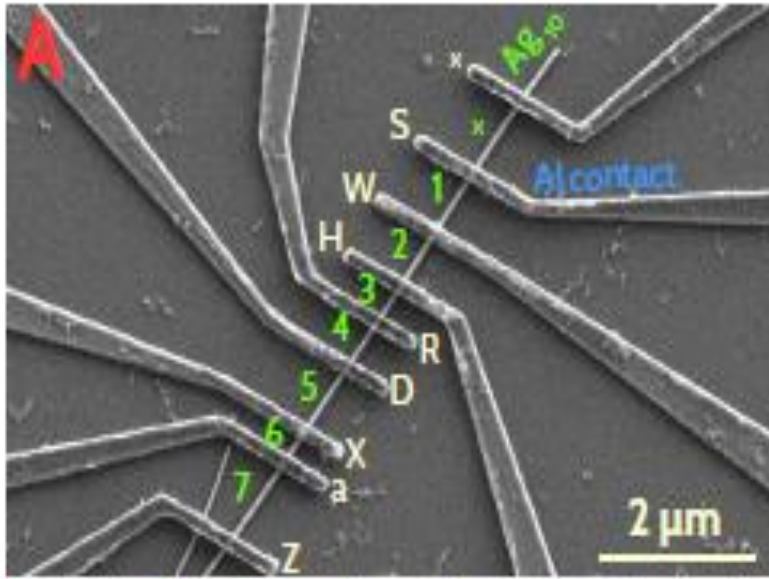
$\frac{I_c^{long diff}}{I_c^{long bal}} = \frac{E_{Th}^{bal}}{E_{Th}^{diff}} \times \frac{R_N^{diff}}{R_N^{bal}}$

$\frac{I_c^{long bal}}{I_c^{long diff}} = \frac{\tau_{diff}}{\tau_{bal}} \times \frac{L}{l_e}$

$\frac{I_c^{long bal}}{I_c^{long diff}} = \frac{L^2 / l_e^2}{L^2 / l_e^2}$

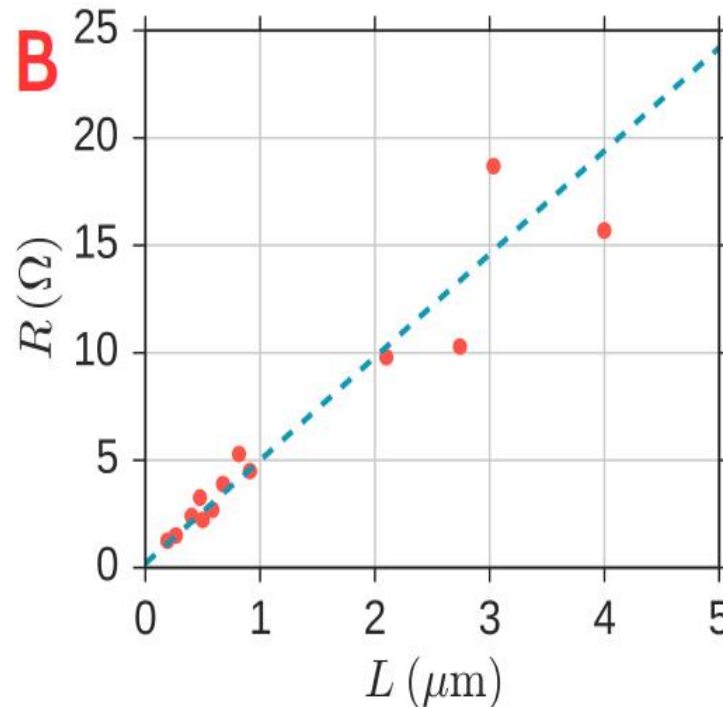
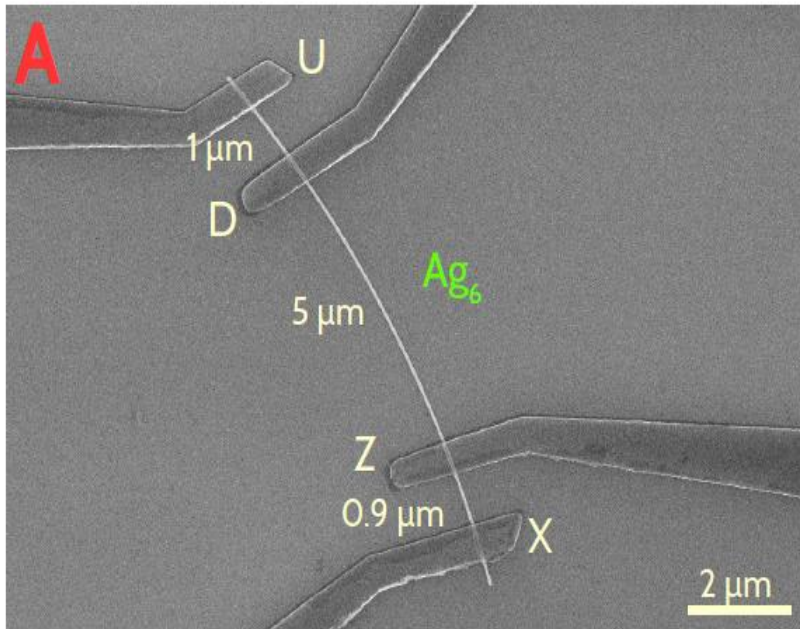
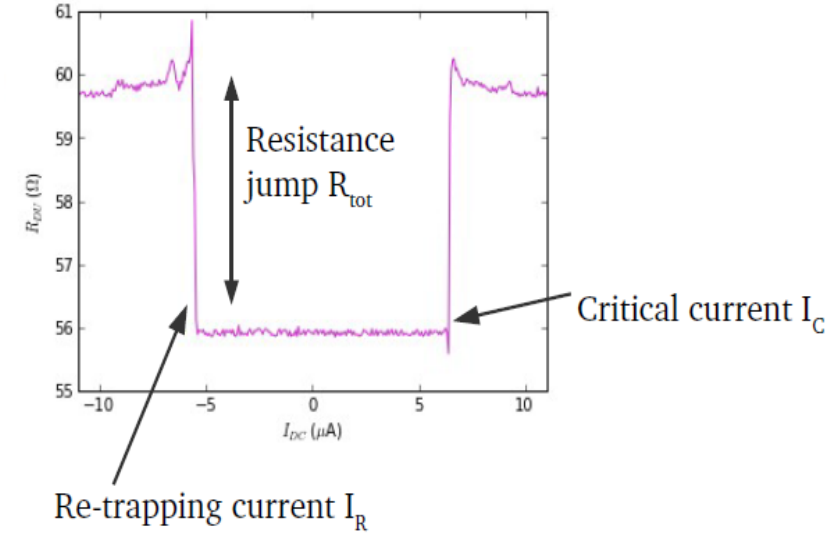
$R^{ballistic} = \frac{\hbar}{e^2} \frac{1}{\pi} \frac{1}{\frac{\pi}{2} \frac{L}{l_e}} = \frac{\hbar}{e^2} \frac{1}{\pi}$

# channels  $\frac{\text{Section}}{\Delta_F^2}$



# Reference example: Silver nanowires (50 nm diameter) based Josephson junctions

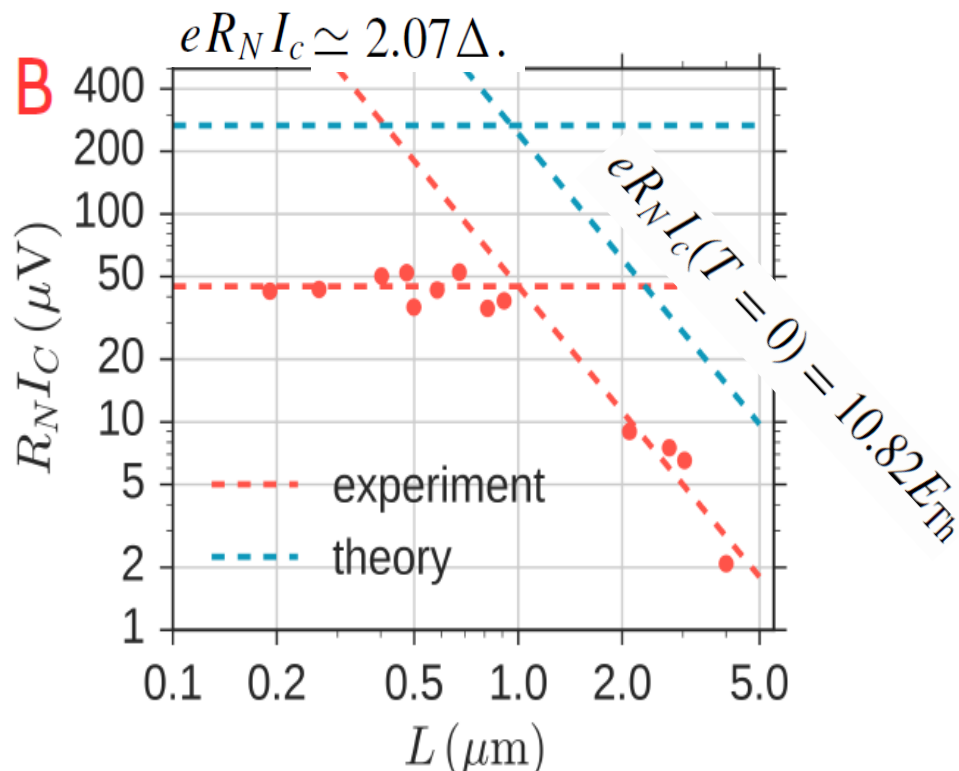
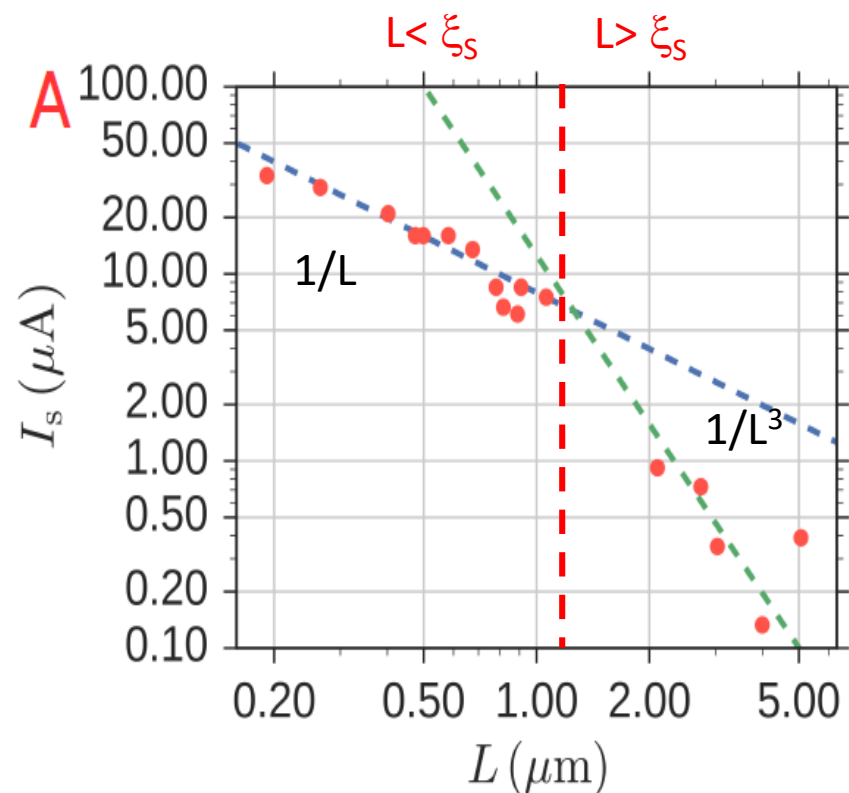
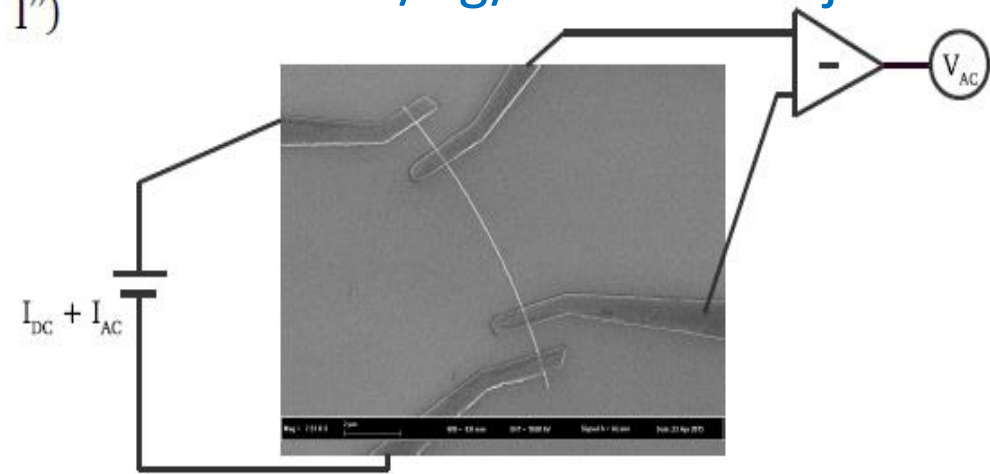
Murani et al., in preparation



$$R = R_c + R_Q M l e / L$$

Diffusive normal state conduction

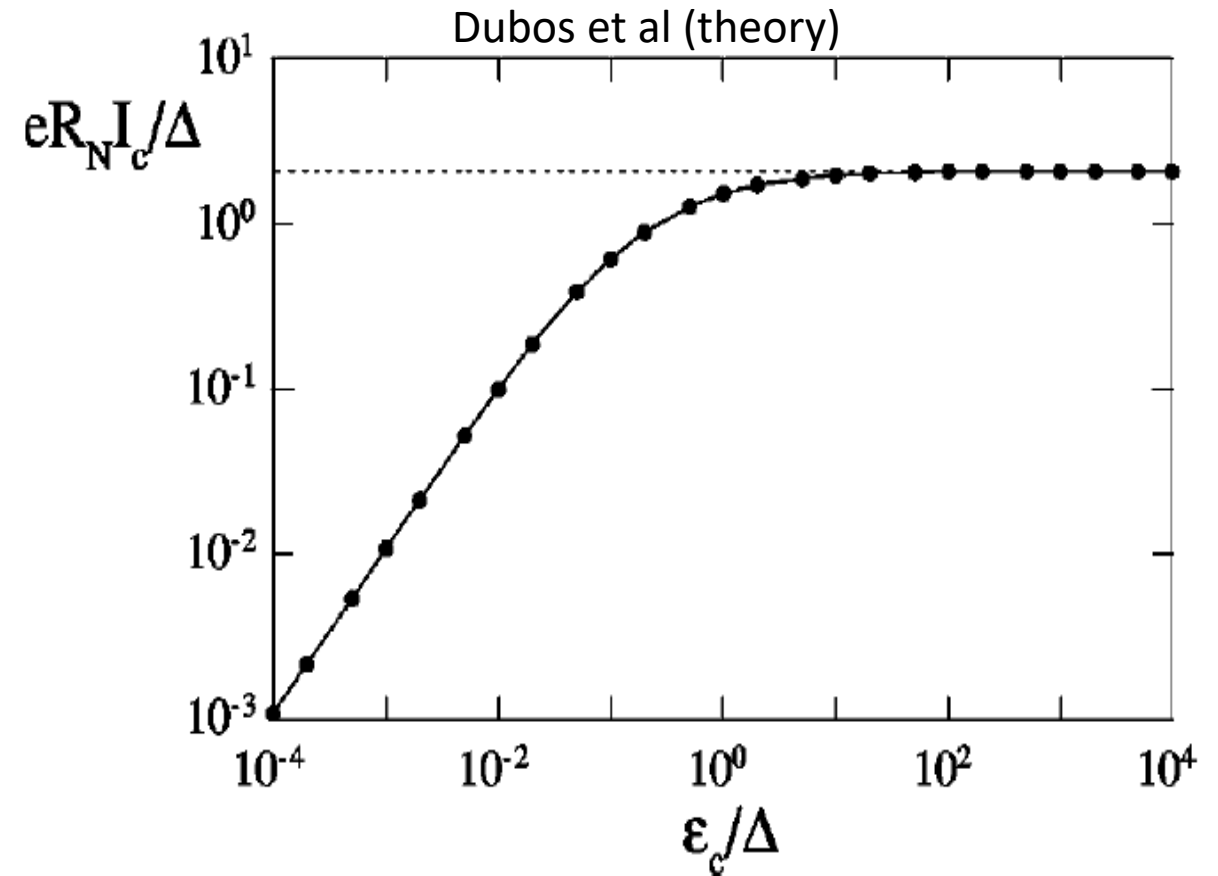
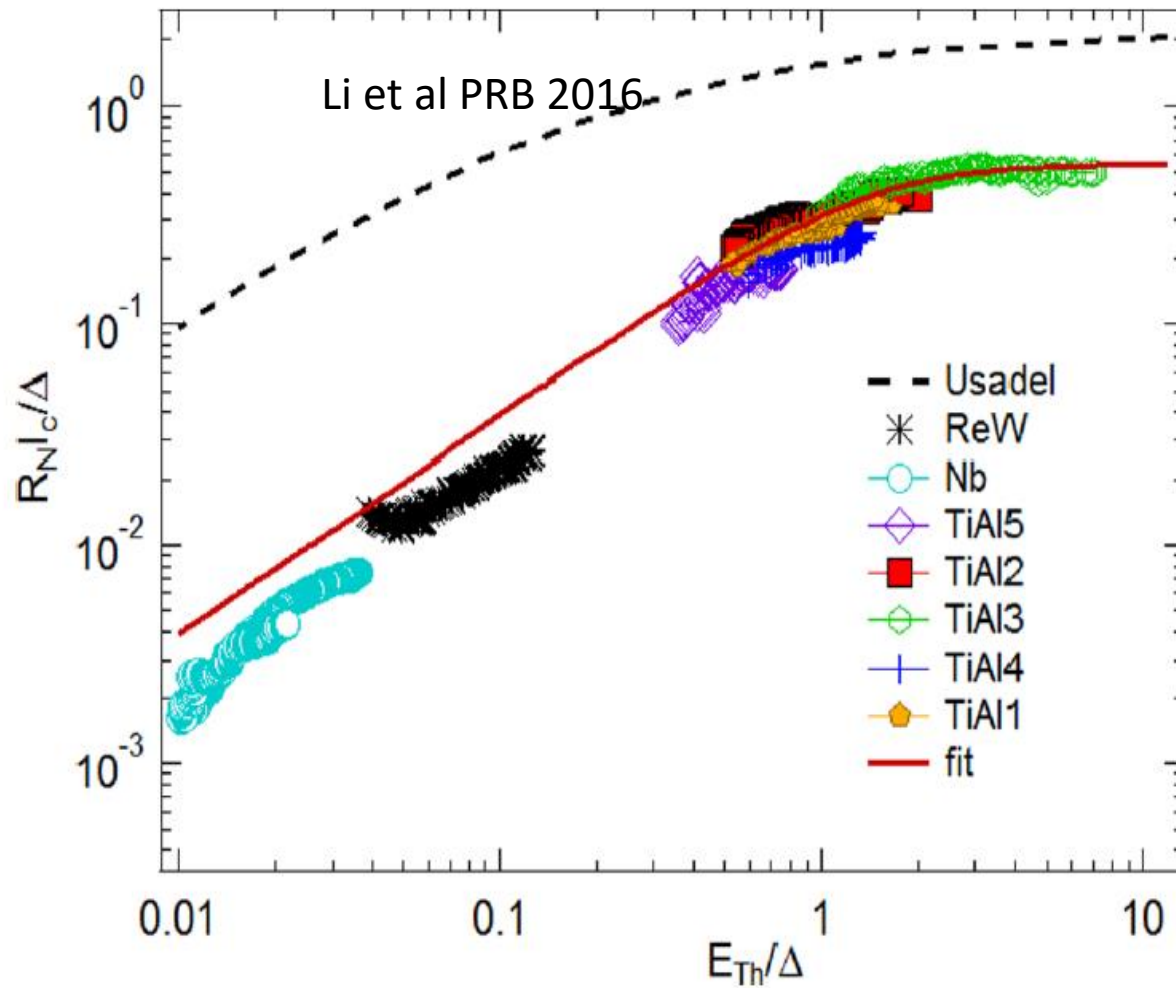
I<sup>'''</sup>) S/Ag/S reference junction, with varying lengths



S/Ag/S reference junction: crossover from short to long junction

# Crossover from short to long junction also seen in graphene samples

Gate voltage modulates the number of carriers and the diffusion coefficient



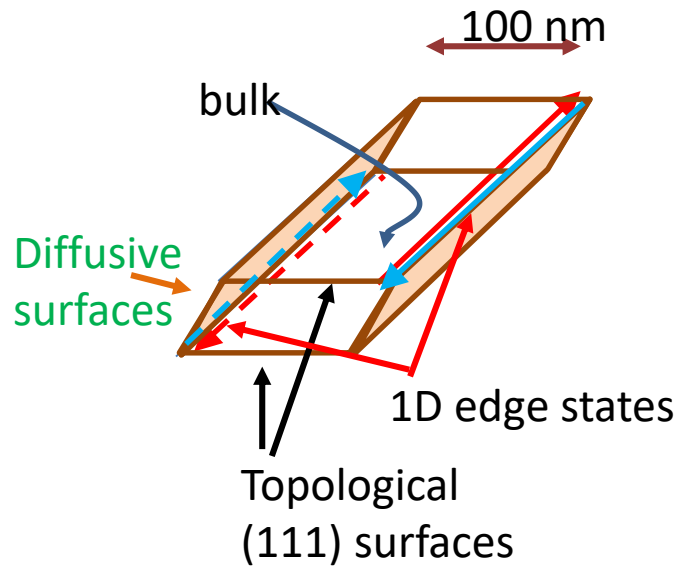
Qualitative agreement but critical currents are lower than expected theoretically



# Induced superconductivity enhances contribution of Quantum Spin Hall states

- Critical current carried by diffusive states is much smaller than critical current carried by ballistic states

~ 6 ballistic edge channels, ~ 100 diffusive surface channels, elastic mean free path  $l_e$

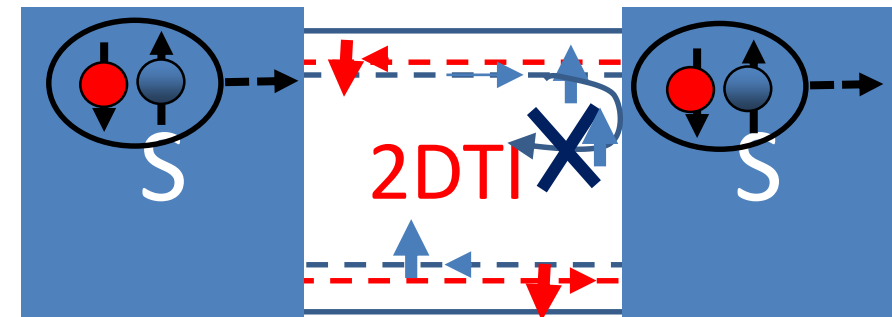


$$I_{c \text{ 1channel, ballistic}} \sim \frac{\hbar v_F}{L} \frac{h}{e^2}$$

$$I_{c \text{ 1channel, diffusive}} \sim \frac{\hbar v_F}{L} \frac{h}{e^2} \left( \frac{l_e^2}{L^2} \right)$$

100 to 1000 times smaller than ballistic

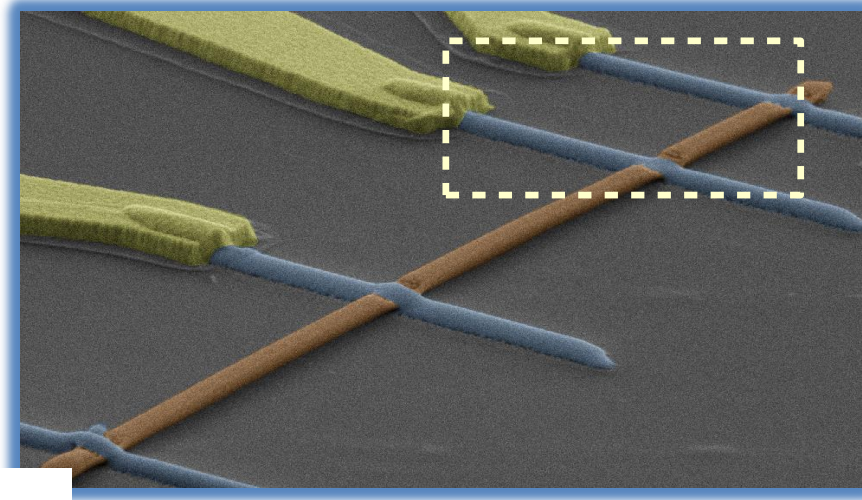
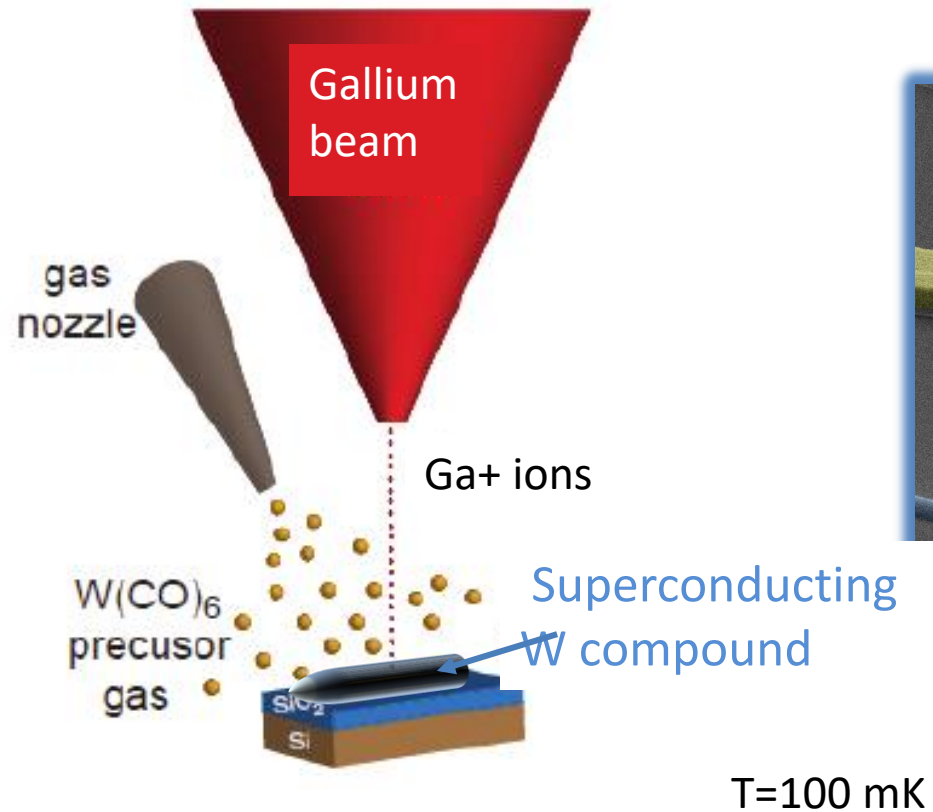
- In addition, Quantum spin Hall edges should have perfect transmission into S (not true of diffusive channels)



End of first course

# Supercurrent through bismuth nanowire below 2 K

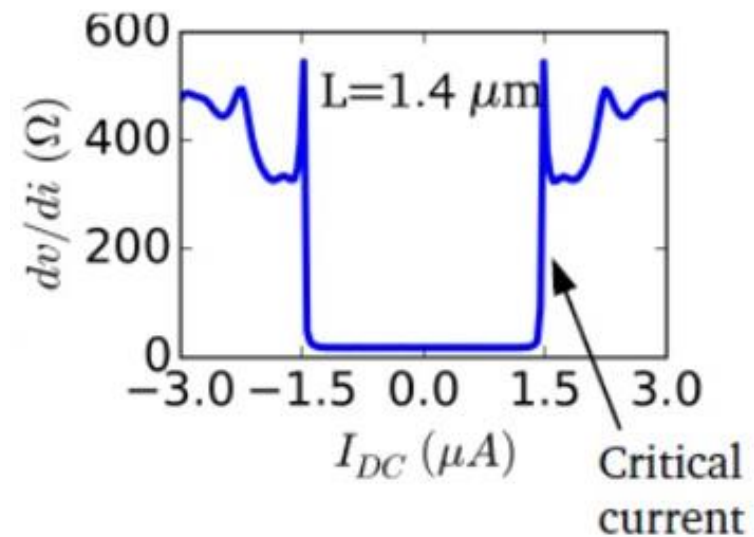
Kasumov 2005



Bismuth nanowire  
with (111) surfaces

Superconducting  
W electrodes

W/Bi/W junction



$$I_{c, \text{ short \& ballistic}} = \Delta / e R_q \sim 100 \text{ nA/channel}$$

~ 15 well transmitted channels

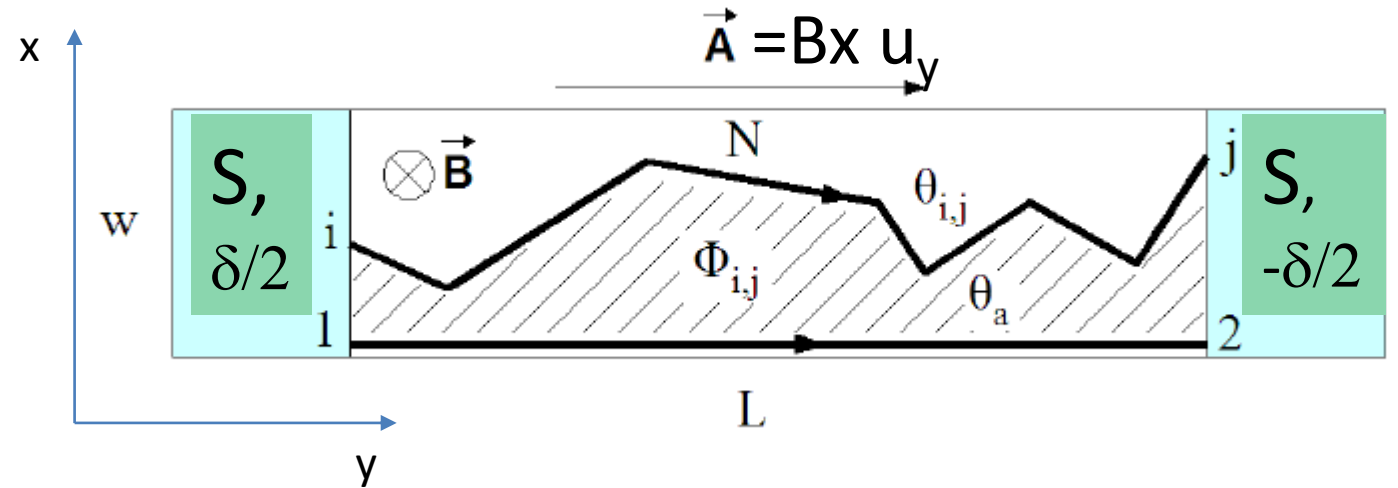
Where does the supercurrent flow?



# Superconducting contacts to exploit macroscopic wavefunction (and its phase): Interference experiments will reveal where supercurrent flows

Gauge invariant Josephson relation:

$$I(\delta) = I_0 \sin \left( \delta - \frac{2e}{\hbar} \int \mathbf{A} \cdot d\mathbf{l} \right)$$



Critical current  $I_c(B)$  = max of integral over all supercurrent paths: interference terms!

$$I_c(B) = \left| \int_{-W/2}^{W/2} J(x) \cdot e^{2\pi i L B x / \Phi_0} dx \right|$$

Critical current  $I_c(B)$  = |Fourier transform of supercurrent distribution  $J(x)$ |

Known interference patterns for :

- Uniform current in wide junctions

- Current at two edges

- Current carried asymmetrically at two edges

$I_c$ : Formula after TF-

$$I_c \propto \left| \int_{-w/2}^{w/2} J(x) e^{iBxL} dx \right|$$

•  $J = \text{const}$

$$I_c \propto \left| \int_{-w/2}^{w/2} e^{iBxL} dx \right| = \left| \frac{\sin \frac{BwL}{2}}{B} \right|$$

•  $J = \delta(\frac{w}{2}) + \delta(-\frac{w}{2})$

$$I_c \propto \left| \int_{-w/2}^{w/2} e^{iBxL} \left( \delta(\frac{w}{2}) + \delta(-\frac{w}{2}) \right) dx \right|$$

$$= \left| e^{iBwL/2} + e^{-iBwL/2} \right|$$

$$= \left| \cos \frac{BwL}{2} \right|$$

•  $J = \delta(\frac{w}{2}) + \alpha \delta(-\frac{w}{2})$

$$I_c = \left| e^{iBwL/2} + \alpha e^{-iBwL/2} \right|$$

$$= \left\{ (e^{iB} + \alpha e^{-iB})(e^{-iB} + \alpha e^{iB}) \right\}^{1/2}$$

$$= \left\{ 1 + \alpha^2 + 2\alpha \cos \frac{BwL}{2} \right\}^{1/2}$$

max  $(1+\alpha)$   
min  $(1-\alpha)$

$\alpha$  small  $I_c = \left| 1 + \alpha \cos \frac{BwL}{2} \right|$

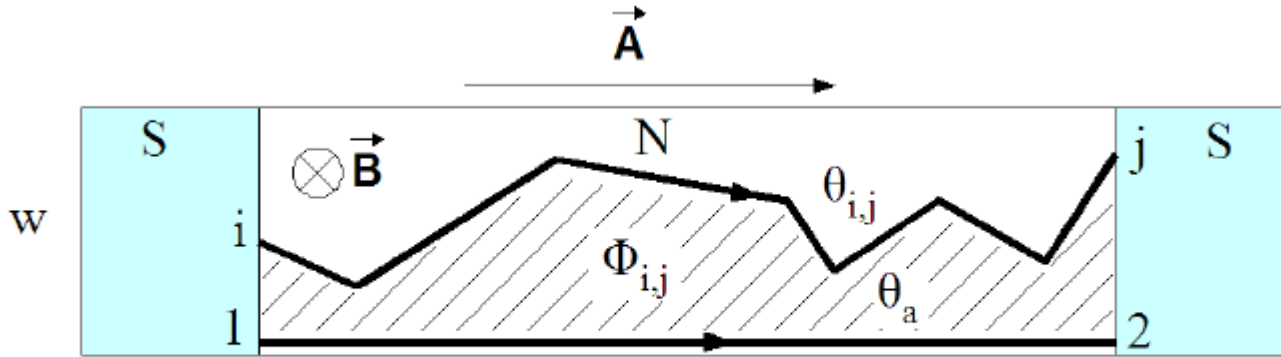
asymmetric SQUID

- Fraunhofer

- SQUID

- asymmetric SQUID

**Narrow diffusive sample with many channels:**  
Flux-dependent phase variation in sample



# Cuevas, Montambaux

$$I_c \propto \left| \langle e^{i\Delta\theta_{i,j}} \rangle_{c_{i,j}} \right| \quad I_c \propto \left| e^{-\langle (\Delta\theta_{i,j})^2 \rangle_{c_{i,j}}/2} \right|$$

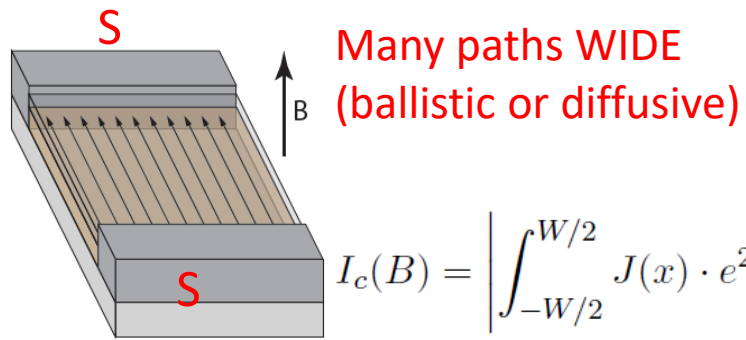
Diffusive trajectories encircle different flux,  
so pick up different phases

$$\Delta\theta_{i,j} = \frac{2e}{\hbar} \left[ \int_i^j A_x dx - \int_1^2 A_x dx \right] = \frac{2e}{\hbar} \oint A_x dx = \frac{2\pi}{\Phi_0} H S_{i,j} = 2\pi \frac{\Phi_{i,j}}{\Phi_0} \quad (2.5)$$

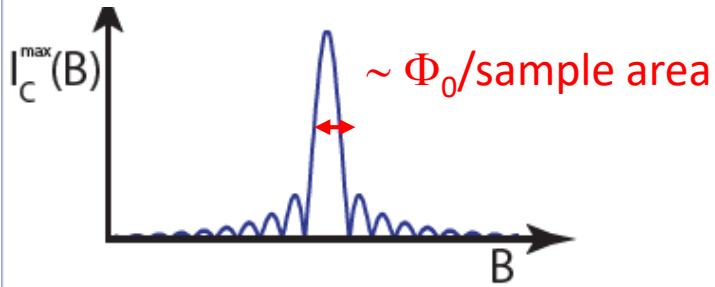
$$I_c \propto \left| e^{-2\pi^2 H^2 \alpha^2 / \Phi_0^2} \right|$$

~ Gaussian decay of  $I_c$  on scale of  $\Phi_0$   
because dephasing by field

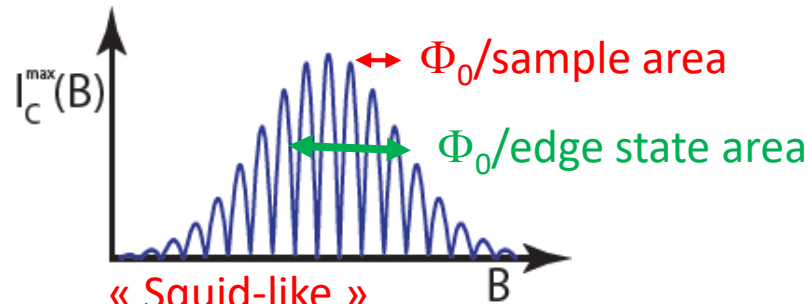
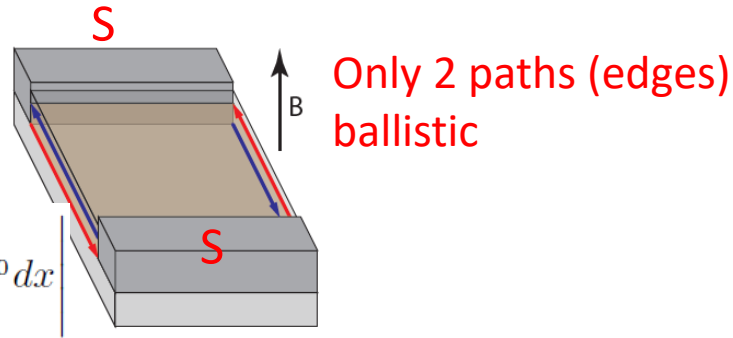
# Critical supercurrent reveals paths taken by pairs (via interference)



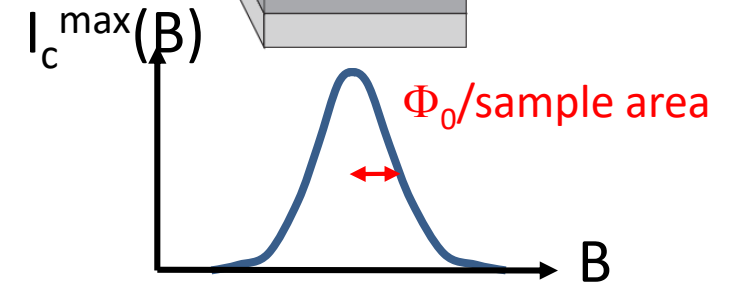
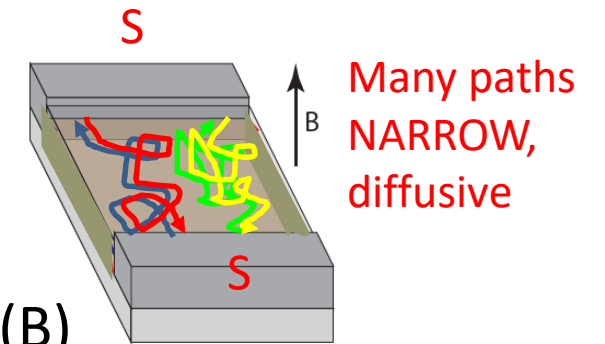
$$I_c(B) = \left| \int_{-W/2}^{W/2} J(x) \cdot e^{2\pi i L B x / \Phi_0} dx \right|$$



« Fraunhofer pattern »

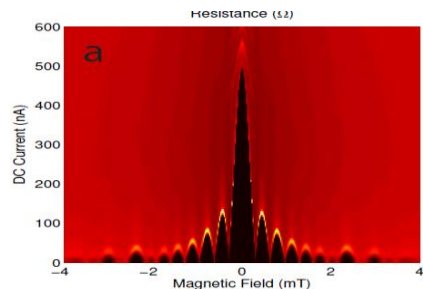


« SQUID-like »

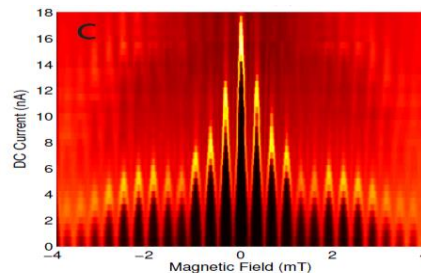


Many diffusive paths  
Gaussian decay

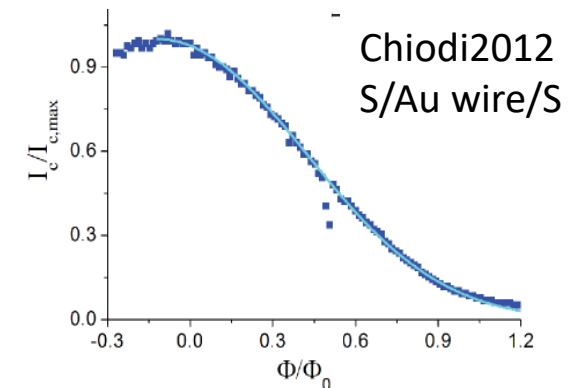
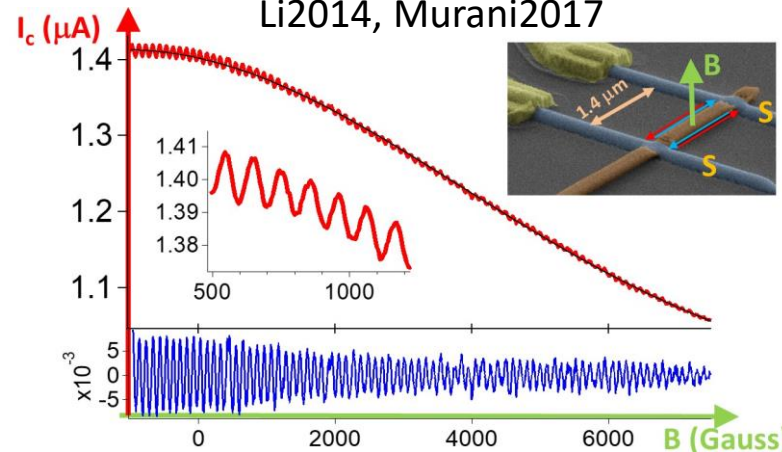
S/Non topo HgTe QW/S,  
Hart 2014



S/Topo/S HgTe QW,  
Hart 2014



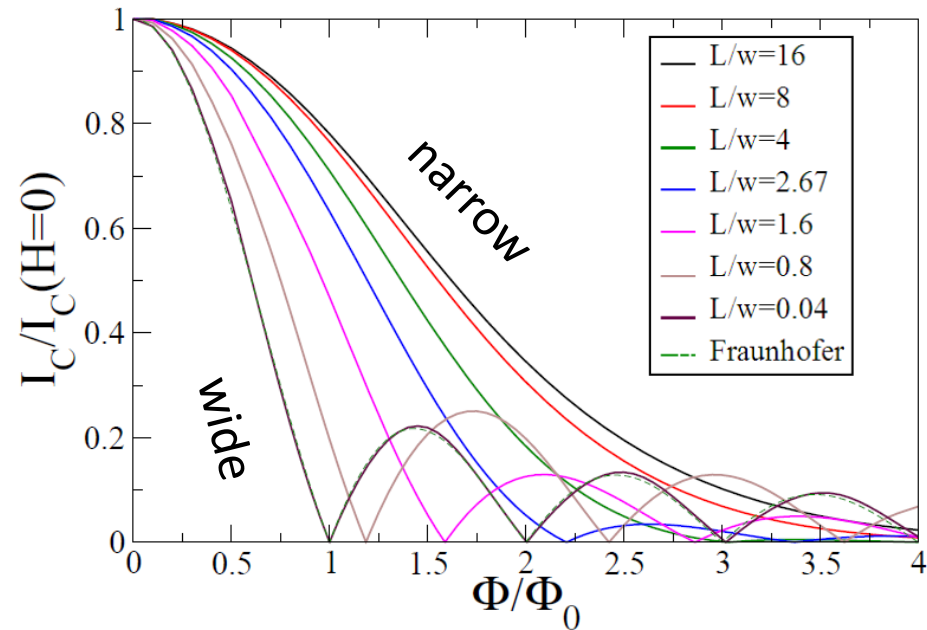
Bismuth nanowire,  
Li2014, Murani2017





# Role of geometry demonstrated in (diffusive!) SNS junctions

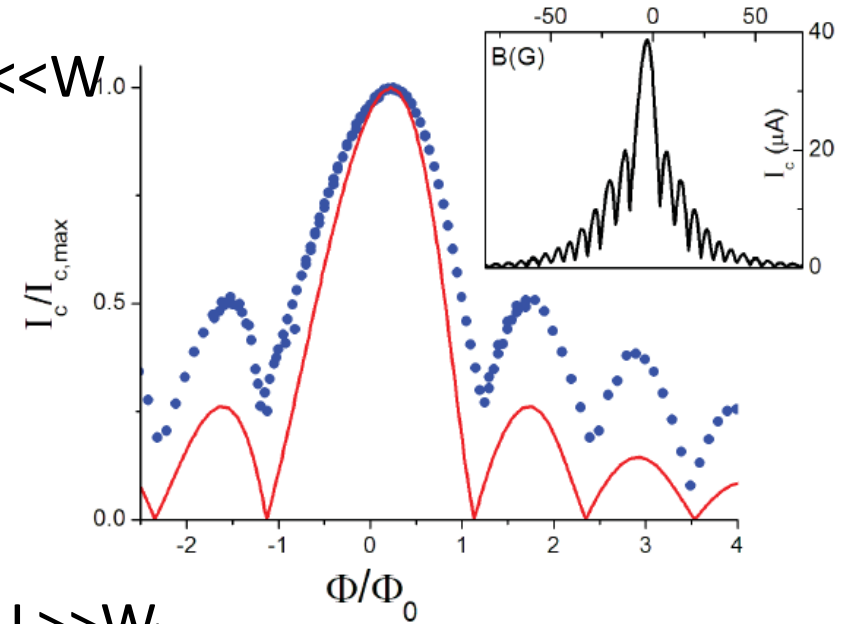
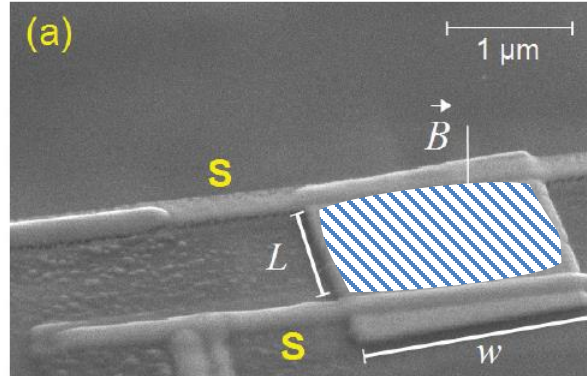
Theory: Bergeret Cuevas 2008



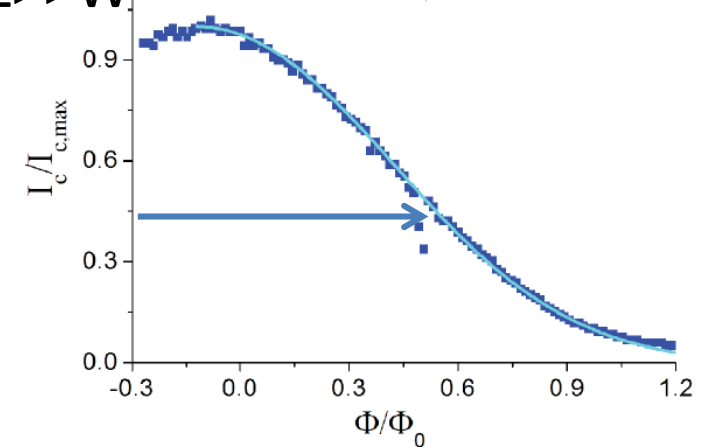
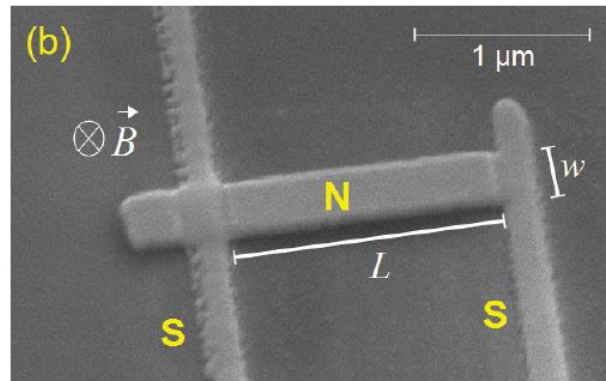
Depends on whether most dephasing by potential vector occurs at S interface or during propagation through N

Exp: Chiodi 2012

wide:  $L \ll W$



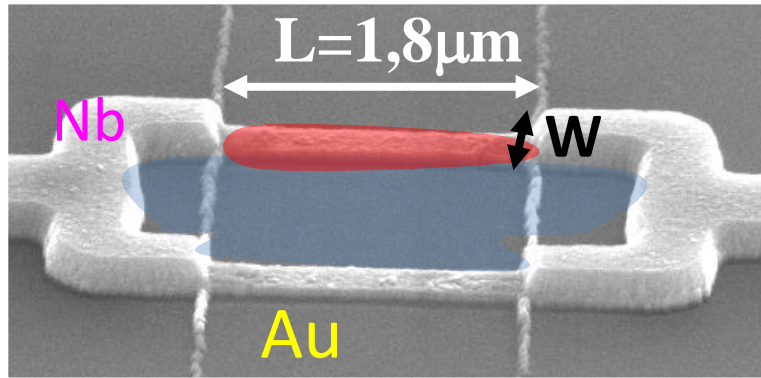
Narrow:  $L \gg W$



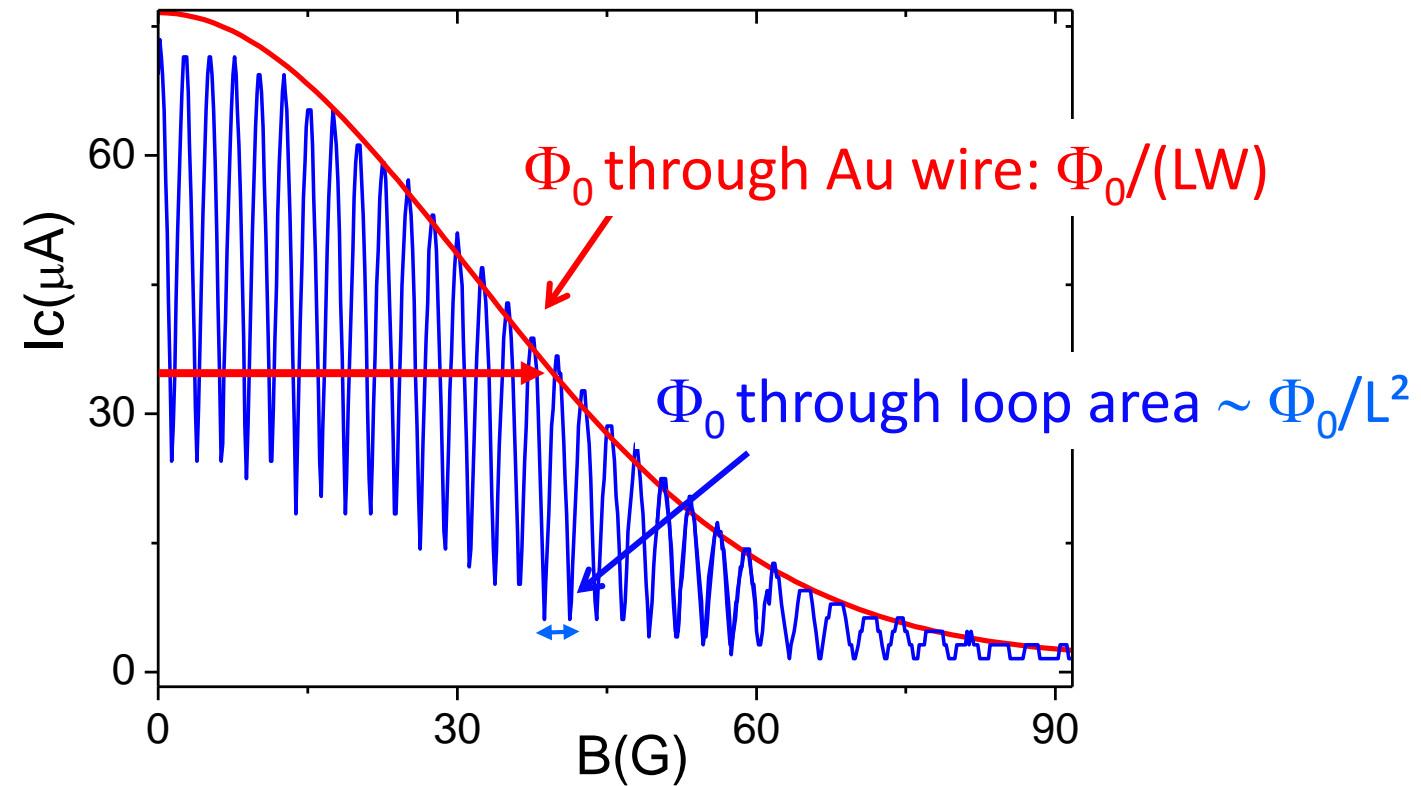
$I_c$  decays on scale of  $\Phi_0$  through sample surface (100 G)

# SNS squid junction has it all

$B \uparrow$



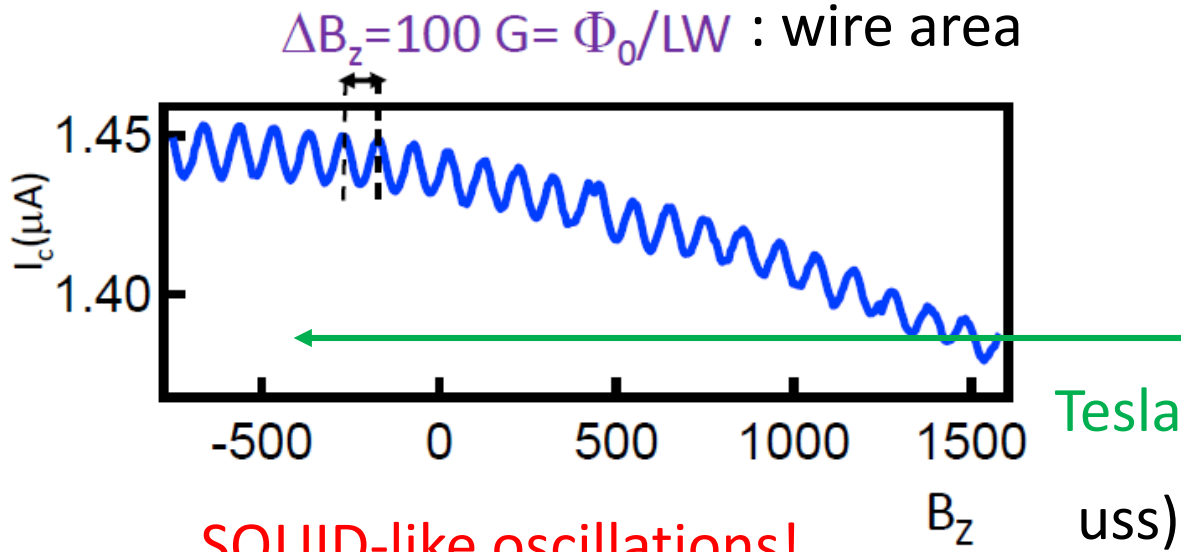
Angers 2008



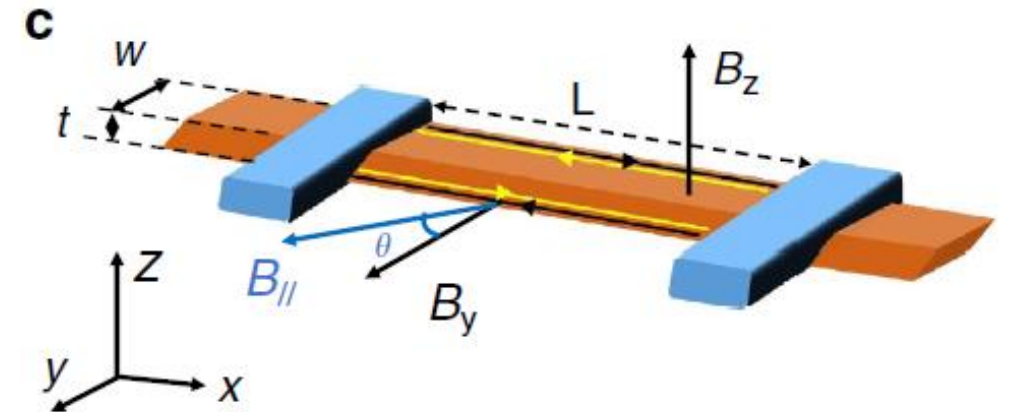
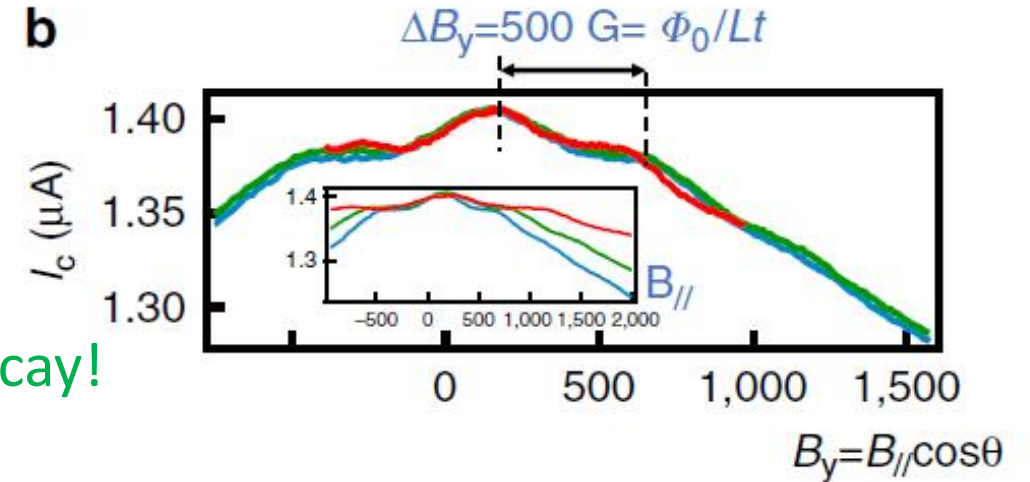
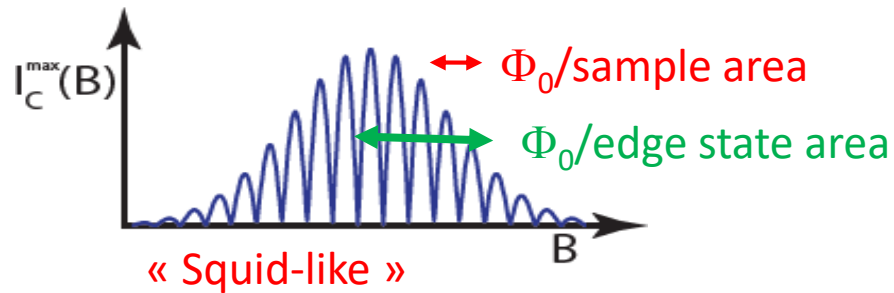
Modulation period a few G : loop area

Decay scale  $\sim 50$  G : current-carrying path area

## What about bismuth nanowires?



SQUID-like oscillations!



- Oscillations: supercurrent travels at the two acute wire edges
- High field decay scale : narrow channels (nm!)
- High critical current : well transmitted channels

# Beyond interference paths revealed by $I_c(B)$ of SNS junction

- There is a way to determine the transport regime in the N part (weak link)
- Need to reveal specific Andreev Bound States that form in weak link
- (Short) tutorial on Andreev Bound States and the supercurrent they carry
- The phase-biased configuration is essential



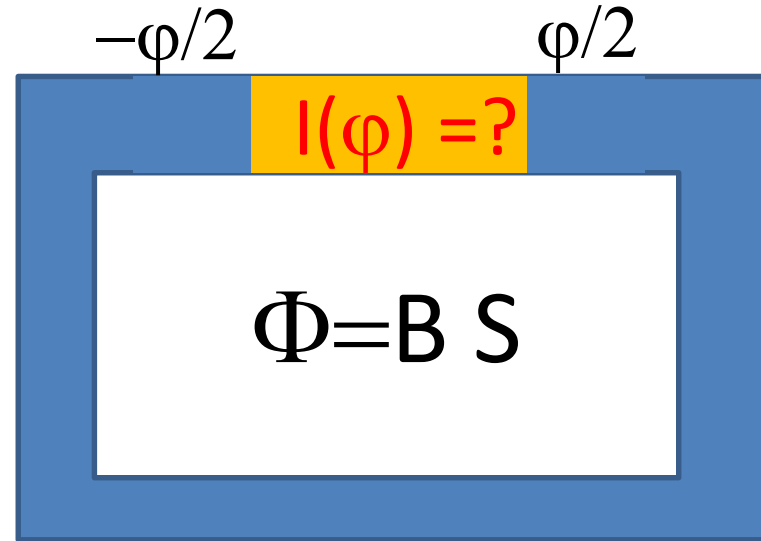
# Better than critical current: supercurrent versus phase relation

Usual two contact SNS configuration



$I_c = \max I(\varphi)$ ,  $\varphi$  not controlled

Better: Ring geometry allows «phase biasing»

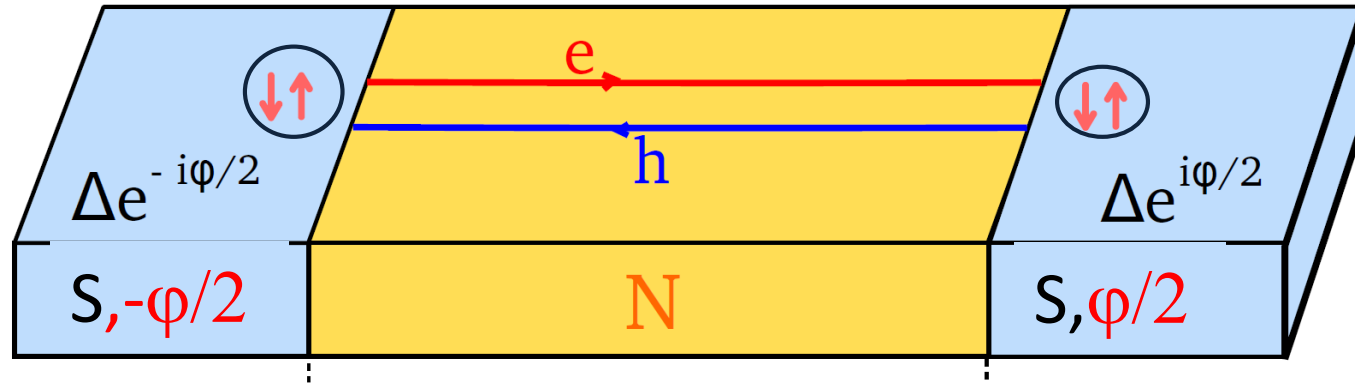


$\varphi$  controlled, proportional to applied magnetic flux

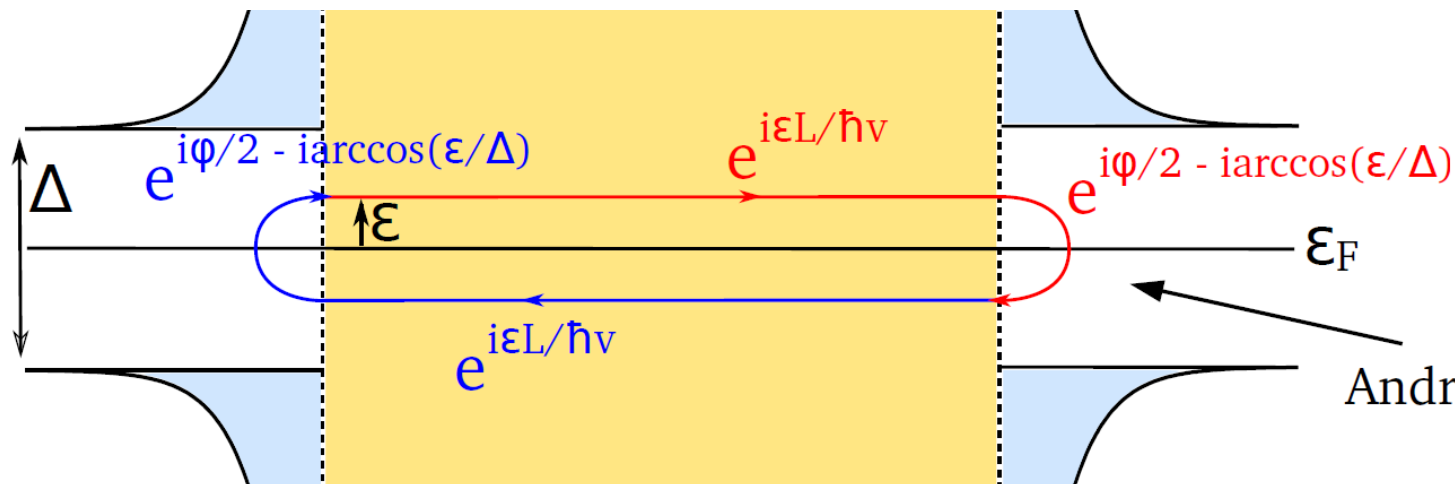
$$\varphi = -2\pi\Phi/\Phi_0$$

$I(\varphi)$  depends on the transport regime in the N (diffusive, ballistic)

# Andreev Bound States in a phase-biased SNS junction



Resonance condition on accumulated phase :  
Andreev Bound States with eigenenergies  $\varepsilon_m$ .



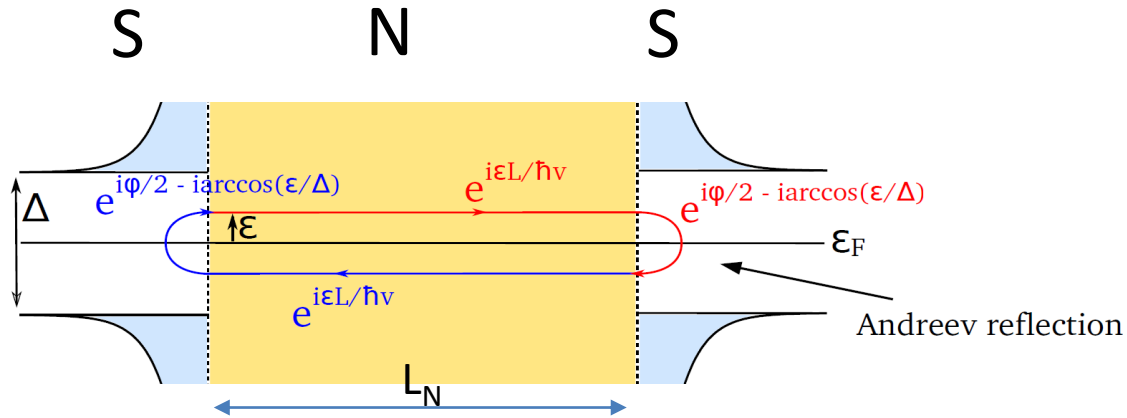
$$\frac{2\varepsilon L_N}{\hbar v_F} - 2 \arccos \frac{\varepsilon}{\Delta_0} \pm \Delta\phi = 2\pi m$$

Propagation Through N      Interface reflection      Superconducting phase difference

Andreev reflection

Andreev bound states carry the supercurrent.  
Spectrum, supercurrent, depend on N and phase

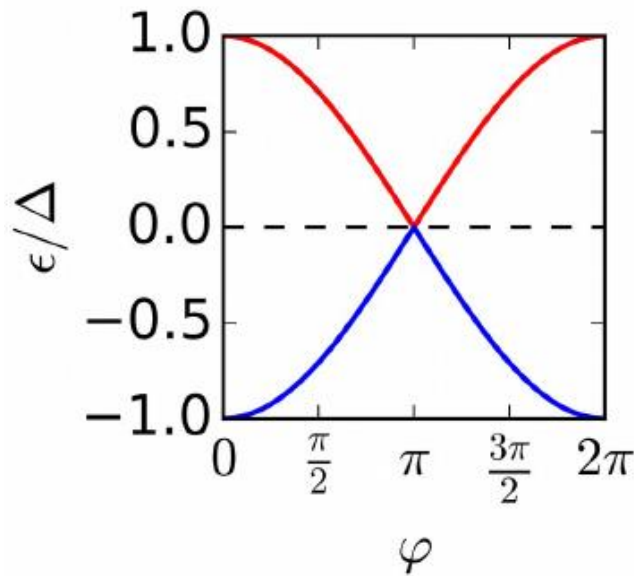
# Andreev spectrum and supercurrent in short ballistic junction



$$\cancel{\frac{2\epsilon I_N}{\hbar v_F}} - 2 \arccos \frac{\epsilon}{\Delta_0} \pm \Delta\phi = 2\pi m$$

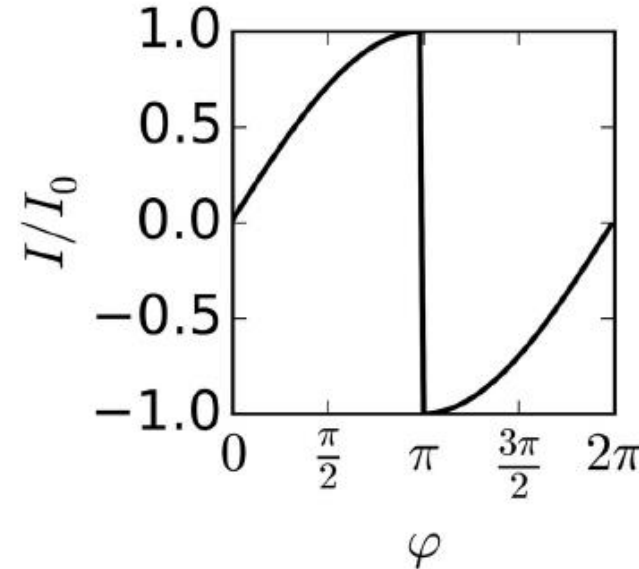
propagation

$\epsilon_n(\varphi) \sim$  branches of  $\cos(\varphi/2)$



$$I = \sum_{-\infty}^0 \frac{\partial \epsilon_n}{\partial \varphi} f(\epsilon_n)$$

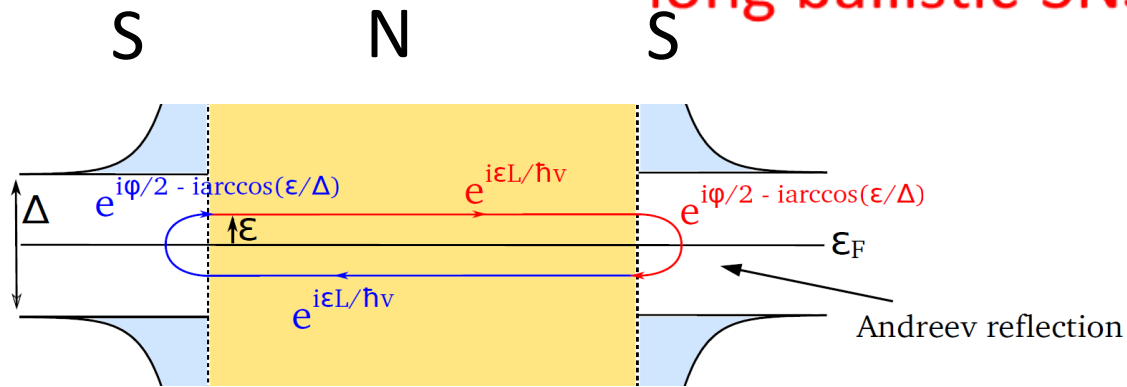
supercurrent



$I(\varphi) \sim$  branches of  $\sin(\varphi/2)$  with jump at  $\pi$

# Example: Andreev spectrum and supercurrent in

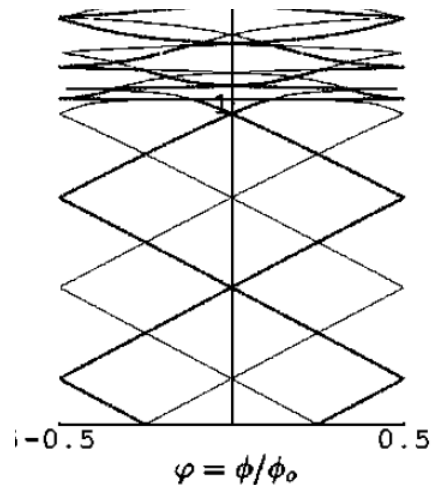
long ballistic SNS junction:  $L \gg \xi_s = \frac{\hbar v_F}{\Delta}$



propagation

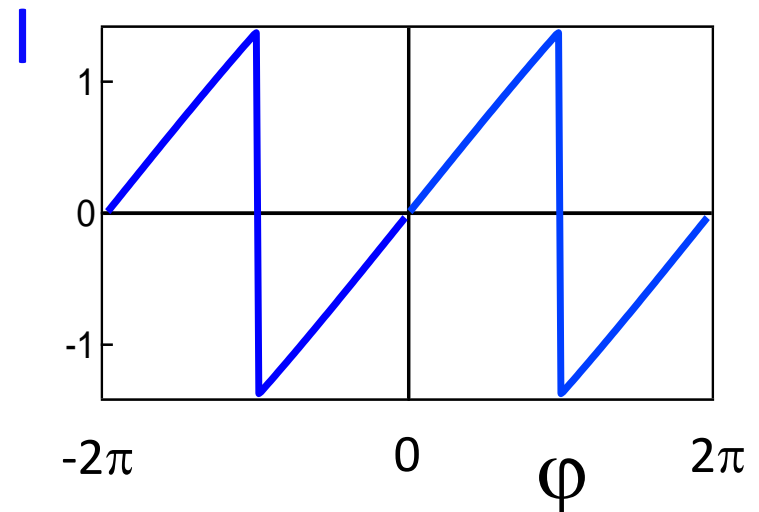
$$\frac{2\epsilon L_N}{\hbar v_F} - 2 \arccos \frac{\epsilon}{\Delta_0} \pm \Delta\phi = 2\pi m$$

$\epsilon_n(\varphi) \sim \varphi$ : linear segments



$$I = \sum_{-\infty}^{\infty} \frac{\partial \epsilon_n}{\partial \varphi} f(\epsilon_n)$$

$I(\varphi) \sim$  linear segments with jumps at  $\pi$



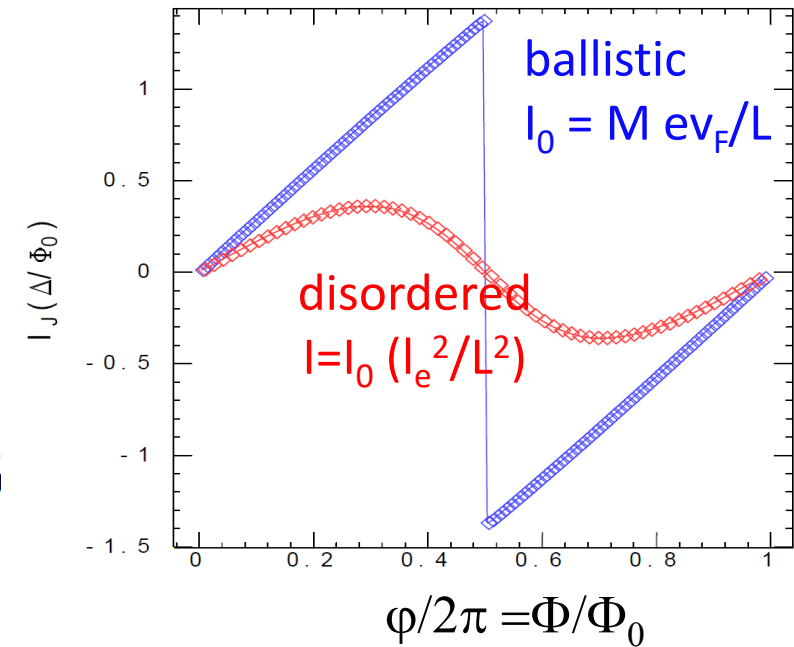
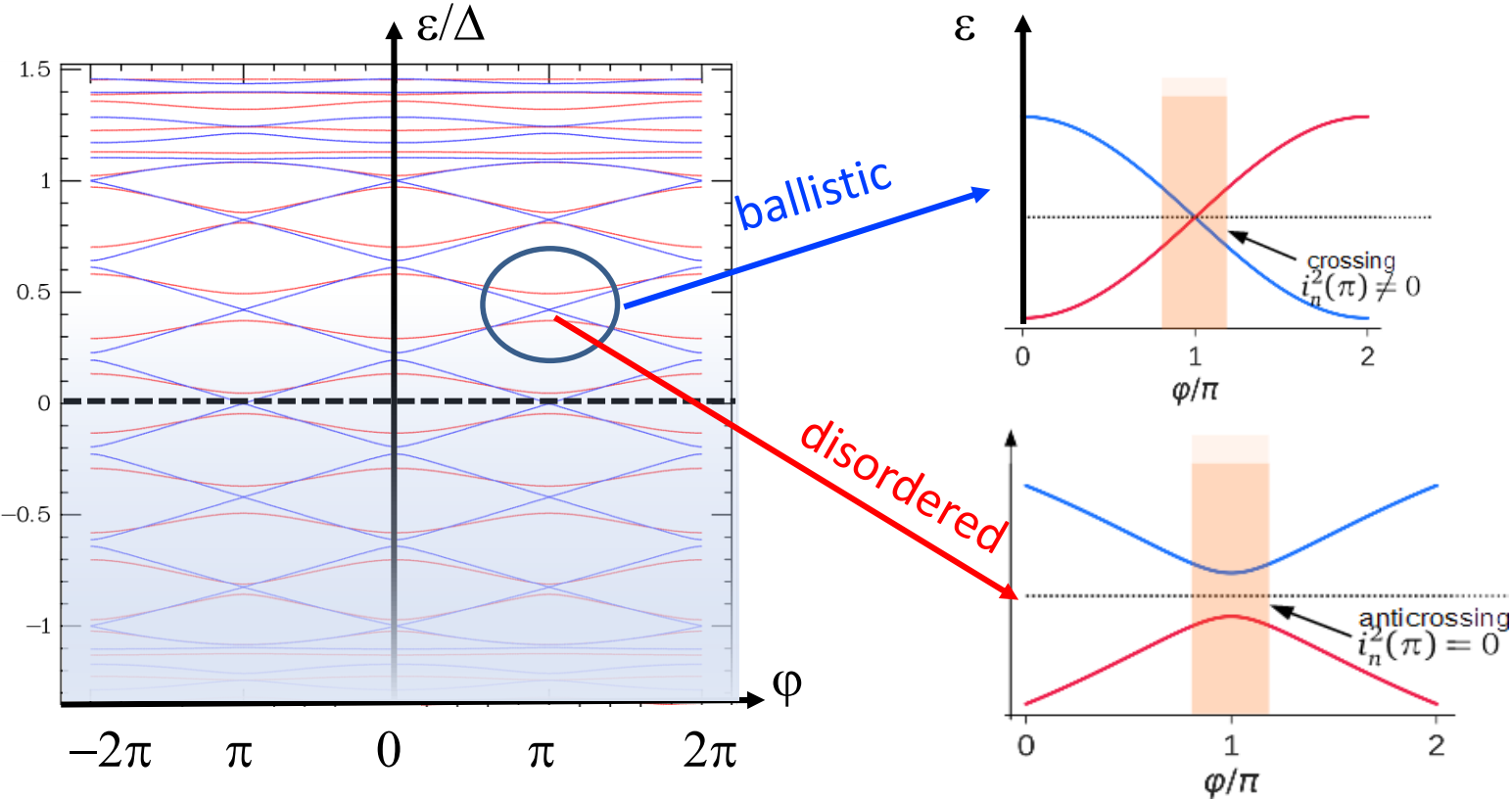
Sawtooth  $I(\varphi)$  characteristic of long ballistic



# Influence of disorder on Andreev spectrum and supercurrent

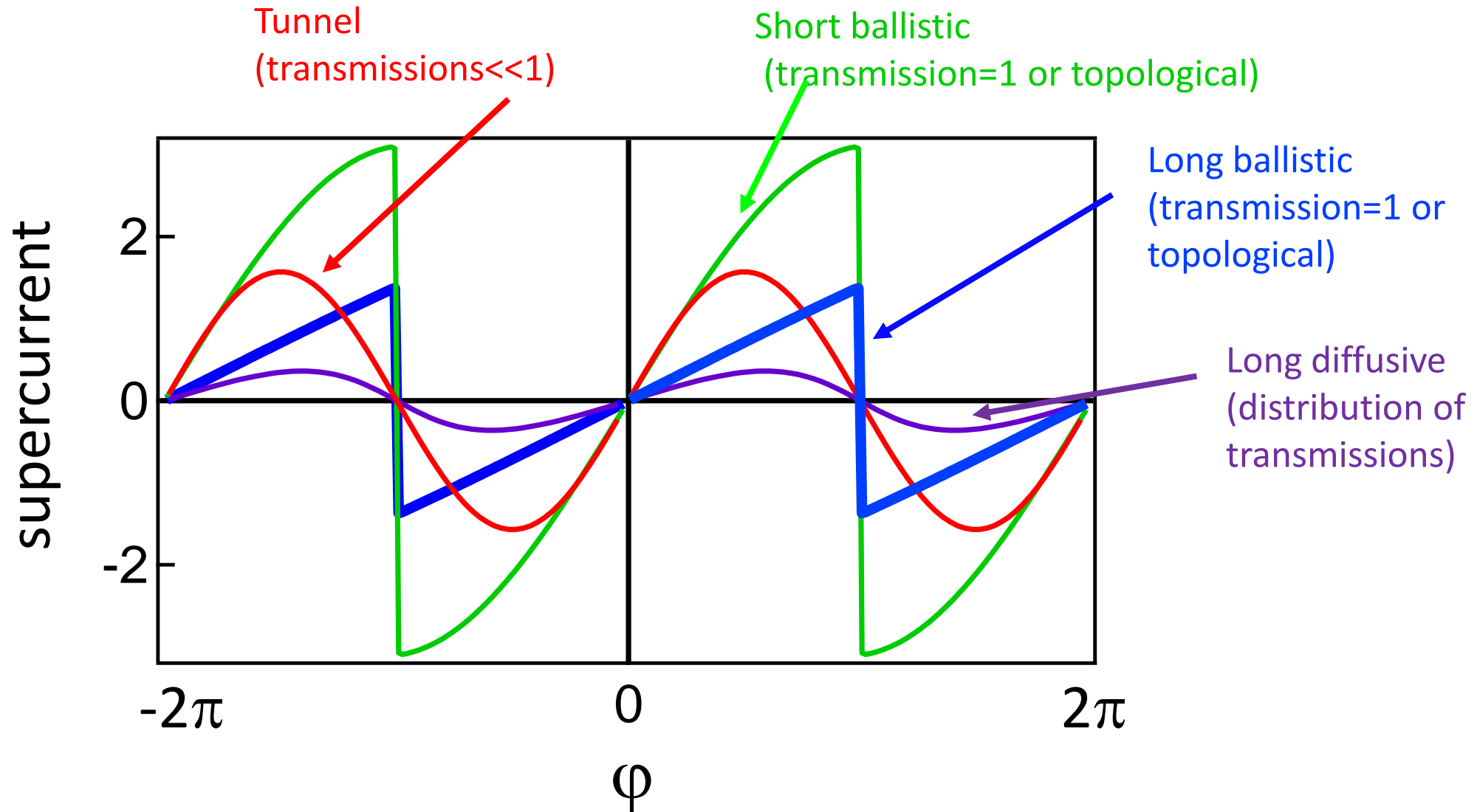
Dc supercurrent versus phase

$$I = \sum_{-\infty}^{\infty} \frac{\partial \epsilon_n}{\partial \varphi} f(\epsilon_n)$$



Disorder lifts Andreev level degeneracy at  $\pi$  and rounds  $I(\varphi)$

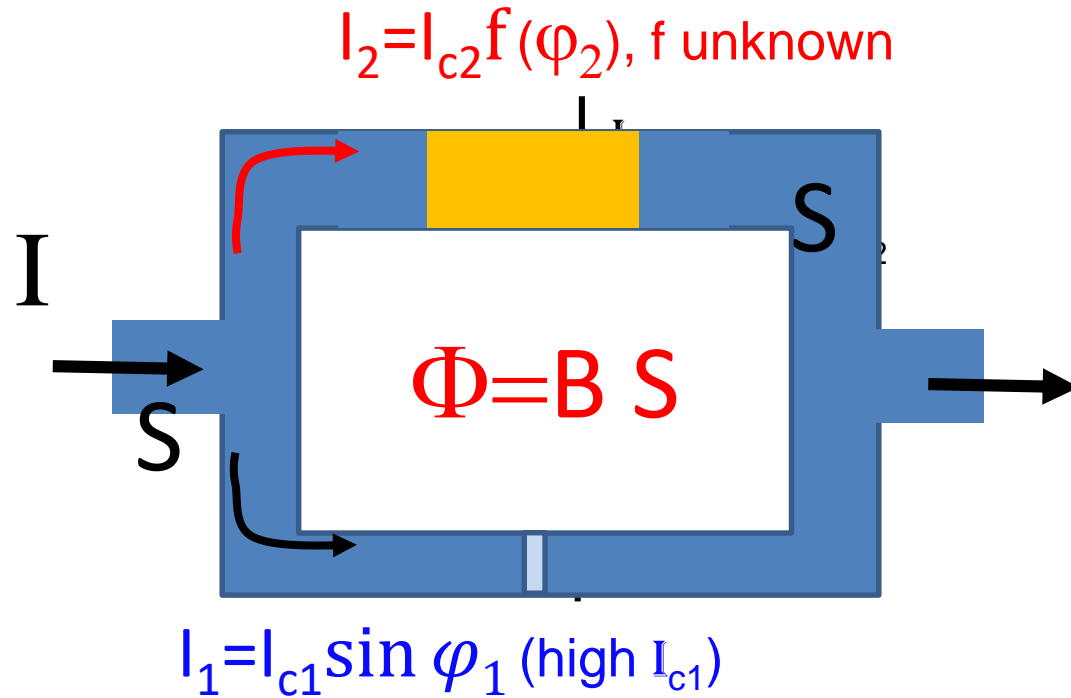
# Supercurrent vs phase: expectations



# Current-phase measurement with an asymmetric SQUID

## Need ring geometry and second junction

Della Rocca et al 2007



$$I = I_{c1} \sin \varphi_1 + I_{c2} f(\varphi_2)$$

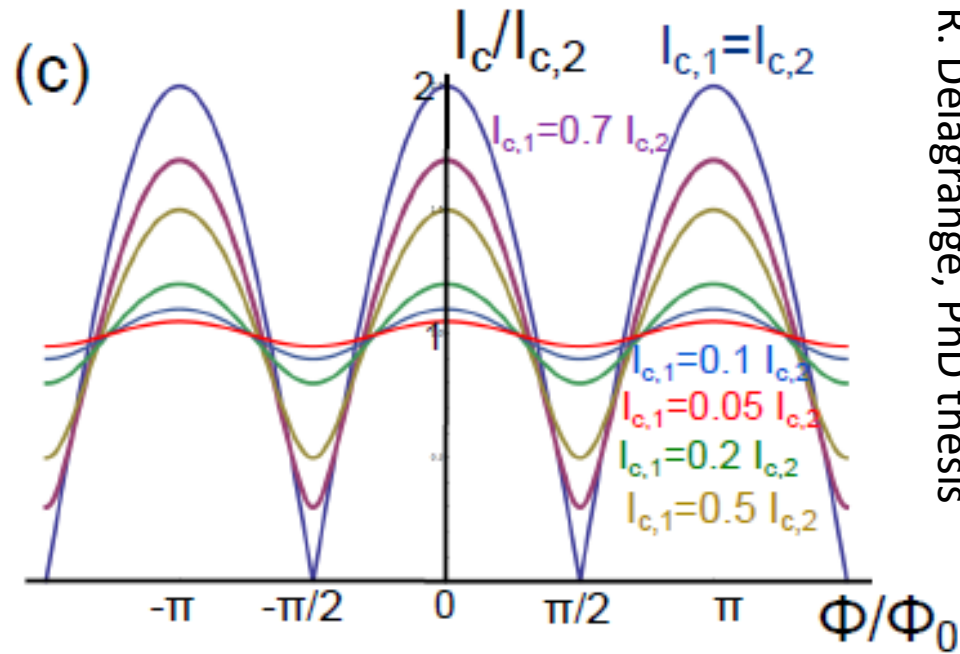
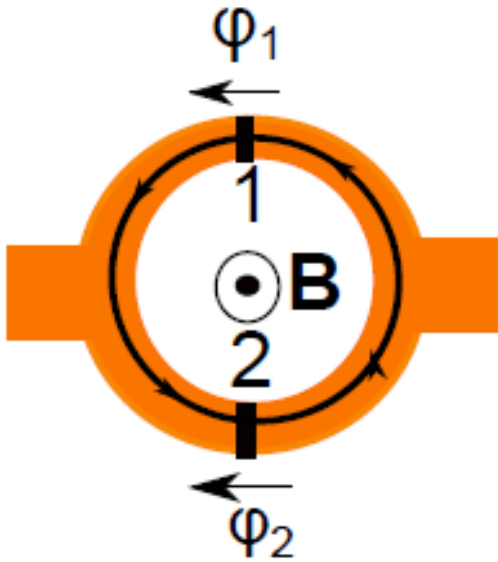
$$\varphi_1 - \varphi_2 = -2\pi\Phi/\Phi_0$$

$I_c$  achieved for  $\varphi_1 \approx \pi/2$

$$I_c \sim I_{c1} + I_{c2} f\left(\frac{\pi}{2} + 2\pi \frac{\Phi}{\Phi_0}\right) \quad \text{to first order in } I_{c2}/I_{c1}$$

Critical current  $I_c$  of asymmetric SQUID yields current-phase relation  $I_{c2} f(\varphi_2)$  of junction with smallest critical current

## Critical current of a SQUID: from symmetric to asymmetric



R. Delagrangé, PhD thesis

$$I_c^2 = (I_1 - I_2)^2 + 4I_1I_2 \cos^2\left(\pi \frac{\Phi}{\Phi_0}\right)$$

Asymmetric:  $I_2 \ll I_1$

$$I_c = I_2 + I_1 \sin\left(2\pi \frac{\Phi}{\Phi_0} + \pi/2\right)$$

Current-phase relation of junction with smallest critical current (on top of the critical current of largest junction)

Handwritten derivation of the critical current for an asymmetric SQUID:

Top part (symmetric case):

$$J = \delta\left(\frac{\omega}{2}\right) + \delta\left(-\frac{\omega}{2}\right)$$

$$I_c \propto \left| \int_{-\omega/2}^{\omega/2} e^{iBxL} \left( \delta\left(\frac{\omega}{2}\right) + \delta\left(-\frac{\omega}{2}\right) \right) dx \right|$$

$$= \left| e^{iB\omega L/2} + e^{-iB\omega L/2} \right|$$

$$= 2 \left| \cos \frac{B\omega L}{2} \right|$$

Bottom part (asymmetric case):

$$J = \delta\left(\frac{\omega}{2}\right) + \alpha \delta\left(-\frac{\omega}{2}\right)$$

$$I_c = \left| e^{iB\omega L/2} + \alpha e^{-iB\omega L/2} \right|$$

$$= \left\{ (e^{iB} + \alpha e^{-iB})(e^{-iB} + \alpha e^{iB}) \right\}^{1/2}$$

$$= \left\{ 1 + \alpha^2 + 2\alpha \cos \frac{B\omega L}{2} \right\}^{1/2}$$

For small  $\alpha$ :

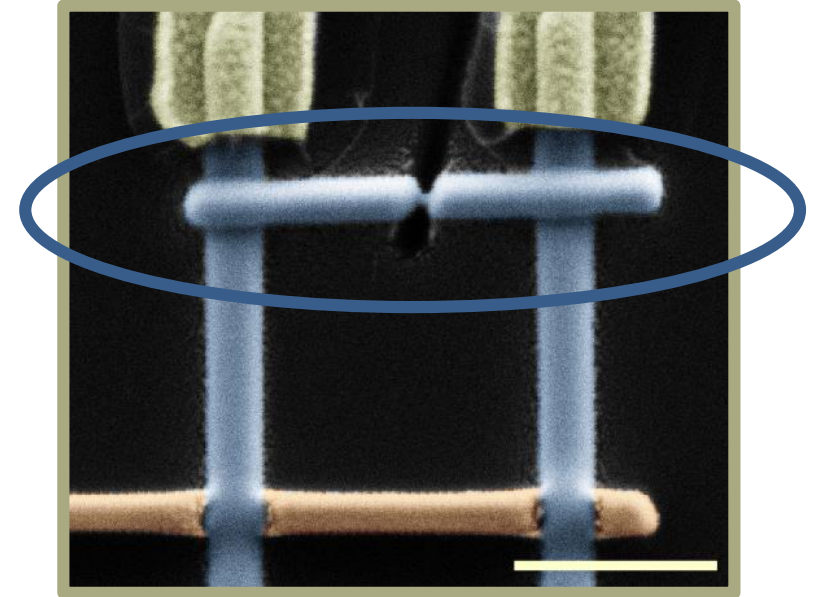
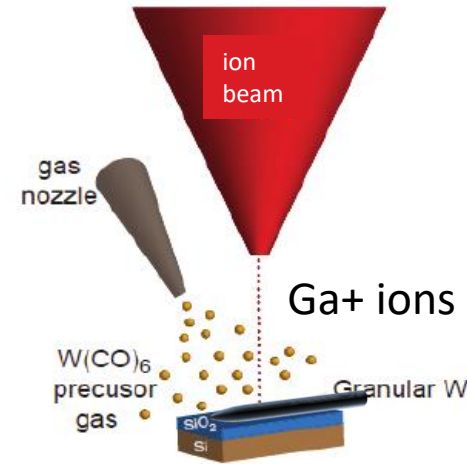
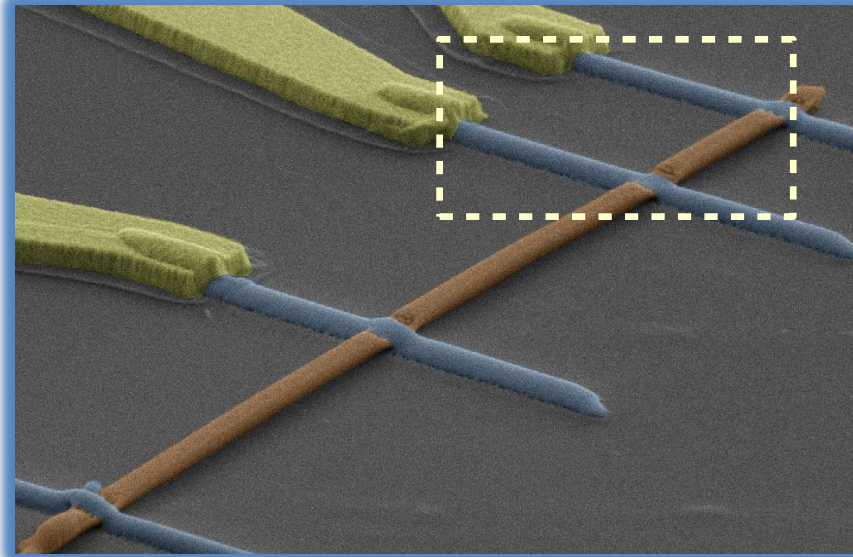
$$I_c \approx \left| 1 + \alpha \cos \frac{B\omega L}{2} \right|$$

asymmetric SQUID



# Measurement of current-phase relation to test channels that carry the supercurrent (on very same sample)

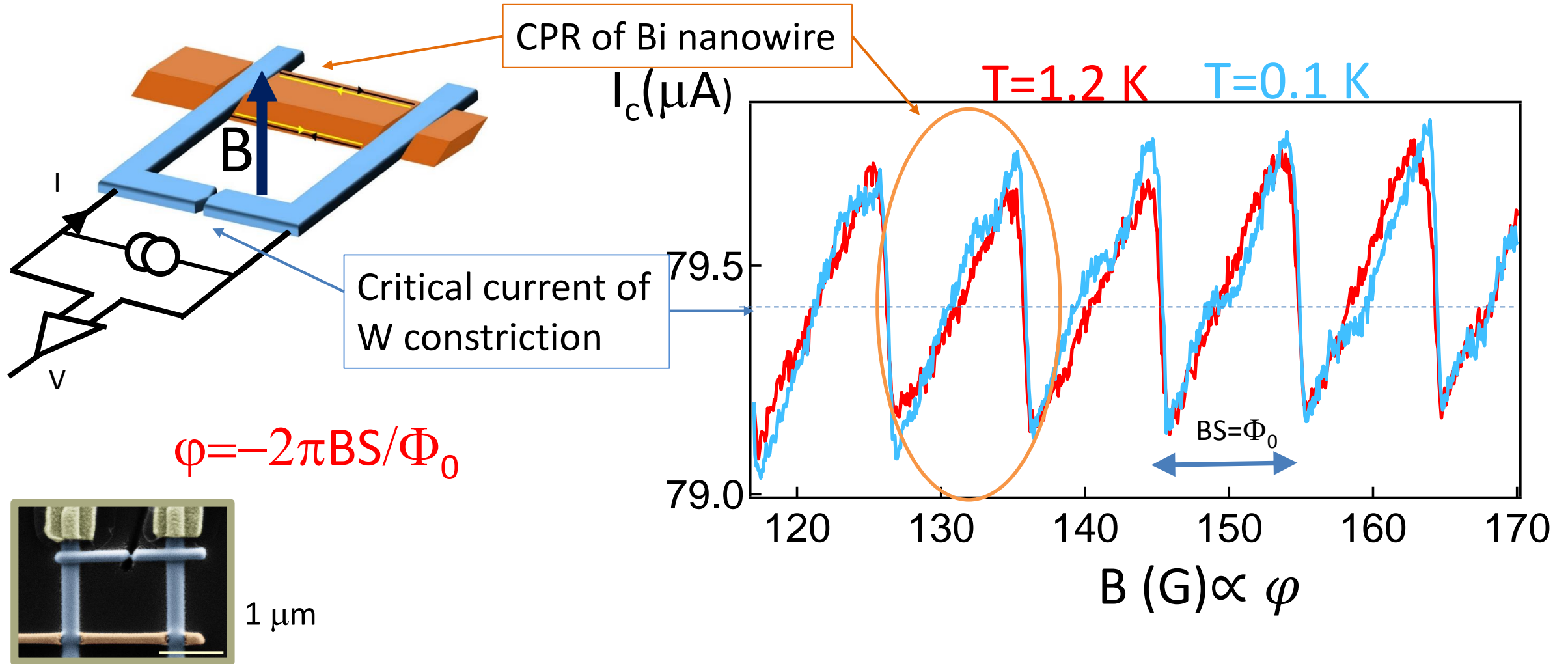
Add superconducting constriction in parallel



1  $\mu\text{m}$

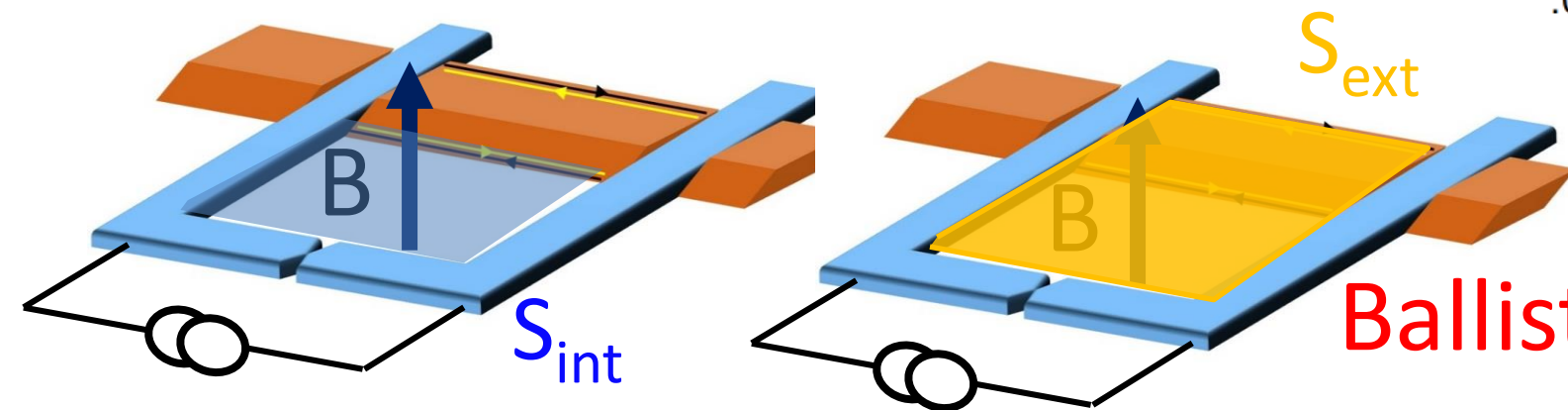
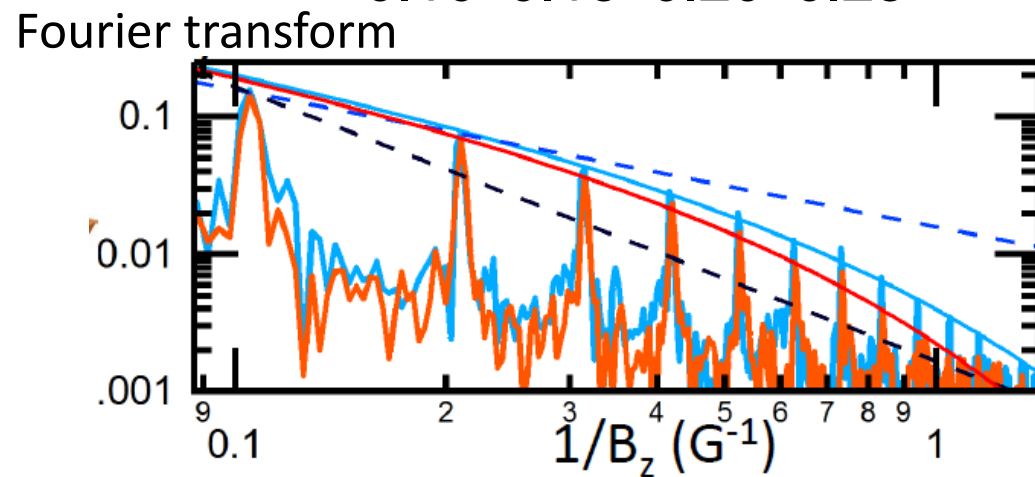
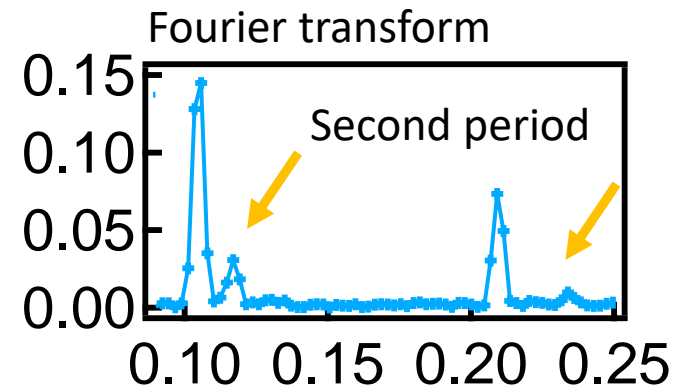
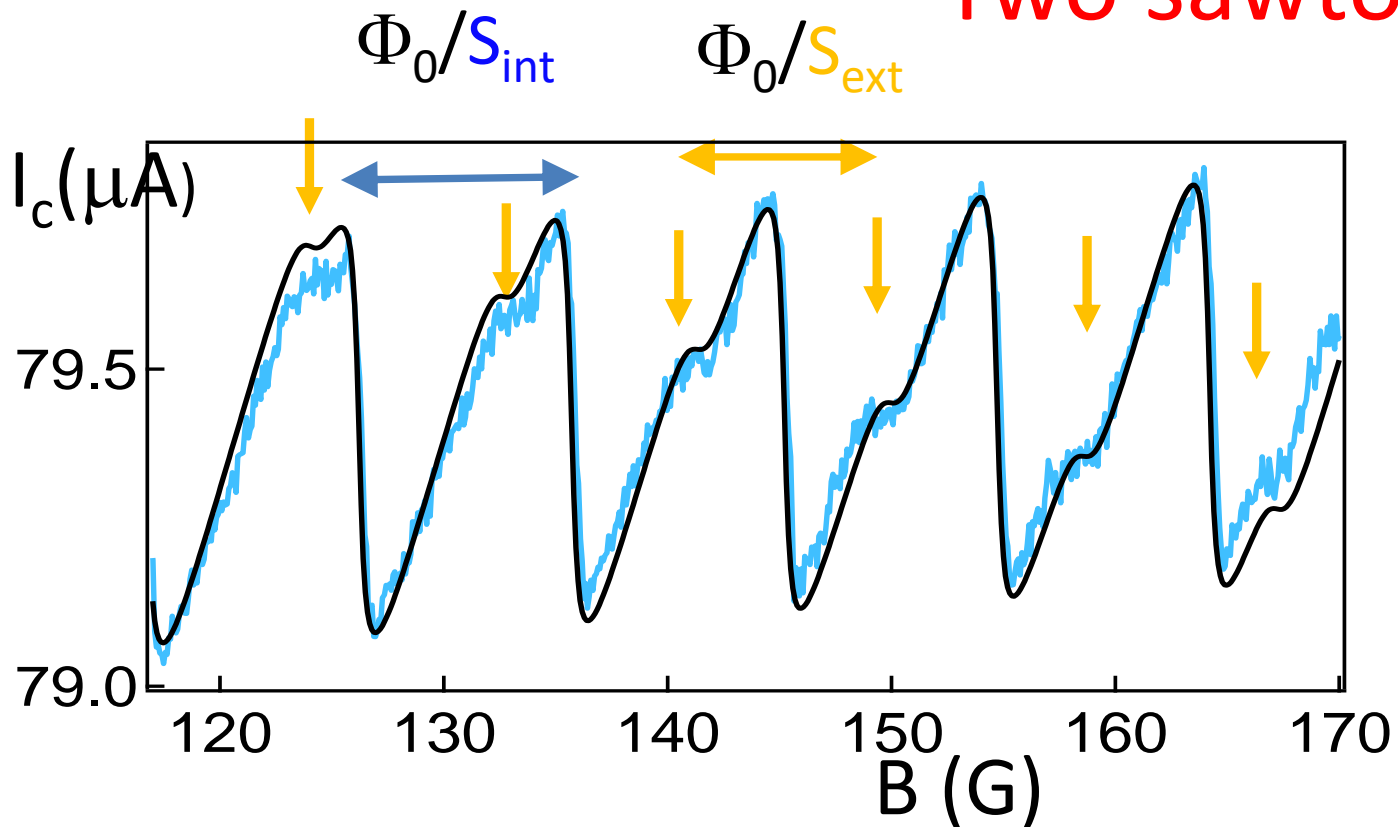
Build an asymmetric SQUID to measure the  $I(\varphi)$  relation

# Supercurrent-versus Phase relations of S/Bi/S: switching current as a function of magnetic flux



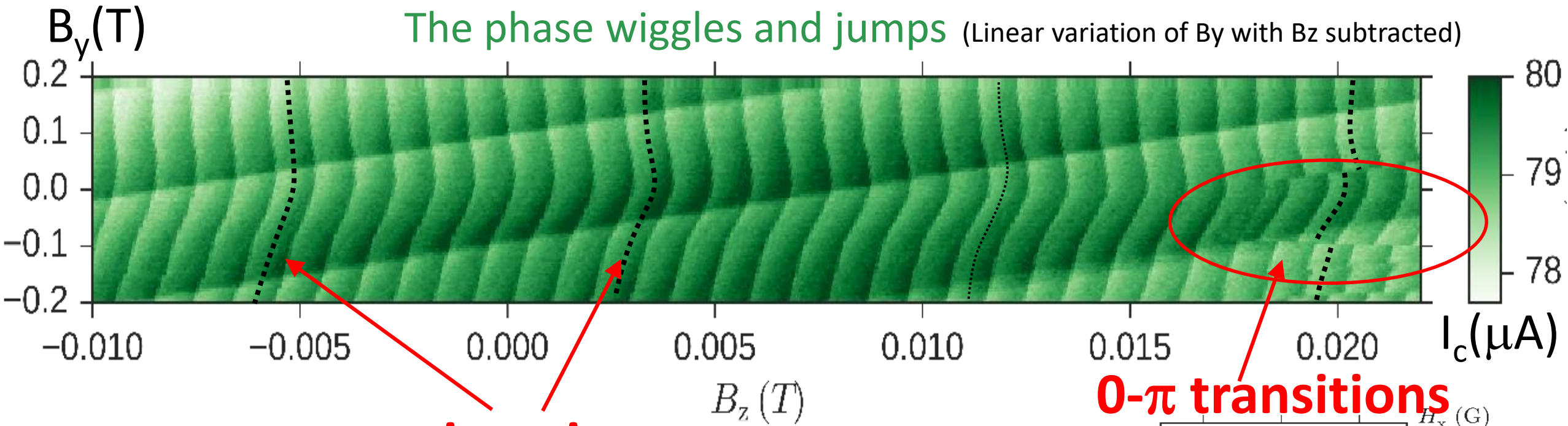
Sawtooth-shaped current phase relation: long ballistic!

# Two sawtooths?

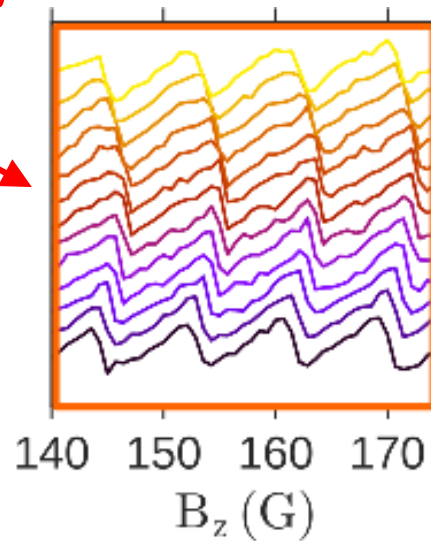
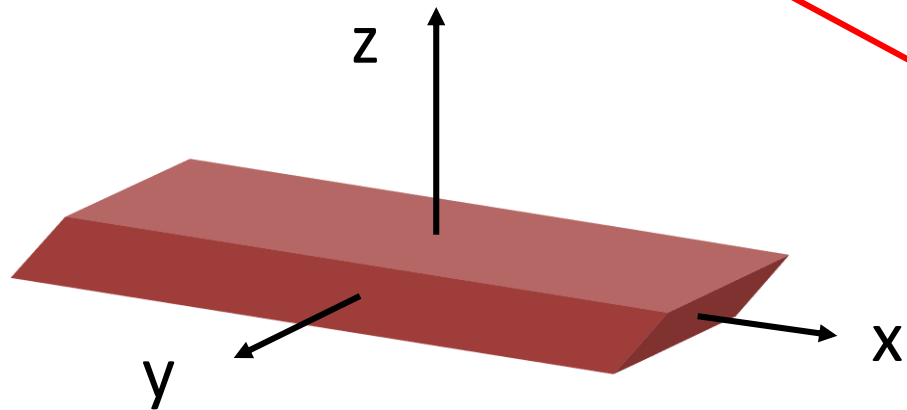


Ballistic states at two edges

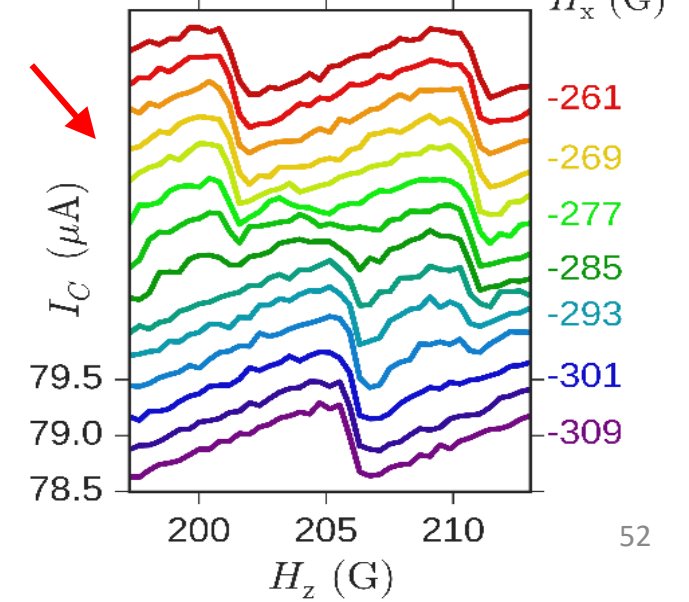
# In plane magnetic field affects the phase of the $I(\varphi)$



$\phi_0$  junctions

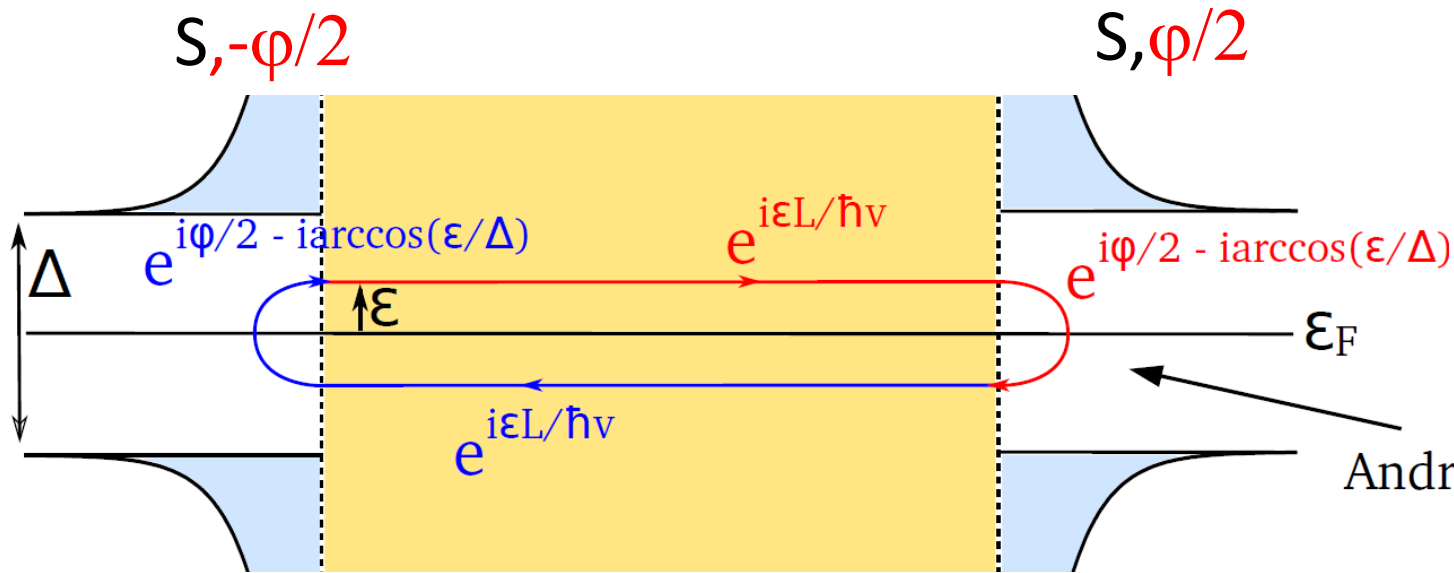


**0- $\pi$  transitions**





# Effect of magnetic field on Andreev states

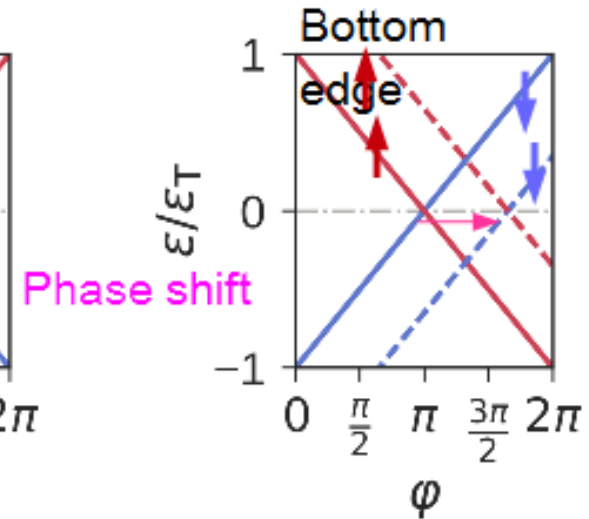
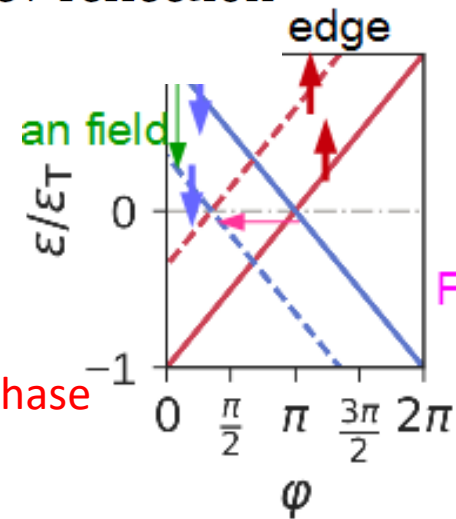


Resonance condition on accumulated phase :  
Andreev Bound States

Andreev reflection

$$\frac{\pm g\mu_B BL}{\hbar v_F} + \frac{2\epsilon L_N}{\hbar v_F} - 2 \arccos \frac{\epsilon}{\Delta_0} \pm \Delta\phi = 2\pi m$$

Zeeman effect      propagation      Interface reflection      Superconducting phase difference

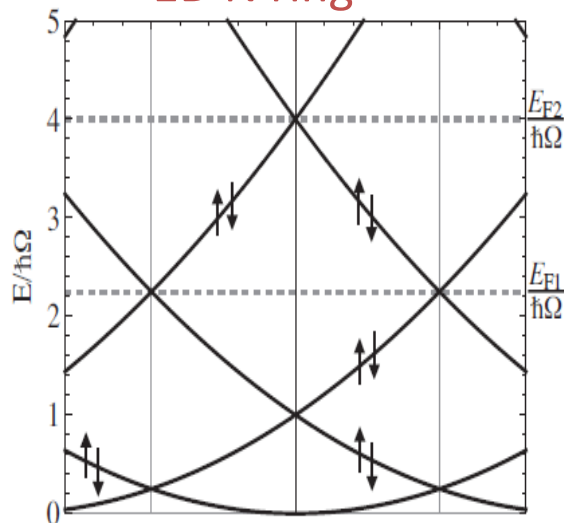


Andreev spectrum splits with field,  
and shifts if spin-orbit scattering, because spin-dependent  $v_F$



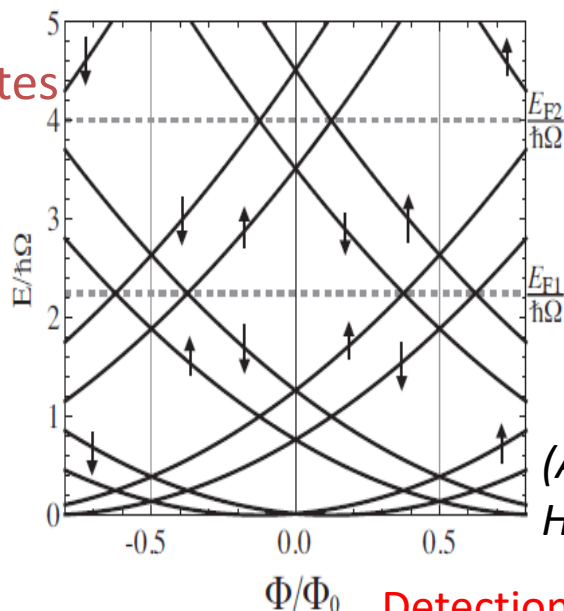
# Flux dependent spectrum of a ring in the presence of spin orbit

1D N ring



Phase shifted  
Spin  $\uparrow$  and  $\downarrow$  states

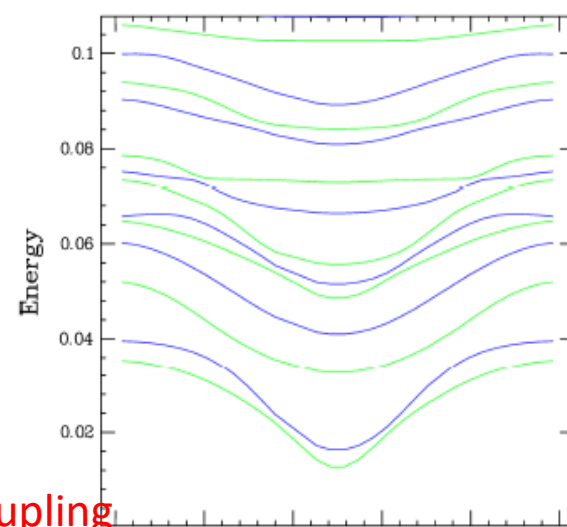
$$\delta\phi = \pm k_{so}L$$



Multichannel

NS ring Andreev states invariant by TRS

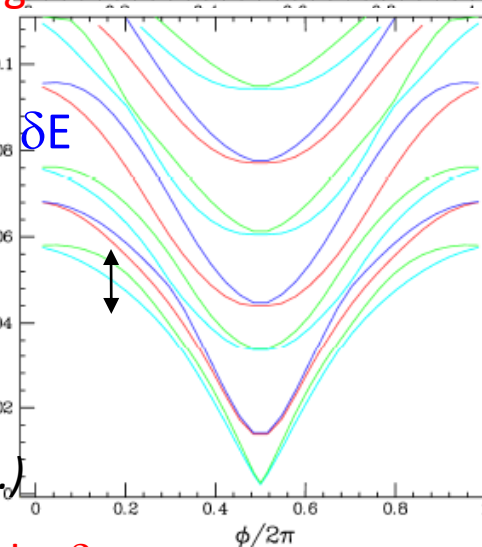
No SO coupling



With Rashba SO coupling

$\lambda = E_{SO}/E_F = 0.3$   
decreased effective  
disorder

spin split AS at  $\phi \neq 0, \pi$   
TRS breaking  $\delta E = \lambda \Delta^2 \tau_D$



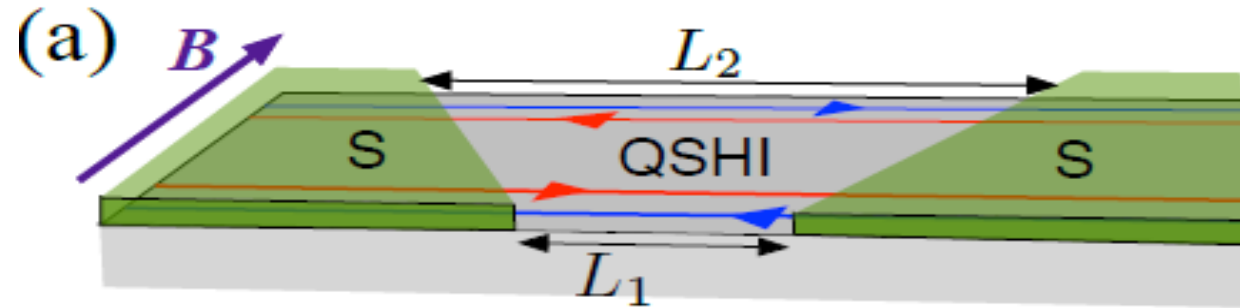
(A. Murani, A. Chepelianskii  
H.B. Simulations of BdG equ.)

Detection of level crossings at 0 and  $\pi$  ?

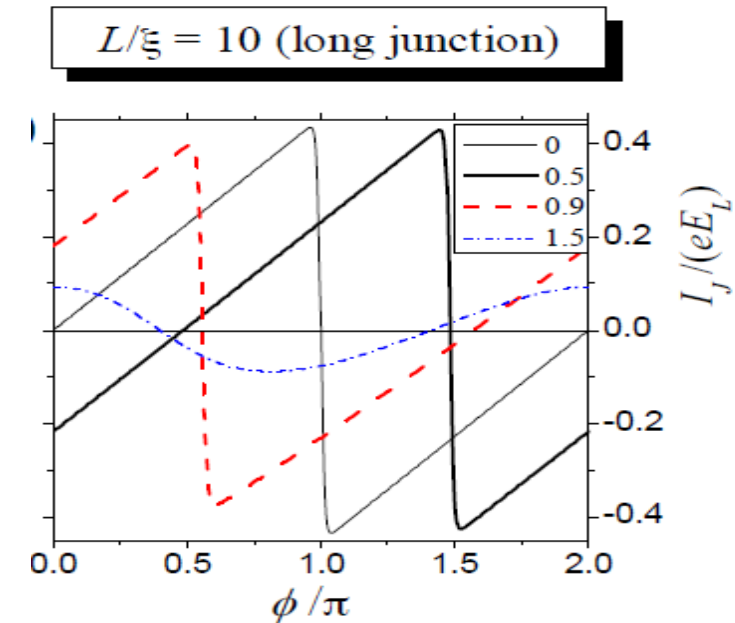
# Topological Josephson $\phi_0$ junction expected in field

Dolcini, Houzet,  
Meyer 2016

...If 2 edges with different lengths



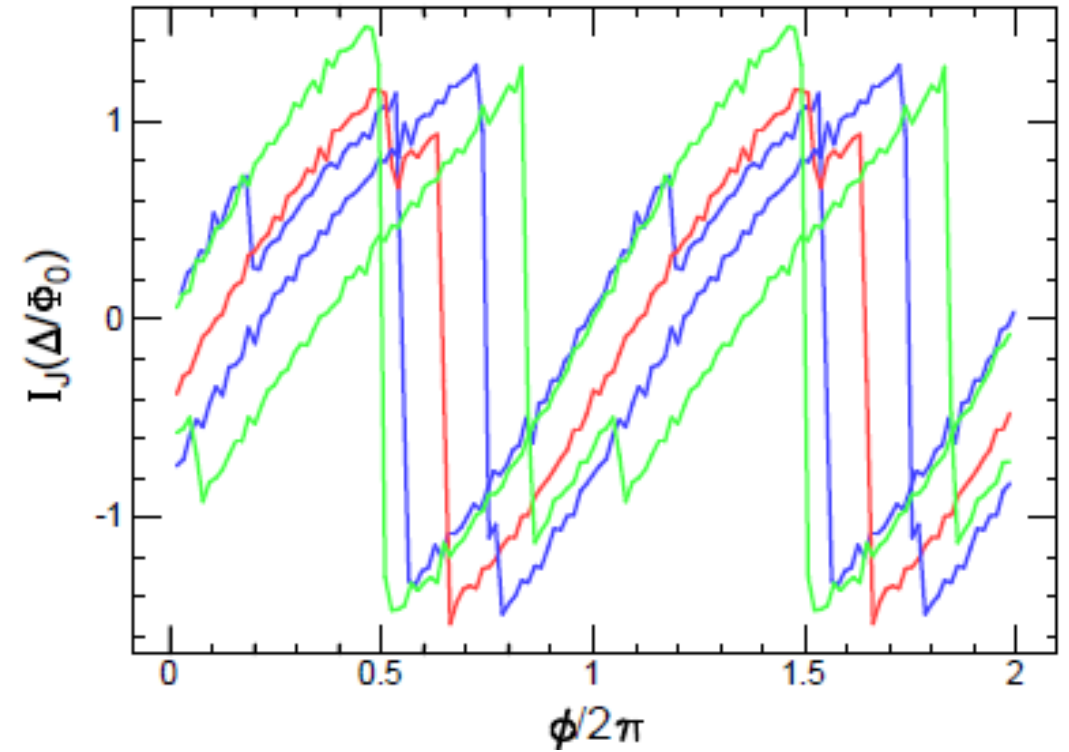
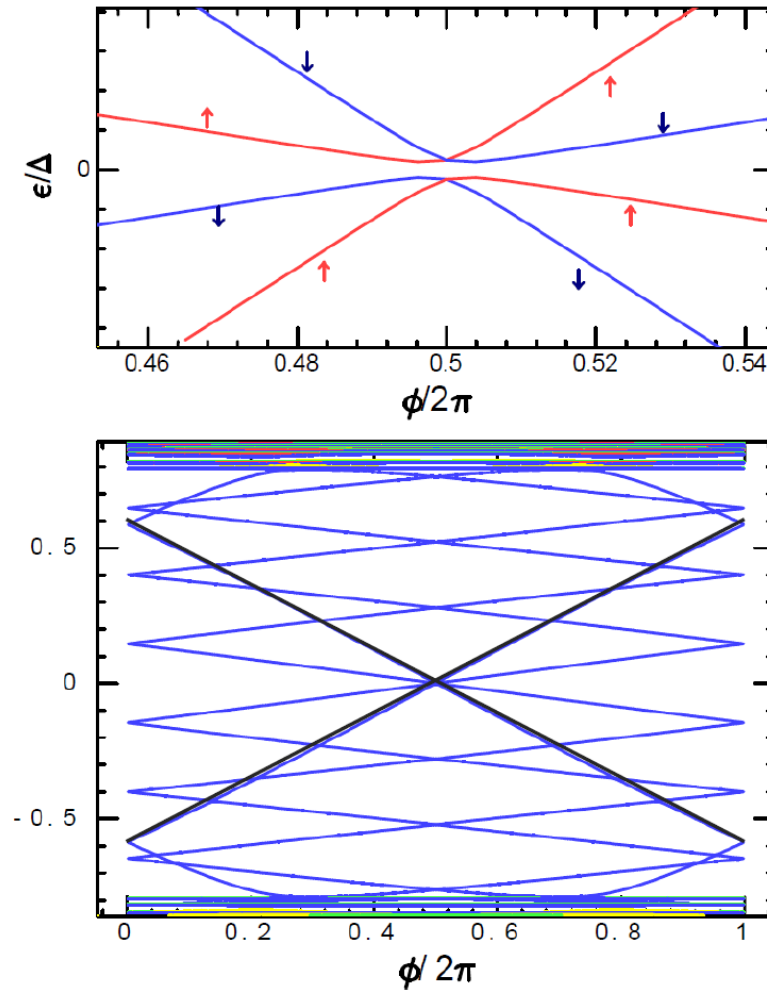
$$2 \arccos \left( \frac{E_n + h}{\Delta_0} \right) - \frac{2(E_n + h)}{E_L} = \phi + 2\pi n$$



# Topological Josephson $\varphi_0$ junction expected in field

...If 2 channels with different transmission

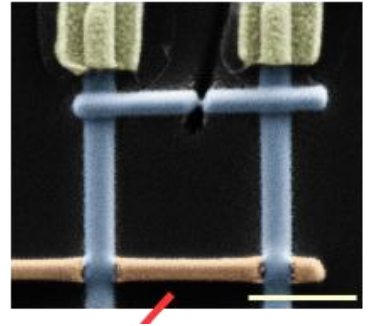
Murani,  
Chepelianskii,  
Bouchiat  
2017



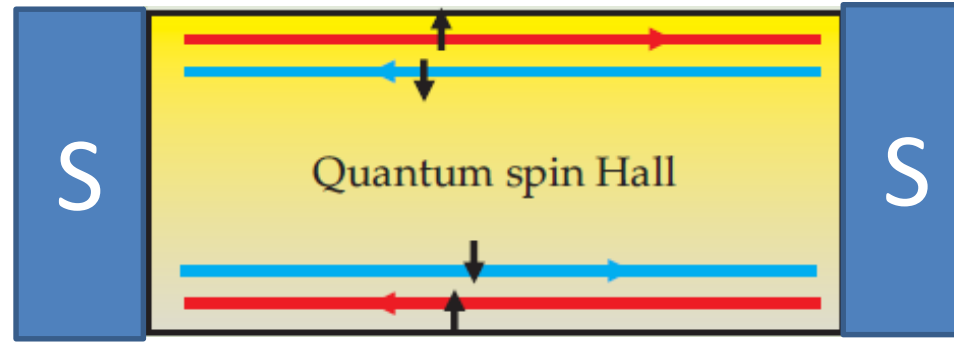
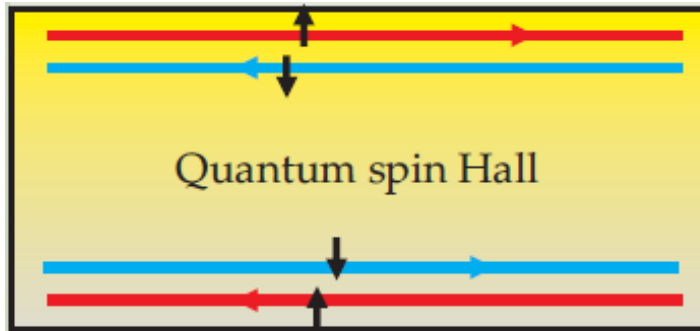
ac probing of the Andreev spectrum of a Quantum Spin Hall state:

- ac Josephson effect
- $2\pi$  and  $4\pi$
- Several ways to probe the dynamic response of a system

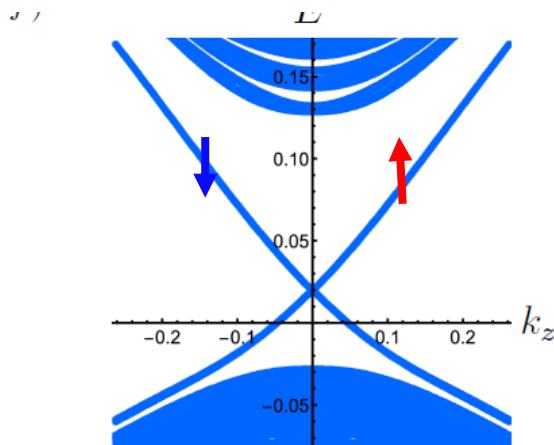
Susceptibility  $\chi = dI/d\phi$  probes topological protection and dynamics



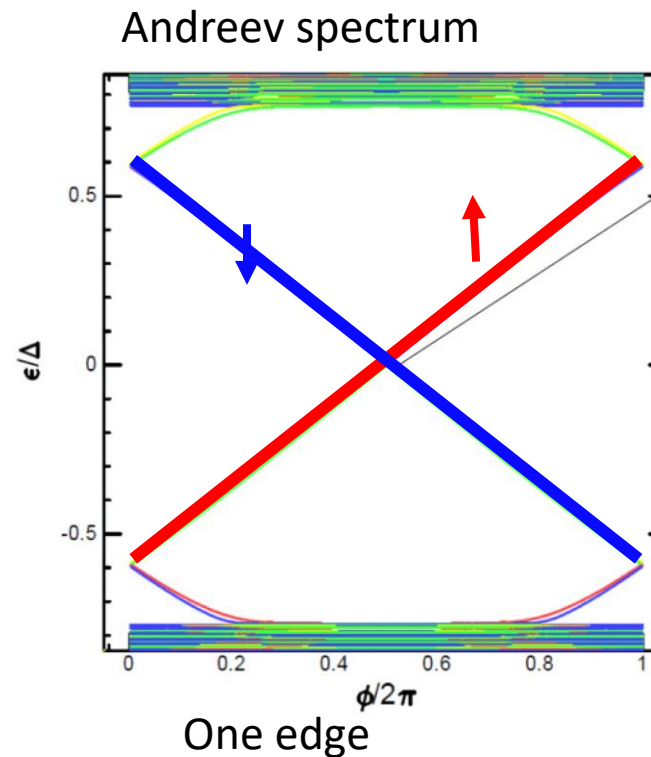
# Specificities of the S/Quantum Spin Hall/S junction



QSH, helical = « half » ballistic 1D



One edge

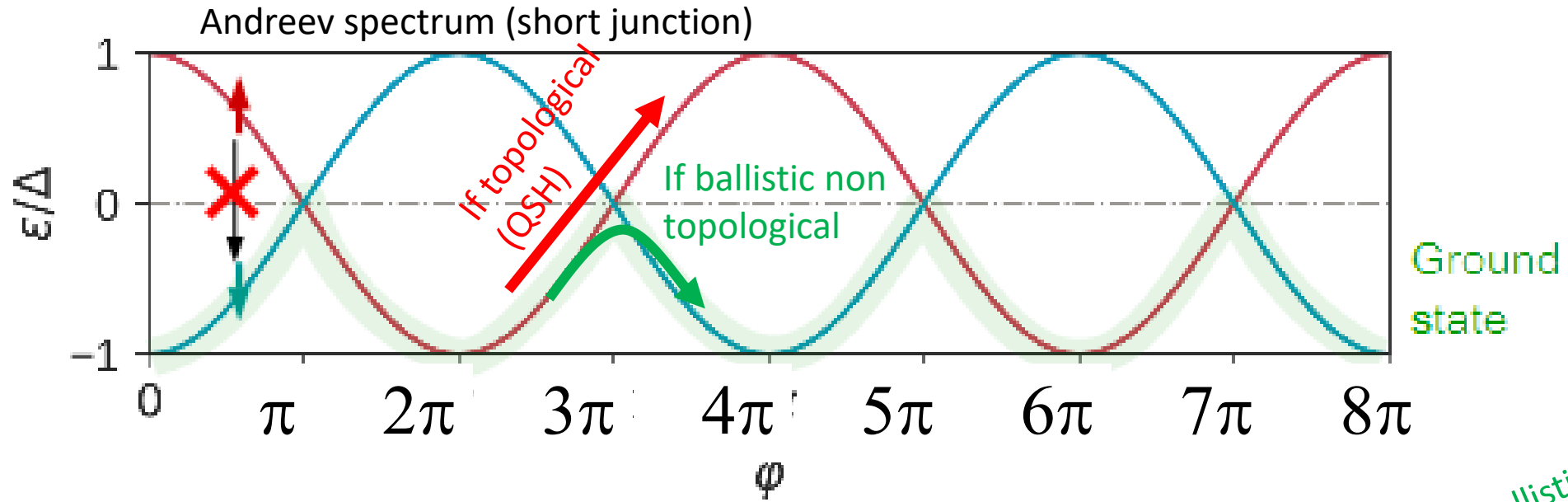


One edge

- Andreev spectrum is « half » of S/1D ballistic/S Andreev spectrum on one edge
- If parity is conserved, no way to backscatter: perfect level crossing at  $\pi$ :  $\approx$  no disorder
- $4\pi$  periodicity



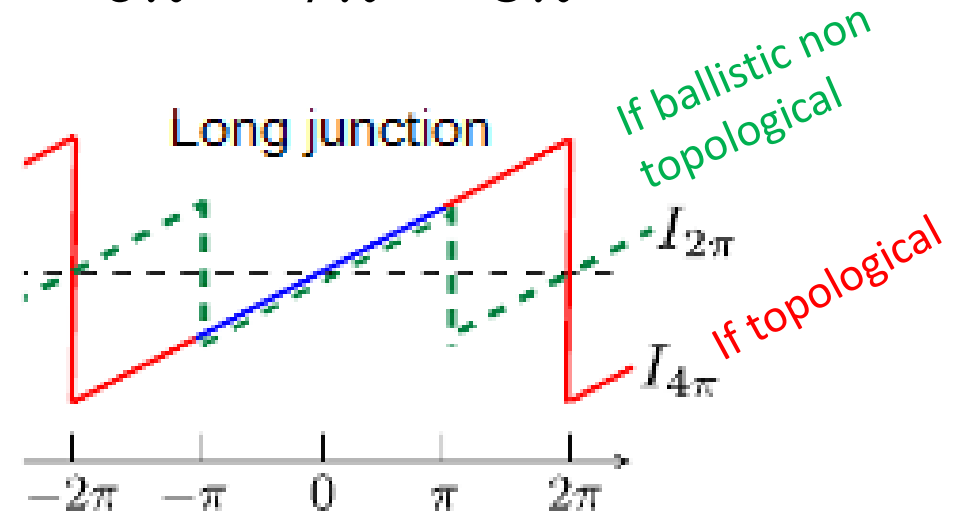
# Consequence of helicity on current phase relation?



Fu Kane 2009

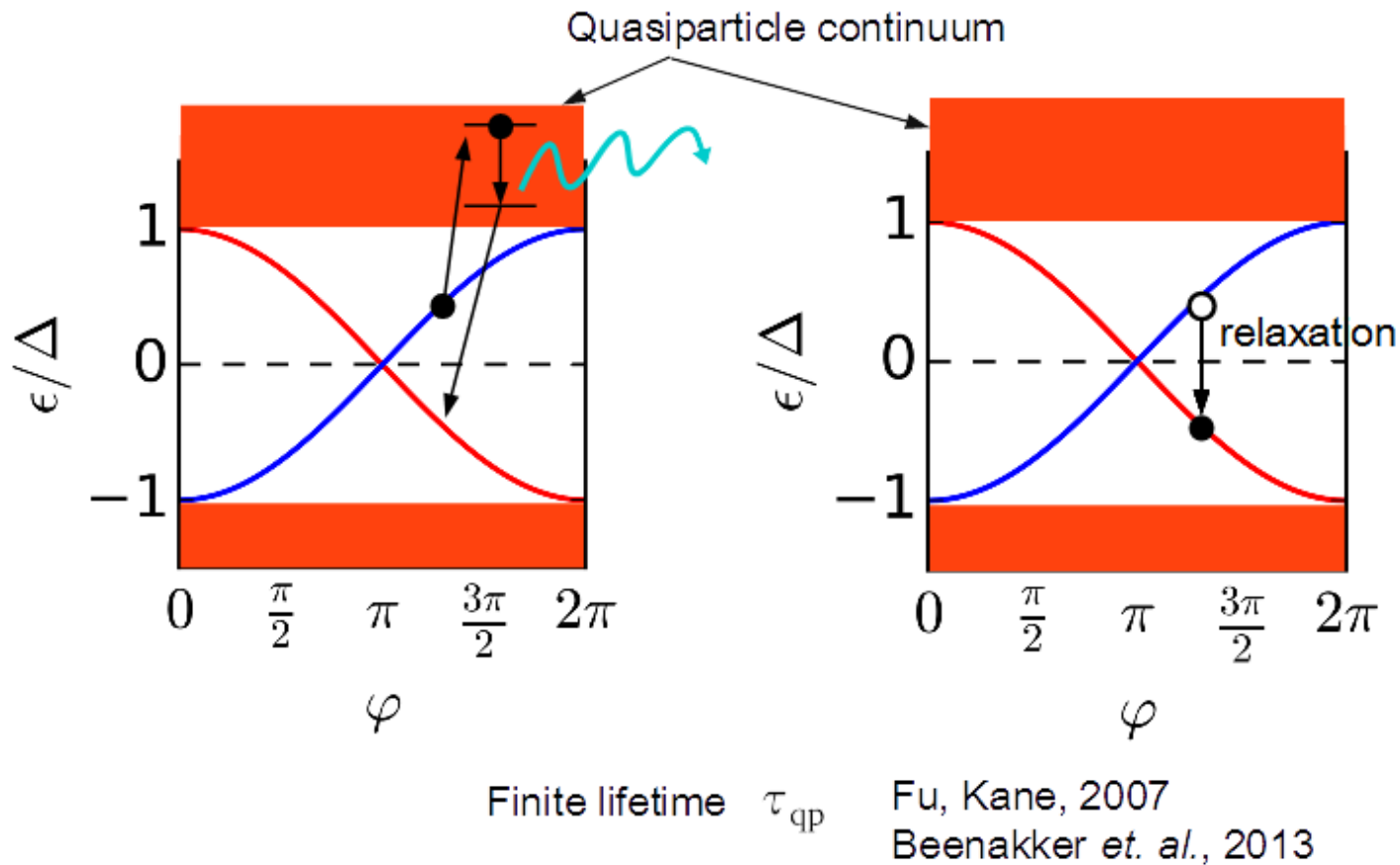
Beenakker 2013, Trauzettel 2014

$$I = \sum_{-\infty}^0 \frac{\partial \epsilon_n}{\partial \varphi} f(\epsilon_n)$$



Supercurrent through QSH edge should be  $4\pi$  periodic, whereas  $2\pi$  periodicity if ballistic non topological.

But poisoning can return periodicity to  $2\pi$

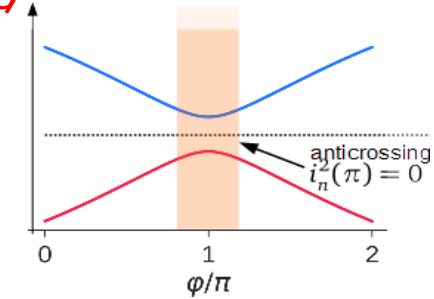
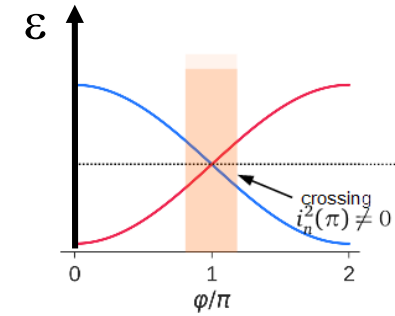
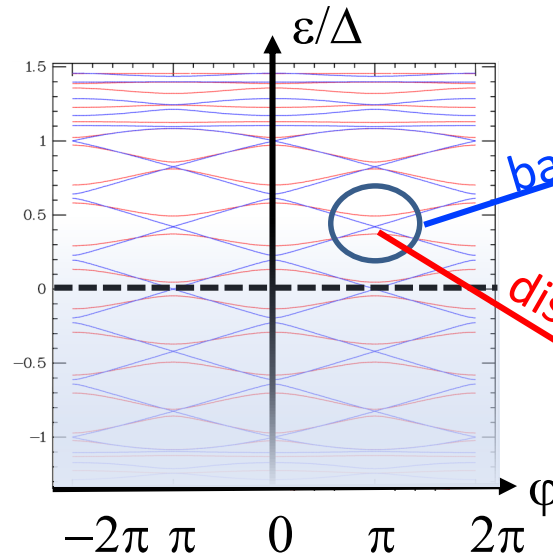


Need to go beyond dc current phase measurements:

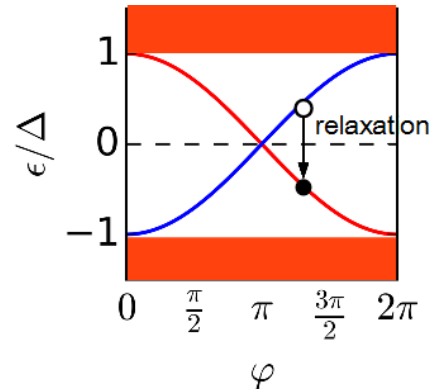
Measure high frequency response (especially near crossings) to beat poisoning/relaxation rate: measure at  $\omega \gg \gamma_p$ !

# ac experiment can probe:

- Perfect crossing
- Rate of parity relaxation



Splitting due to coupling between two edges



# Suggestion to use thermal noise to probe topological crossing

PHYSICAL REVIEW B 79, 161408(R) (2009)



## Josephson current and noise at a superconductor/quantum-spin-Hall-insulator/superconductor junction

Liang Fu and C. L. Kane

Department of Physics and Astronomy, University of Pennsylvania, Philadelphia, Pennsylvania 19104, USA

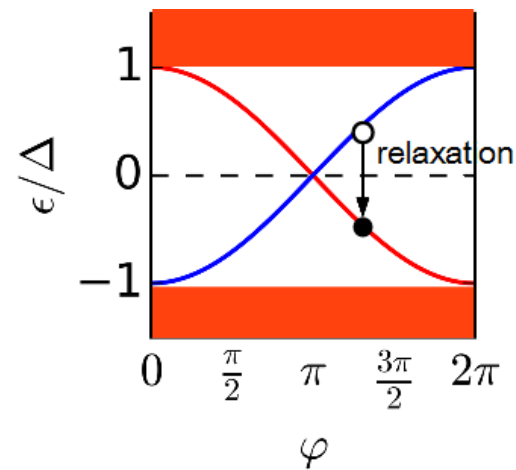
(Received 28 April 2008; revised manuscript received 11 February 2009; published 28 April 2009)

We study junctions between superconductors mediated by the edge states of a quantum-spin-Hall insulator. We show that such junctions exhibit a fractional Josephson effect, in which the current phase relation has a  $4\pi$  rather than a  $2\pi$  periodicity. This effect is a consequence of the conservation of fermion parity—the number of electron mod 2—in a superconducting junction and is closely related to the  $Z_2$  topological structure of the quantum-spin-Hall insulator. Inelastic processes, which violate the conservation of fermion parity, lead to telegraph noise in the equilibrium supercurrent. We predict that the low-frequency noise due these processes diverges exponentially with temperature  $T$  as  $T \rightarrow 0$ . Possible experiments on HgCdTe quantum wells will be discussed.

Noise power  $S(\omega)$ : gives time dependence of current

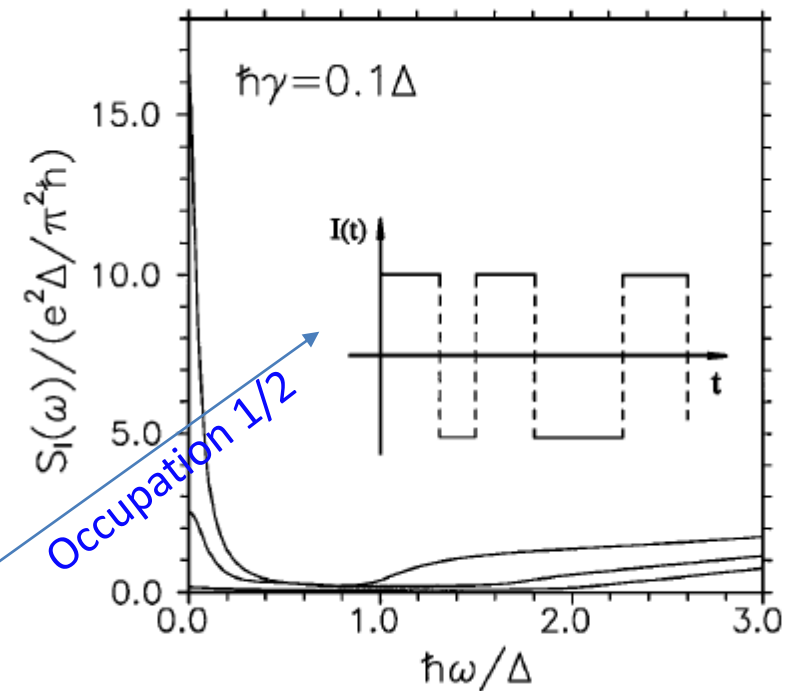
$$S(\omega) = 2 \int_{-\infty}^{\infty} e^{i\omega t} \langle I(t) I(0) \rangle$$

$$S(\omega) = \frac{4I_0^2}{\cosh^2 \epsilon_0(\phi)/2T} \frac{\tau}{1 + \omega^2 \tau^2}$$



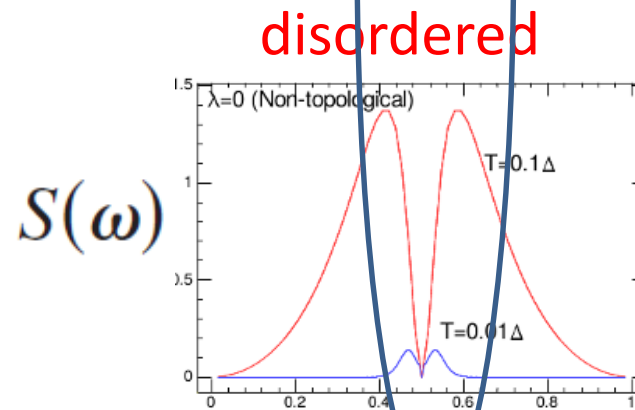
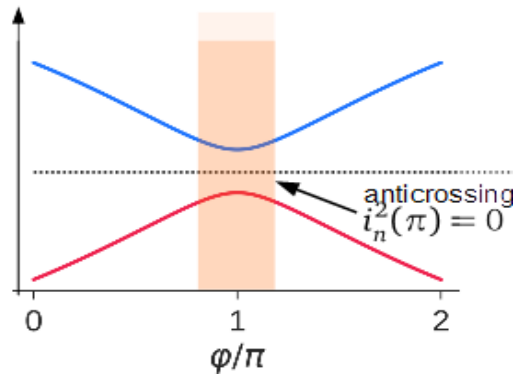
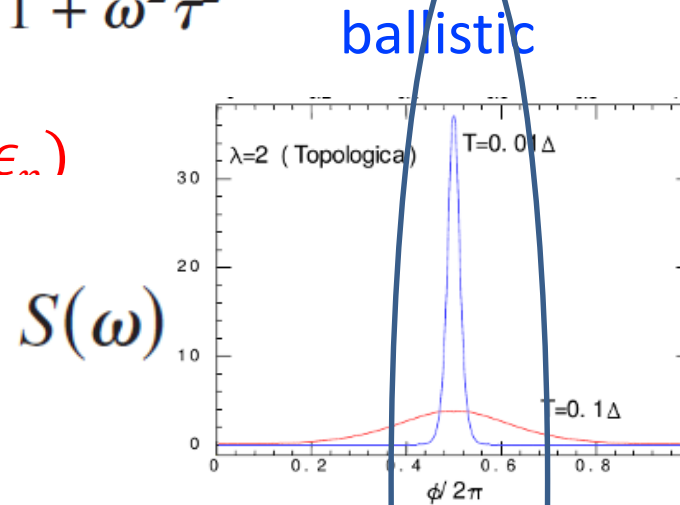
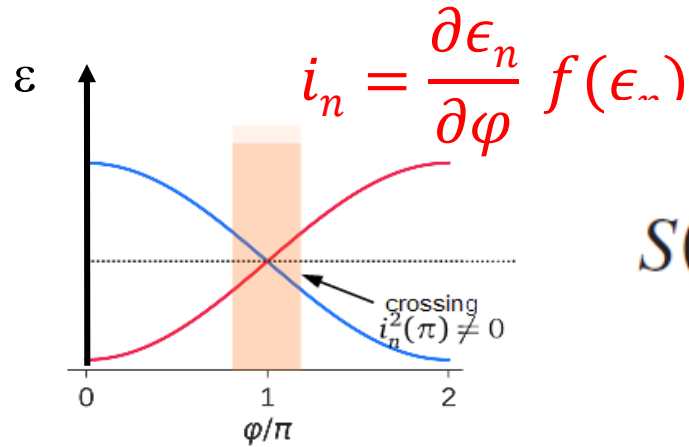
HUGE telegraphic noise of supercurrent if perfect crossing and low temperature

Averin Imam 1996



# Suggestion to use thermal noise to probe topological crossing

$$S(\omega) = \frac{4I_0^2}{\cosh^2 \epsilon_0(\phi)/2T} \frac{\tau}{1 + \omega^2 \tau^2}$$



Prediction:

Telegraphic noise of supercurrent is **huge** (at  $\pi$ ) if perfect crossing and low temperature, and **zero** if avoided crossing at  $\pi$ .

$$S_I(\omega) = \frac{2}{\pi} \frac{k_B T \chi''(\omega)}{\omega}$$

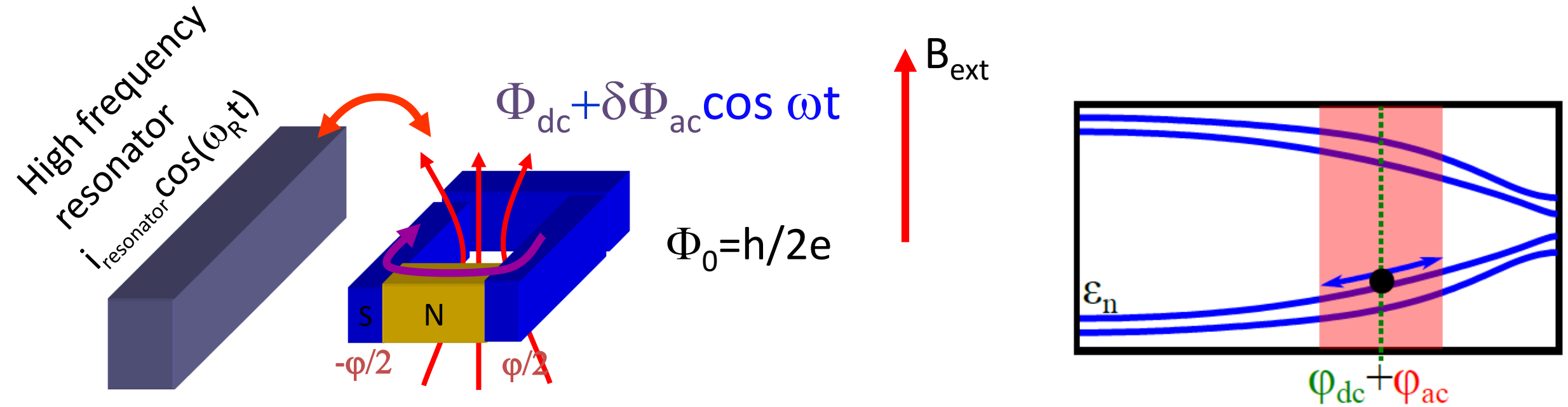
Noise=fluctuations

$\chi''$ =dissipation

Instead of probing noise, we will probe susceptibility (equivalent via Fluctuation-Dissipation Theorem)



# (dc+) ac phase-driven proximity effect



ac :  $\Phi(t) = \Phi_{\text{dc}} + \delta\Phi_{\text{ac}} \cos \omega t$        $\varphi(t) = 2\pi \Phi(t) / \Phi_0$

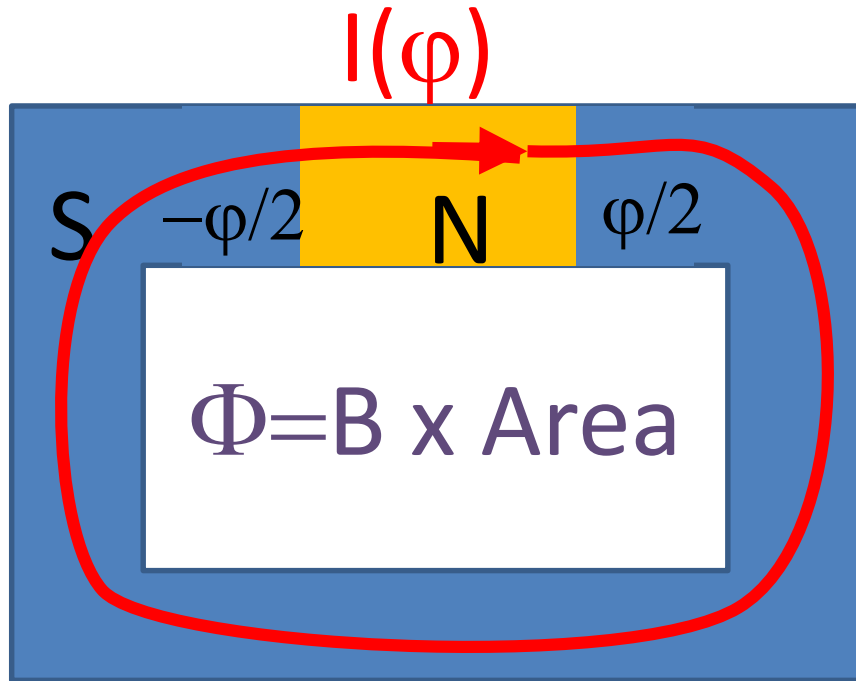
Ring linear response:  $I(t, \varphi, \omega) = I_{\text{dc}} + \varphi_{\text{ac}} (\chi'(\omega) \cos \omega t + \chi''(\omega) \sin \omega t)$

$\chi = \chi' + i\chi''$        $\chi'$  non dissipative       $\chi''$  dissipative

$I(\varphi)$  depends on the transport regime in the N (diffusive, ballistic)

$\chi(\varphi, \omega)$  depends on the spectrum and dynamics

## ac phase-biased junction



$$\varphi = -2\pi\Phi/\Phi_0 \quad \Phi = \Phi_{\text{dc}} + \delta\Phi_{\text{ac}} \cos \omega t$$

Flux-induced current perturbation

$$\hat{I}_s(t) = \hat{I}_s + \delta\hat{I}_s(t),$$

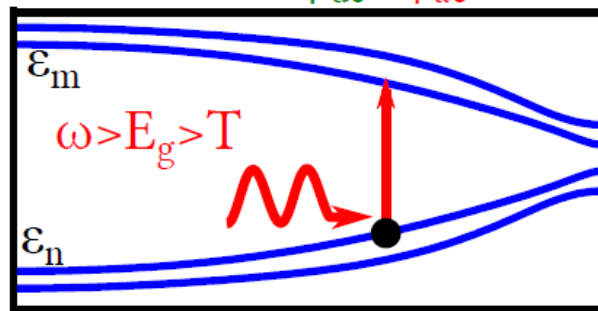
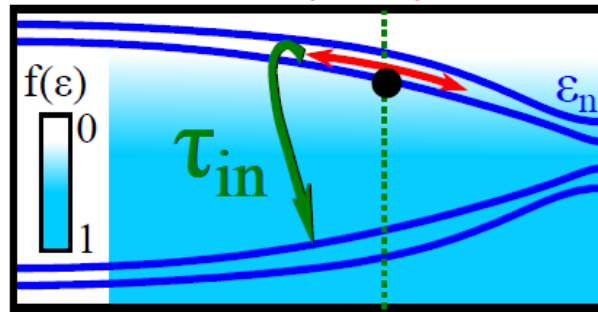
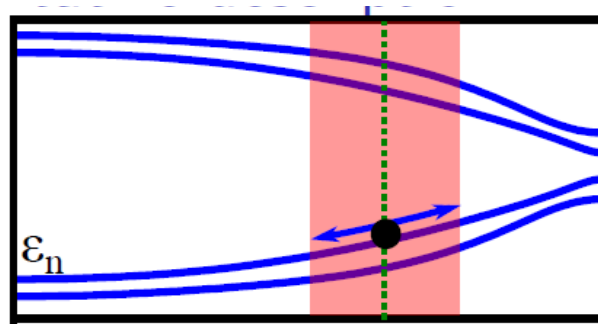
$$\delta\hat{I}_s(t) = -\delta\Phi(t) \frac{\partial^2 H_0}{\partial \Phi^2},$$

$$\langle \hat{I}_s(t) \rangle = \text{Tr}[\hat{I}_s \rho_0] + \text{Tr}[\hat{I}_s \delta\rho(t)] + \text{Tr}[\delta\hat{I}_s(t) \rho_0]$$

$$\chi(\Phi, \omega) = \frac{\delta\langle \hat{I}_s \rangle}{\delta\Phi(\omega)}$$

Susceptibility: Linear response

# Contributions to susceptibility



$\varphi_{dc} + \varphi_{ac}$

Adiabatic response

$$\text{Josephson susceptibility: } \chi_J = -\frac{2\pi}{\Phi_0} \frac{\partial I_J}{\partial \varphi}$$

Diagonal response: population relaxation

$$\delta f_n = \frac{1}{1 - i\omega\tau_{in}} \frac{\partial f_n}{\partial \varphi} \varphi_{ac}$$

$$\chi_D = -\frac{i\omega}{1/\tau_{in} - i\omega} \sum_n i_n \frac{\partial f_n}{\partial \varphi} = -\frac{i\omega}{1/\tau_{in} - i\omega} \sum_n i_n^2 \frac{\partial f_n}{\partial \epsilon_n}$$

Non diagonal response: Transitions between Andreev levels

$$\chi_{ND} = \sum_{n,m \neq n} J_{n,m}^2 \frac{f_n - f_m}{\epsilon_n - \epsilon_m} \frac{i\hbar\omega}{1/\tau_{nm} + i(\epsilon_n - \epsilon_m - \hbar\omega)}$$

# How does a system respond to a high frequency excitation ?

$$\chi(\Phi, \omega) = \underbrace{\frac{\partial I_J}{\partial \Phi}}_{\chi_J} + \underbrace{\sum_n \frac{\omega}{\omega + i\gamma_{nn}} \left( \frac{\partial \epsilon_n}{\partial \Phi} \right)^2 \frac{\partial f(\epsilon_n)}{\partial \epsilon_n}}_{\chi_D} - \underbrace{\hbar\omega \sum_{n \neq m} \frac{|\langle m | \hat{I}_s | n \rangle|^2}{\epsilon_n - \epsilon_m} \frac{f(\epsilon_n) - f(\epsilon_m)}{\epsilon_n - \epsilon_m - \hbar\omega - i\hbar\gamma_{nm}}}_{\chi_{ND}}$$

Static

Derivative of  
dc current-  
phase relation

Delayed response  
Population  
relaxation  
Prop to  $i_n^2$

Transitions: Spectroscopy (in  
some range)

$$I_J(\Phi) = - \sum_n f(\epsilon_n) \frac{\partial \epsilon_n}{\partial \Phi}$$

Most sensitive to  
avoided/protected  
crossing

Applied to normal ring  
(Trivedi Browne PRB 1988),  
and diffusive SNS ring  
(Ferrier PRB 2013,  
Dassonneville 2014)

Terms beyond derivative of dc Josephson relation lead to dissipation!

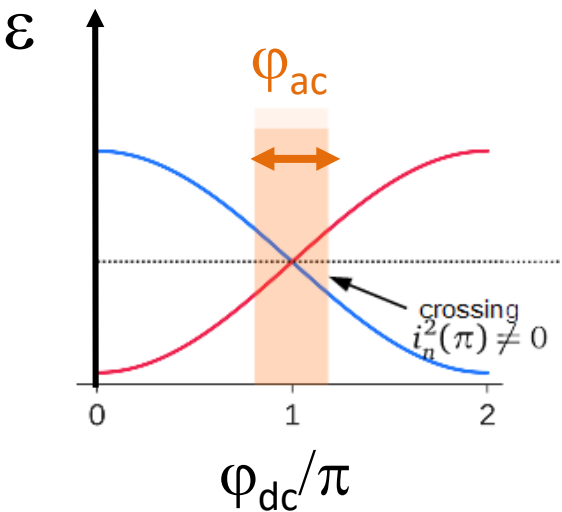
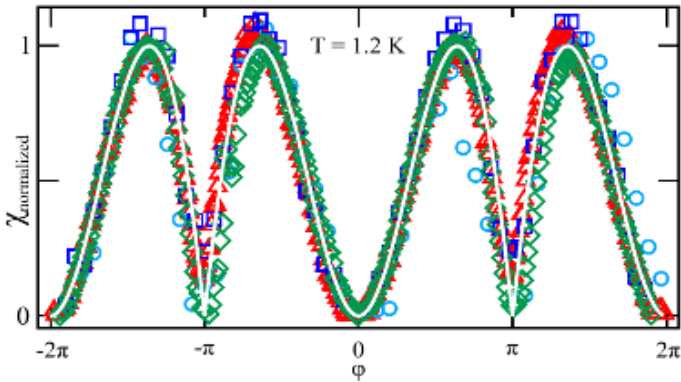
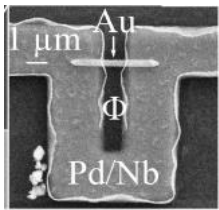
ac susceptibility (especially diagonal absorption)  
 can distinguish between topo/non topological  
 crossings

$$\underbrace{\sum_n \frac{\omega}{\omega + i\gamma_{nn}} \left( \frac{\partial \epsilon_n}{\partial \Phi} \right)^2 \frac{\partial f(\epsilon_n)}{\partial \epsilon_n}}_{\chi_D} i_n^2$$

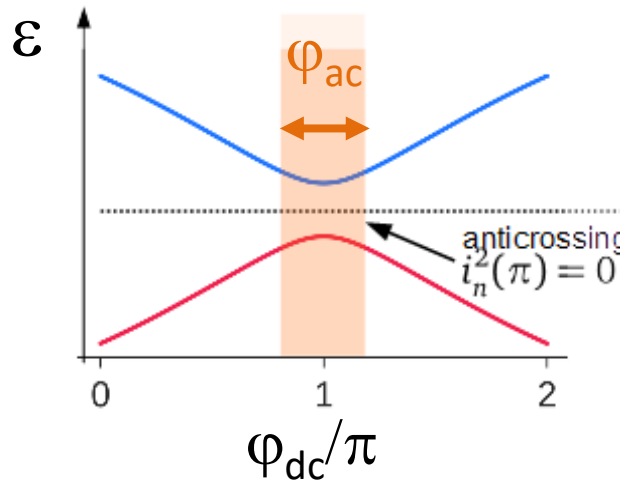
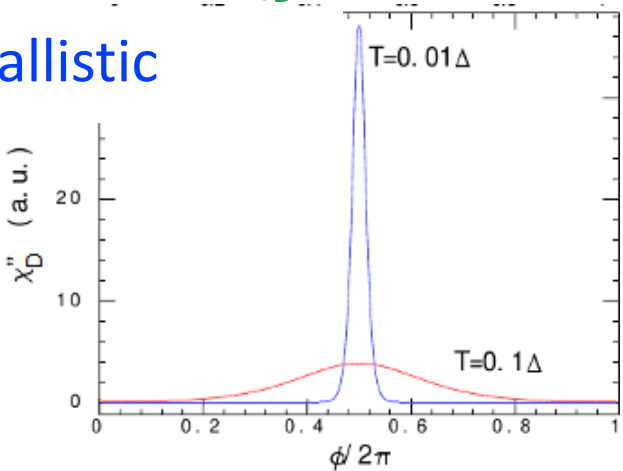
$\chi_D$  probes zero energy level crossings!

Not seen before...

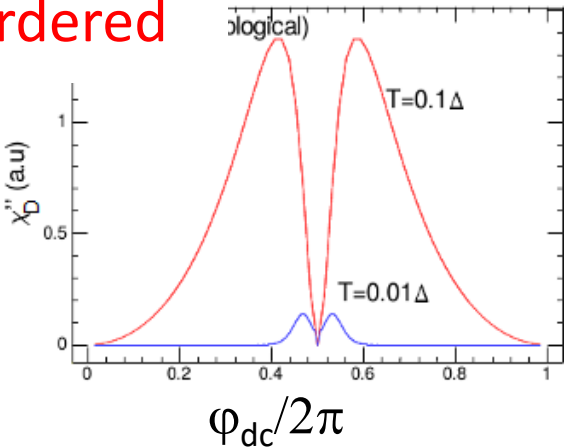
Diffusive SNS ring:  
 Ferrier 2013,  
 Dassonneville 2014,  
 2018



ballistic

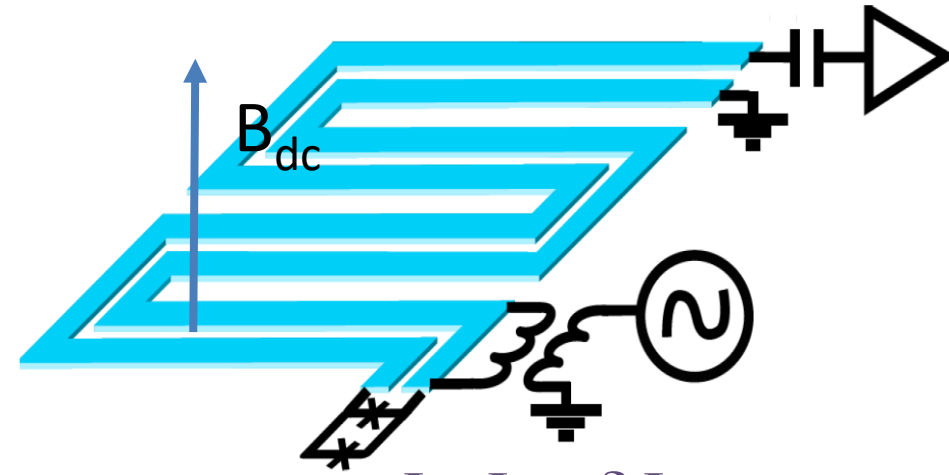
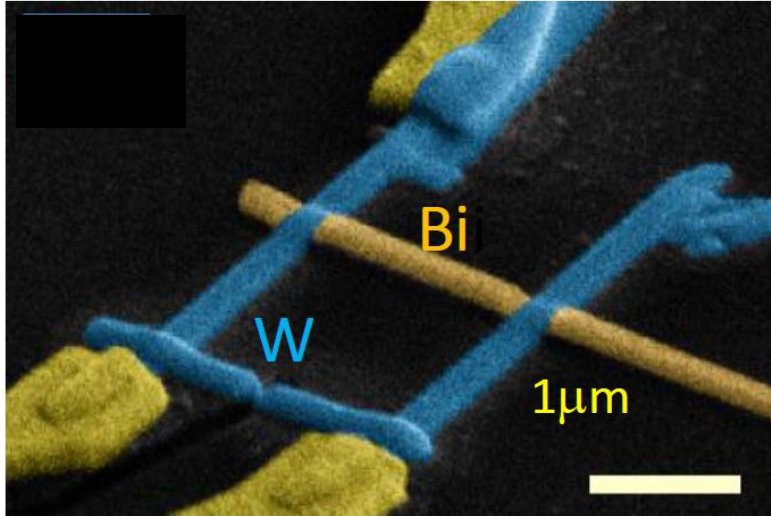


disordered



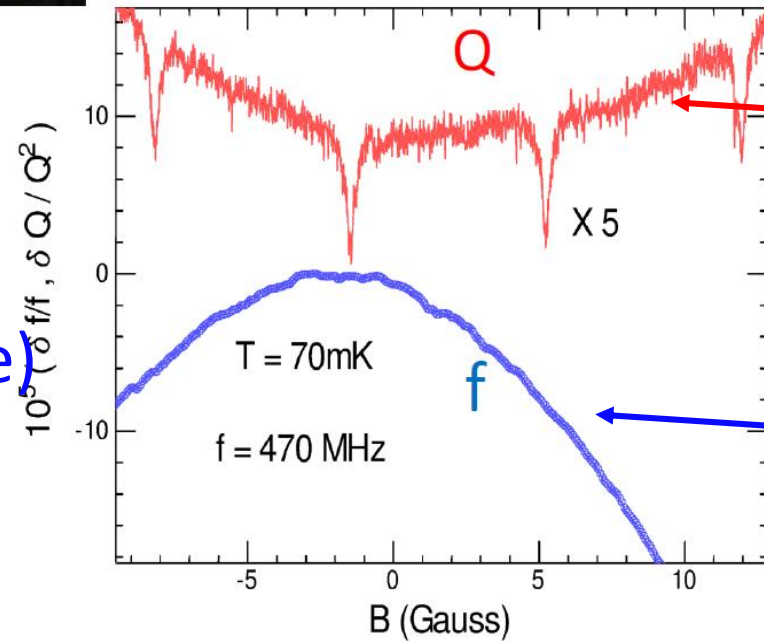


# In practice : multimode resonator coupled to S/Bi/S asymmetric SQUID



$$\Phi = \Phi_{dc} + \delta\Phi_{ac} \cos \omega t$$

Measure  $Q$  and  $f$  variations with  $B$  (at each resonator mode)



Dissipative response

$$\chi''(\varphi) = \frac{L_R}{L_W^2} \delta \left[ \frac{1}{Q_n} \right] (\Phi)$$

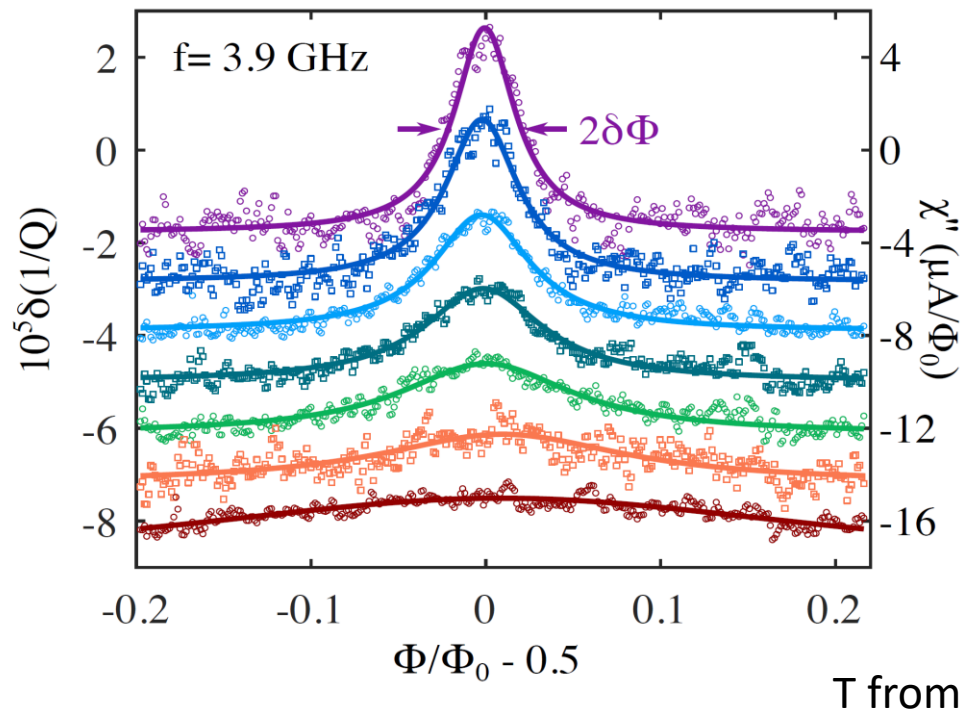
Non-dissipative response

$$\chi'(\varphi) = -\frac{L_R}{L_W^2} \frac{\delta f_n(\Phi)}{2f_n}$$

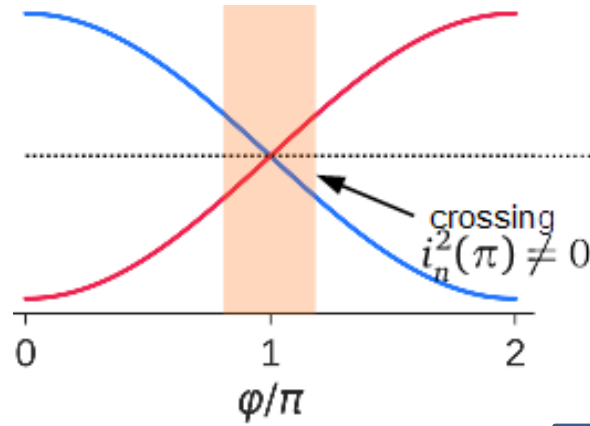
Absorption peaks at  $\pi$  !

# T dependence of absorption peaks at $\varphi=\pi$ OK with protected crossing

$$\delta(1/Q) = L_c^2 / L_R \chi''$$



Noise peaks at level crossing because level occupation fluctuates most (telegraphic noise)



$$\sum_n \frac{\omega}{\omega + i\gamma_{nn}} \underbrace{\left( \frac{\partial \epsilon_n}{\partial \Phi} \right)^2}_{\chi_D} \frac{\partial f(\epsilon_n)}{\partial \epsilon_n} i_n^2$$

$$\chi_D'' = i_0^2 \frac{\omega \gamma}{\omega^2 + \gamma^2} \frac{1}{2T \cosh^2 \left( \frac{\epsilon_T}{2T} (\varphi/\pi - 1) \right)}$$

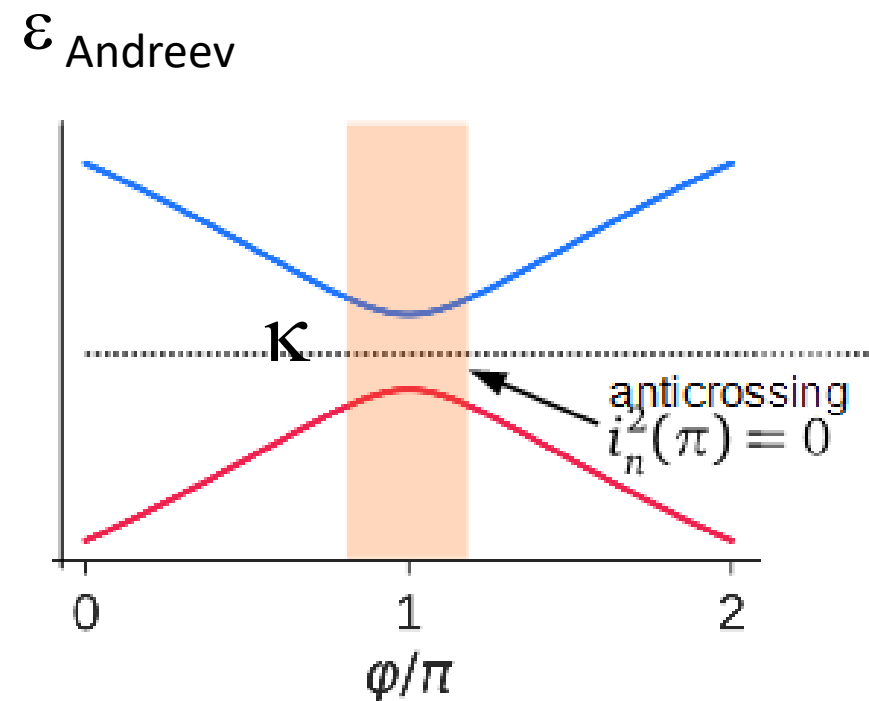
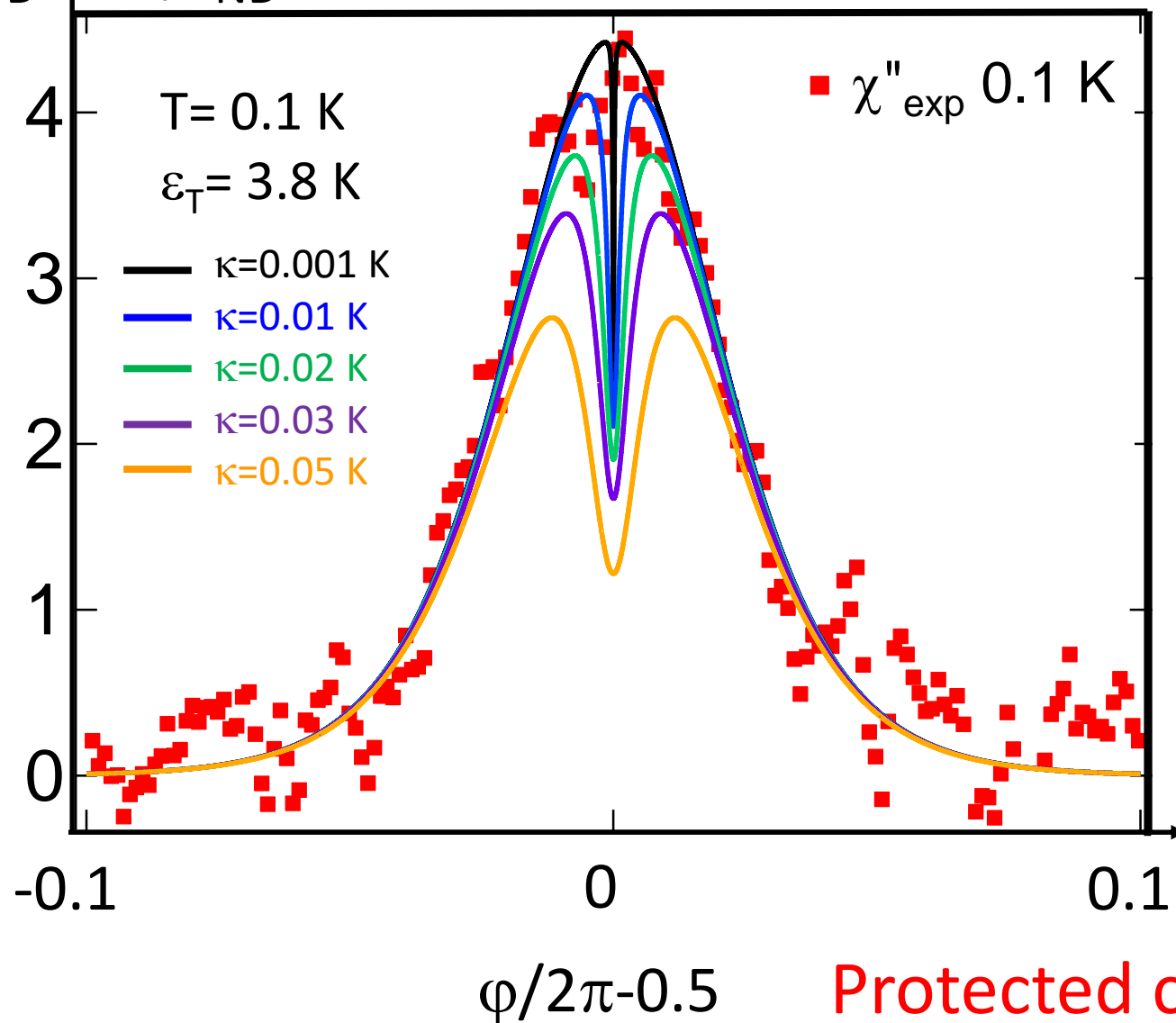
$$i_n = i_0 = E_{Th}/\Phi_0$$

This is the thermal noise of a QSH insulator (Fu Kane)!

$$S(\omega) = \frac{4I_0^2}{\cosh^2 \epsilon_0(\phi)/2T} \frac{\tau}{1 + \omega^2 \tau^2}$$

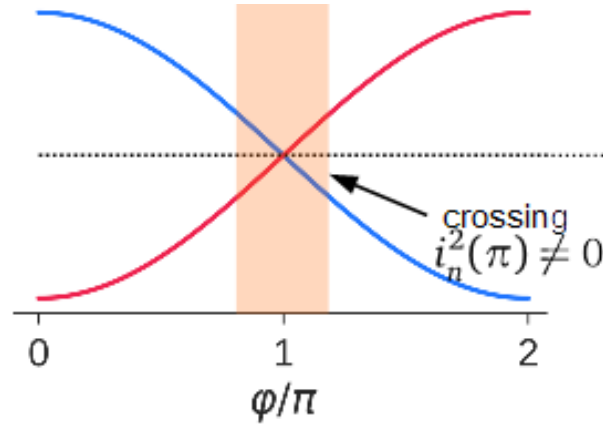
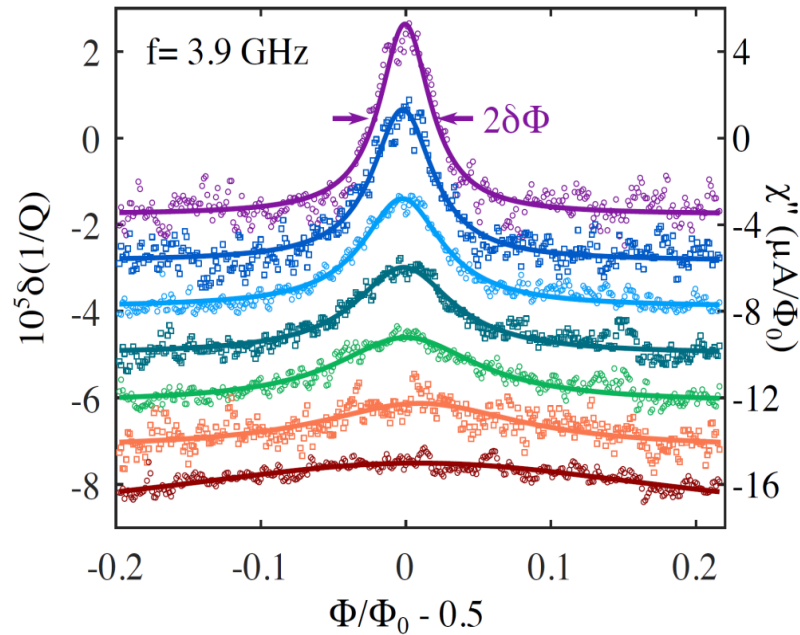
# How protected is protected ?

$$\chi'' = \chi_D'' + \chi''_{ND} \text{ (a.u.)}$$



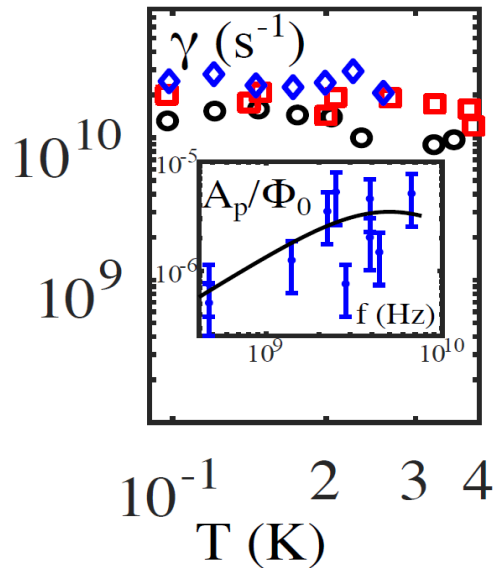
Protected crossing to within 30 mK

# Parity is not conserved! Relaxation occurs



$$\underbrace{\sum_n \frac{\omega}{\omega + i\gamma_{nn}} \left( \frac{\partial \epsilon_n}{\partial \Phi} \right)^2 \frac{\partial f(\epsilon_n)}{\partial \epsilon_n}}_{\chi_D} i_n^2$$

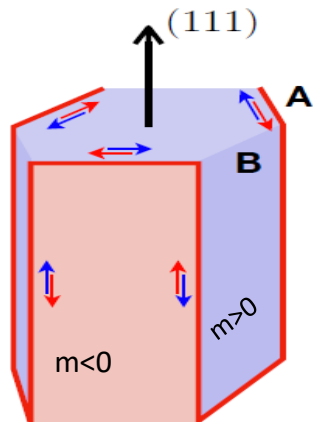
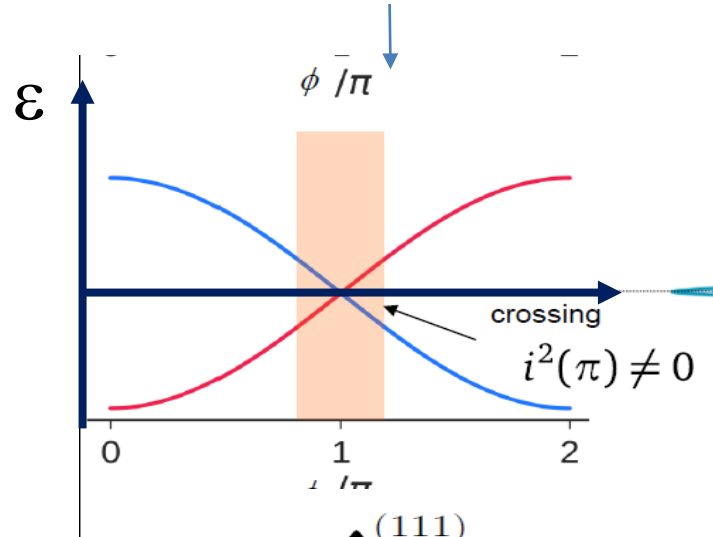
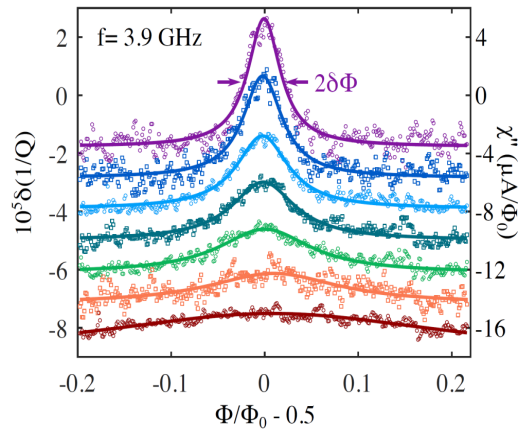
$$\chi_D'' = i_0^2 \frac{\omega \gamma}{\omega^2 + \gamma^2} \frac{1}{2T \cosh^2 \left( \frac{\epsilon_T}{2T} (\phi/\pi - 1) \right)}$$



Fast poisoning!  $\sim 1$ ns

Due to soft gap, quasiparticles, broadband environment

Enabled us to see a response, but room for improvement...



## Conclusion

Superconducting proximity effect is a good tool!

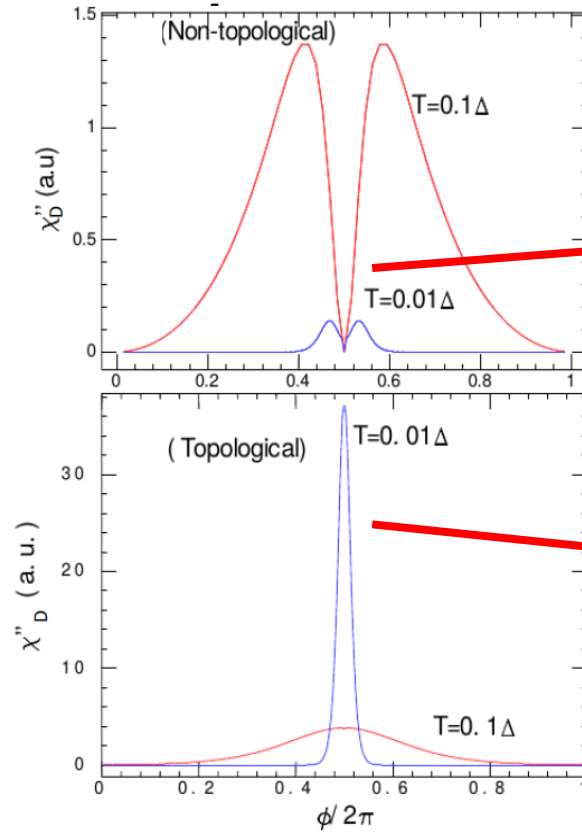
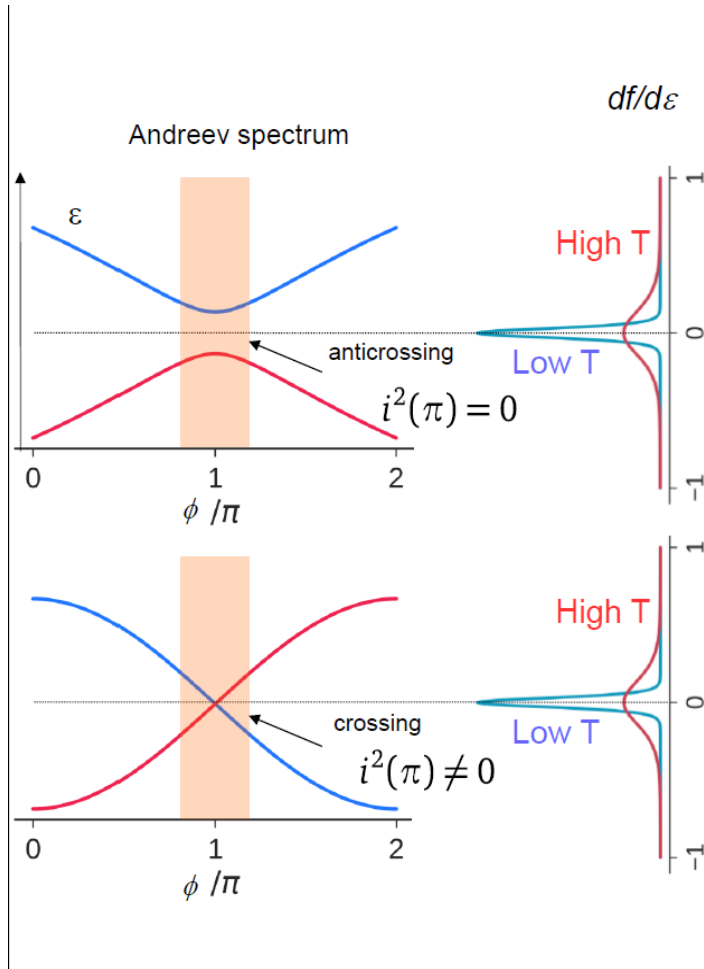
Ballistic edge states with protected (topological) crossing (to within 50 mK). Noisy supercurrent at  $\pi$  reveals topology. Bismuth could well be a Second Order Topological Insulator!

However fast relaxation (parity breaking)

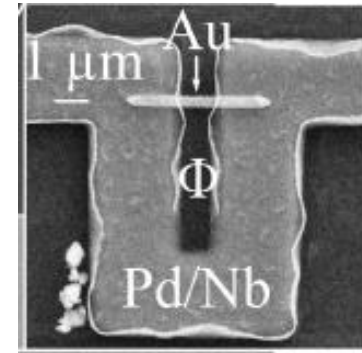
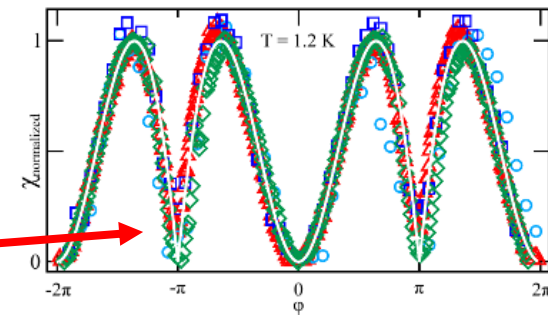
No inductive response... needs further understanding



# Comparison of ac susceptibility of S/Bi/S and S/diffusive Au/S

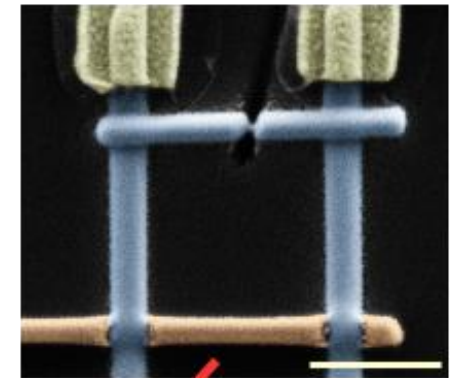
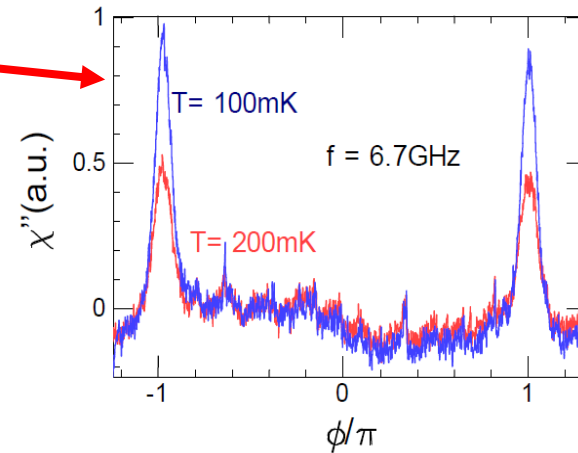


In SNS: zero absorption at  $\pi$ ! S/diffusive Au/S



Dassonneville2013

In S/Bi/S: max absorption at  $\pi$ ! S/Bi/S



Murani2018

## Open questions/ New experiments/ What next?

### Future plans:

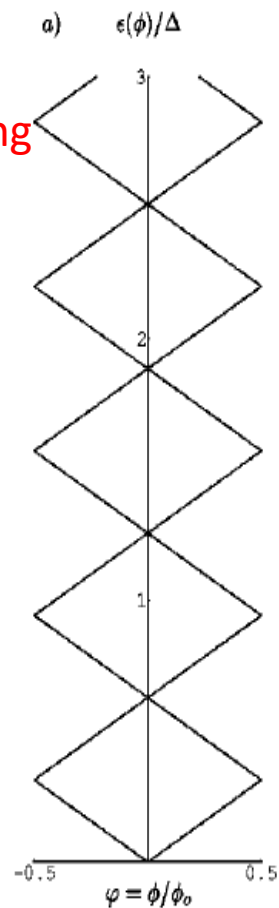
- Measure noise at lower frequency (coupling between edges, MHz) to observe restoration of spin degenerate behavior
- Investigate difference between SOTI and 2DTI
- Other probe of helical edge states? Persistent charge and spin currents of 2DTI/SOTI?

# Compare Normal spectrum to Andreev Bound State spectra

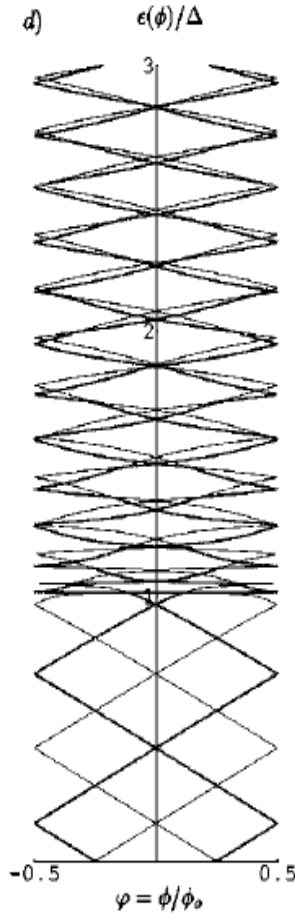
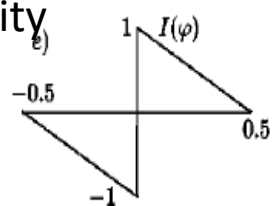
## a) ballistic few channels

Cayssol, Kontos Montambaux 2003.

Normal ring



h/e periodicity

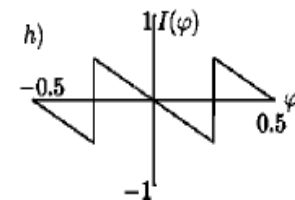


NS ring (long junction)

$h/e$  periodicity above gap (like N)

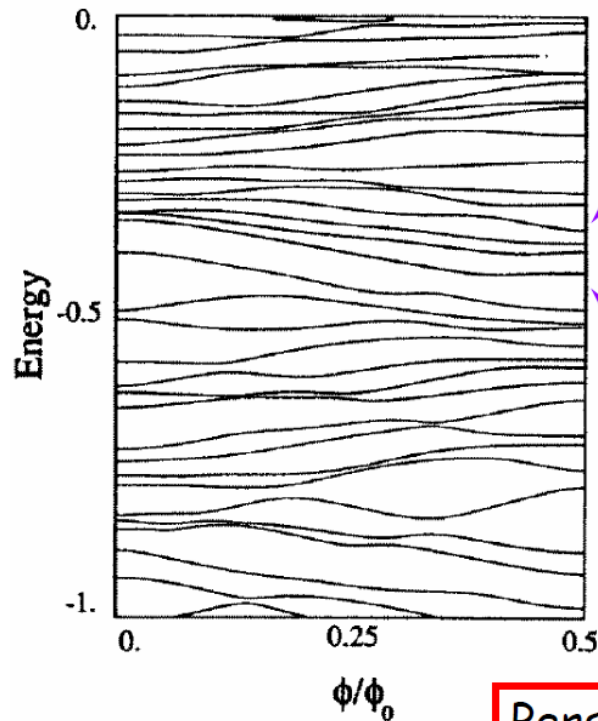
$E = \Delta$

$h/2e$  periodicity in subgap region



$h/2e$  periodicity

# SPECTRUM OF A DISORDERED RING



Correlated spectrum

Thouless energy

$$E_c = h D / L^2 = h / \tau_D$$

$\tau_D = L^2 / D$  diffusion time around the ring

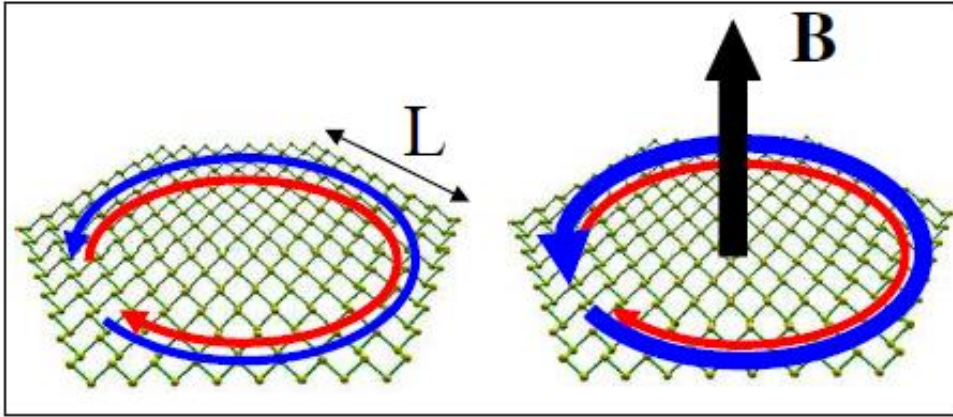
Spectrum described by random matrix theory on this energy scale.

Persistent current: random quantity

$$\langle I^2 \rangle^{1/2} = e / \tau_D = I_0 |e| / L$$

- Diffusive states have tiny persistent current  $\sim e v_F / L$  ( $I_e / L$ ) (as if only one diffusive channel=)
- Topological 1D edge states have  $e v_F / L$ : 100 nA

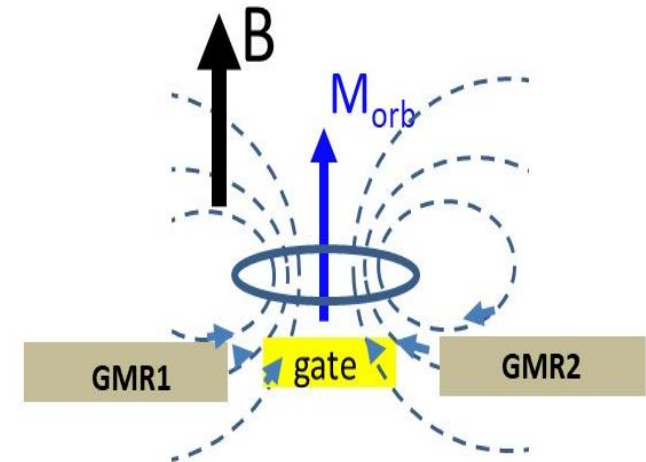
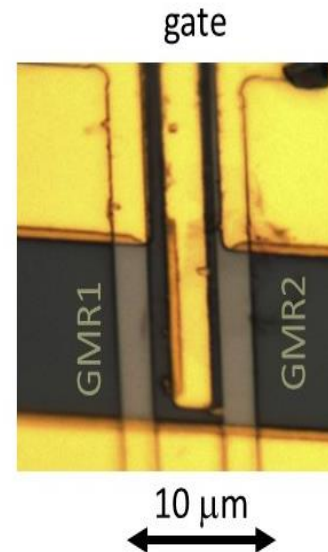
## Persistent (charge) current best discriminator?



- Take a platelet (no need for a ring), no leads
- Diffusive states have tiny persistent current  $\sim e v_F / L$  ( $I_e / L$ ) (as if only one diffusive channel=)
- -1D edge states have  $e v_F / L$ : 100 nA
- Only edge states would have a well-defined period

P. Potasz and J. Fernández-Rossier, Nano Lett. (2015).

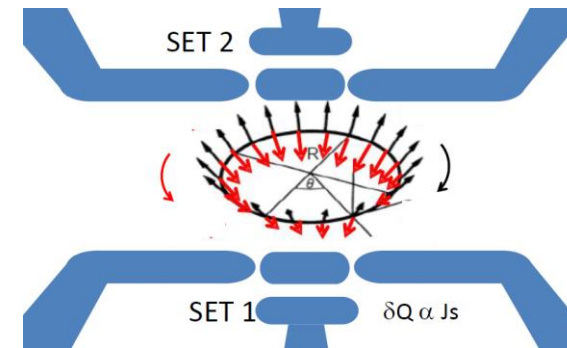
We already have the magnetic probe ready: GMR detector



# Persistent spin current?

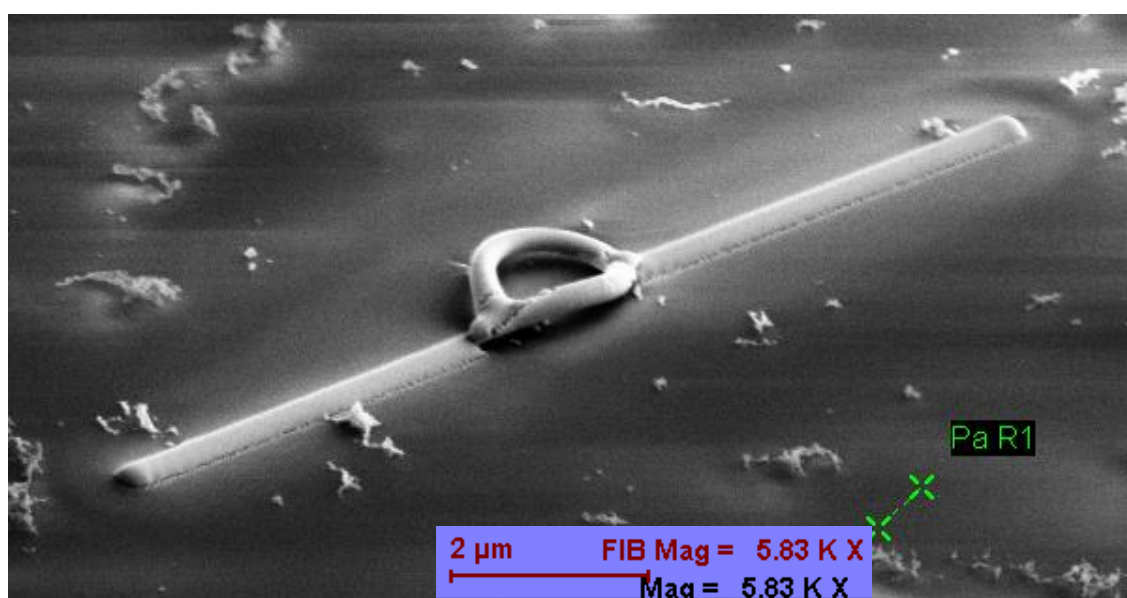
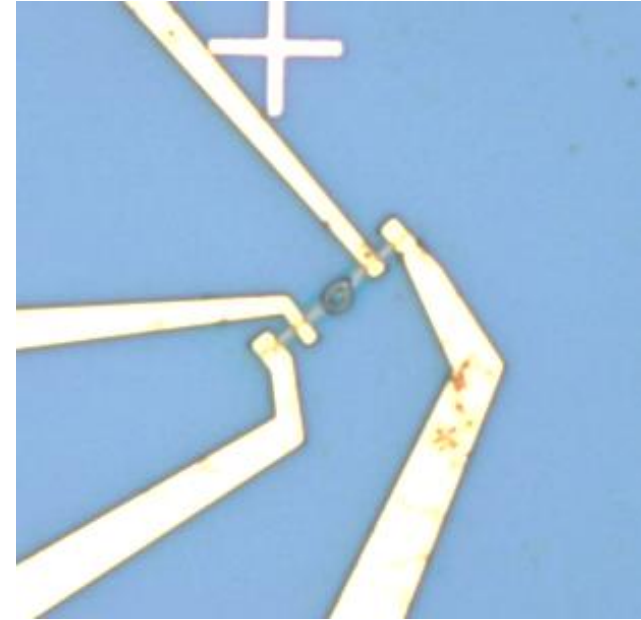
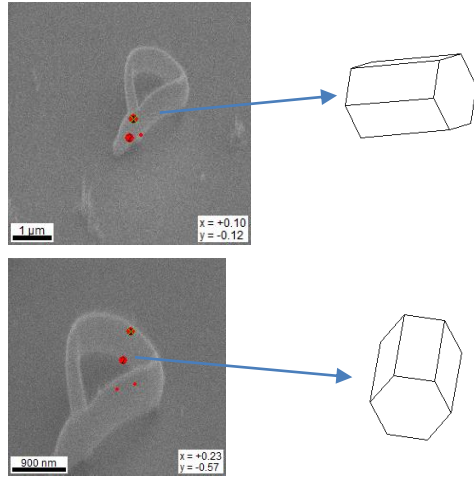
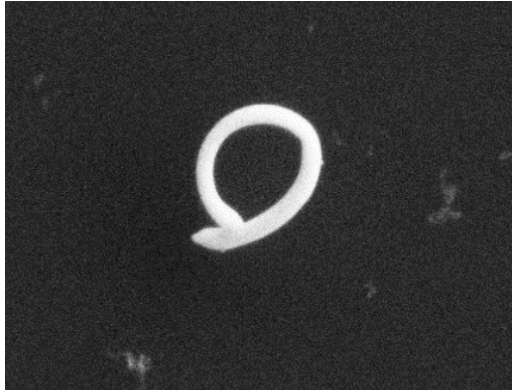
Charge current  $\rightarrow$  magnetic moment

Dual: Spin current  $\rightarrow$  Electric dipole?

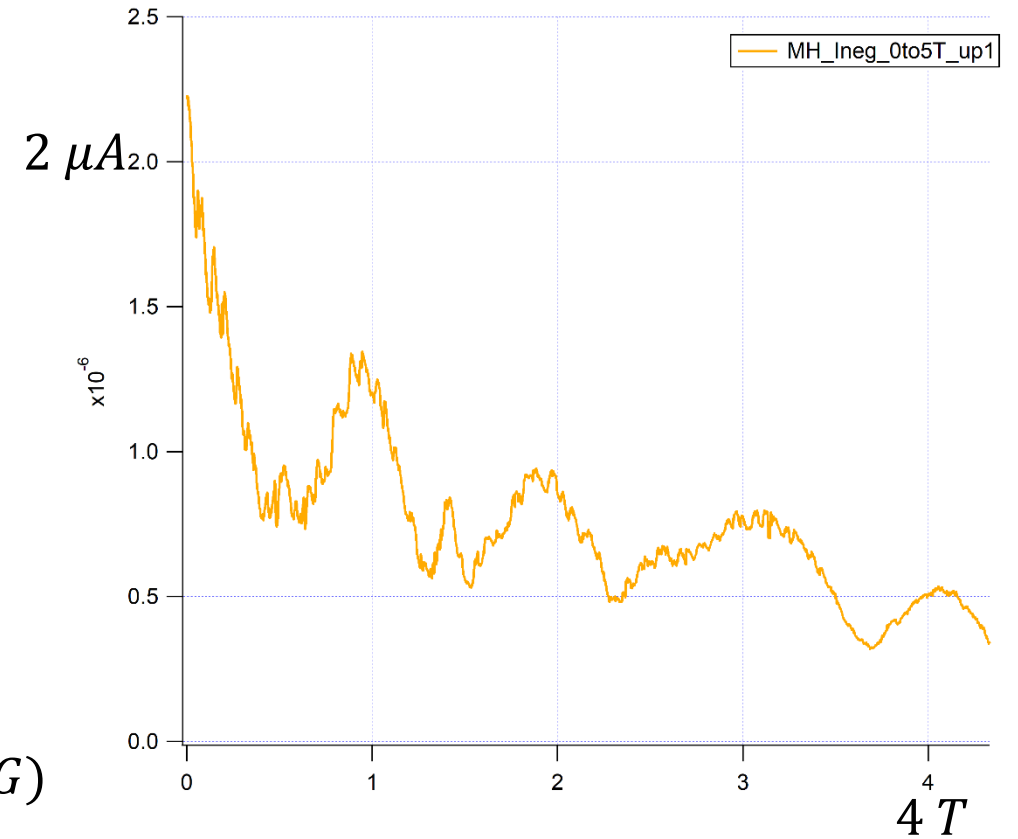
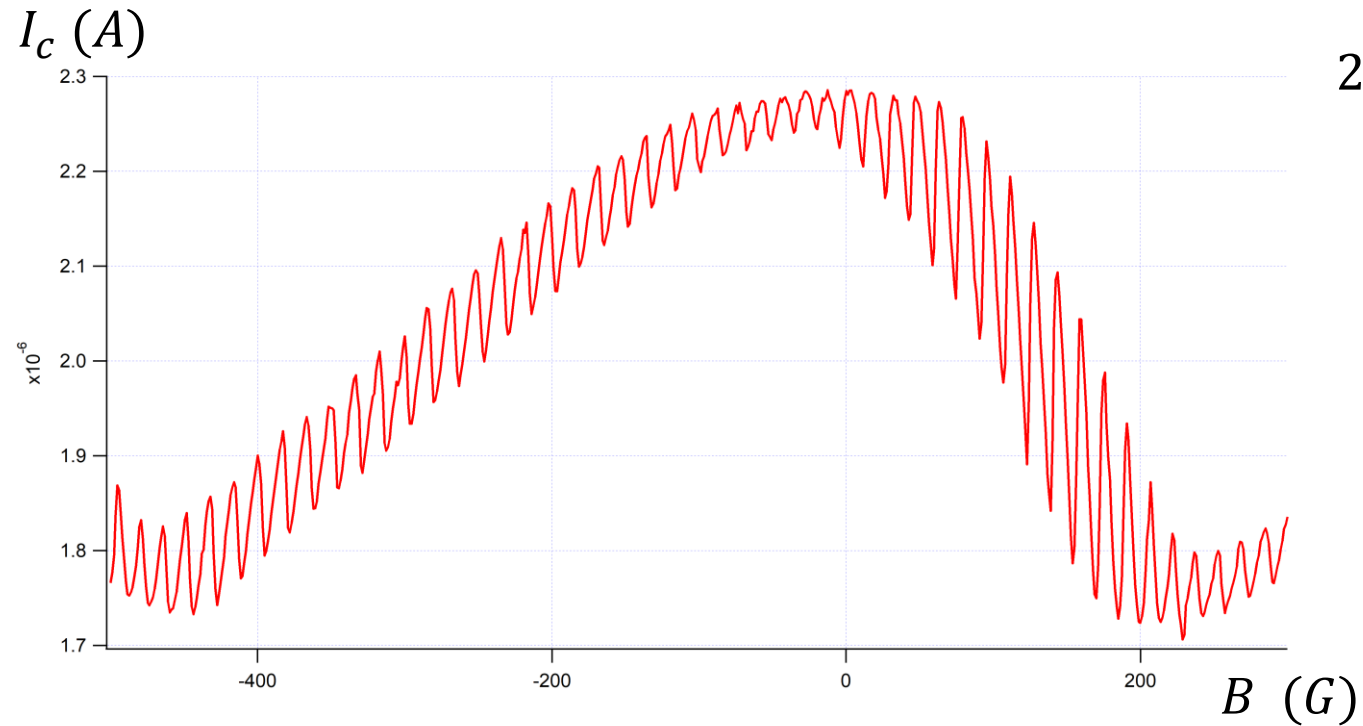
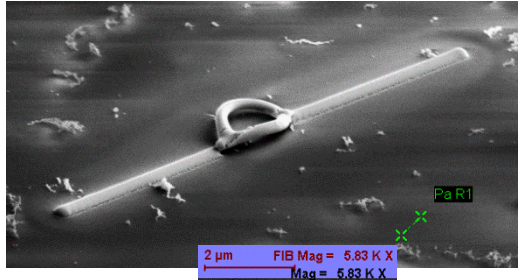




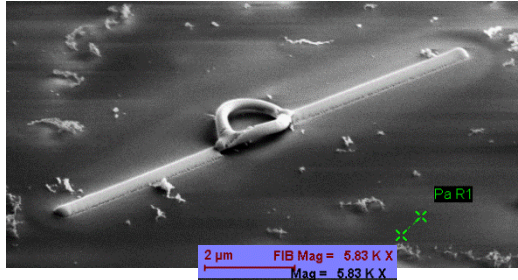
# Ongoing experiments on a bismuth ring



# Supercurrent vs phase: ongoing experiments



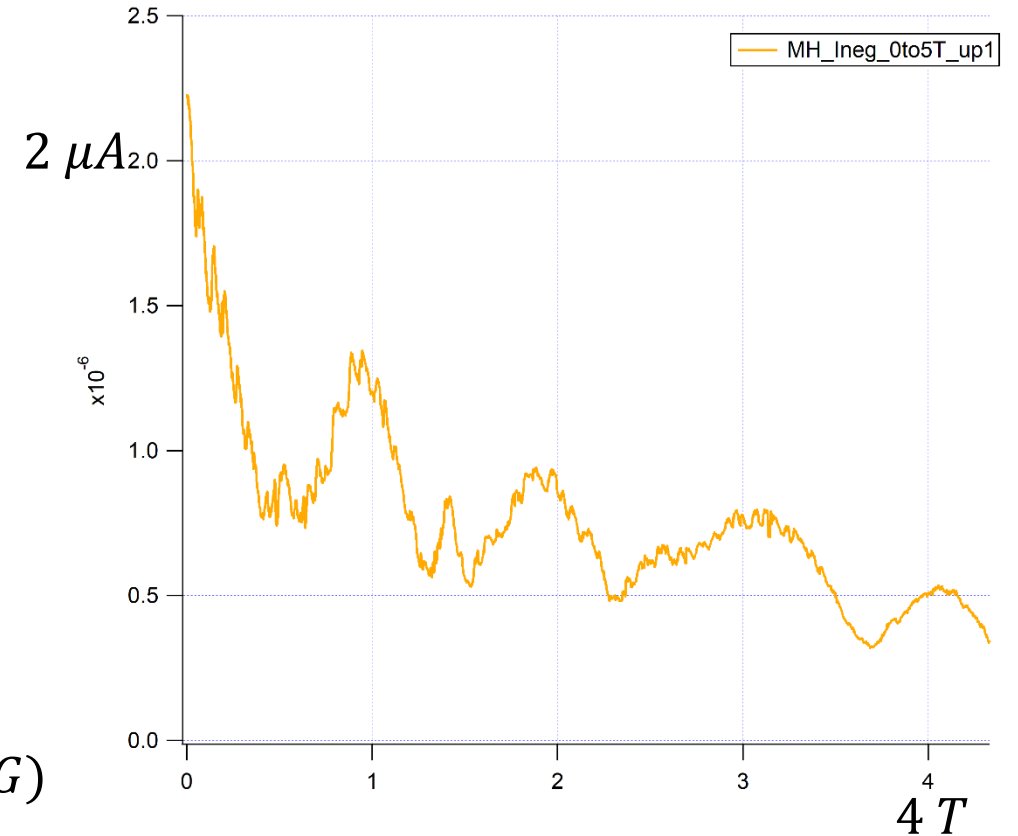
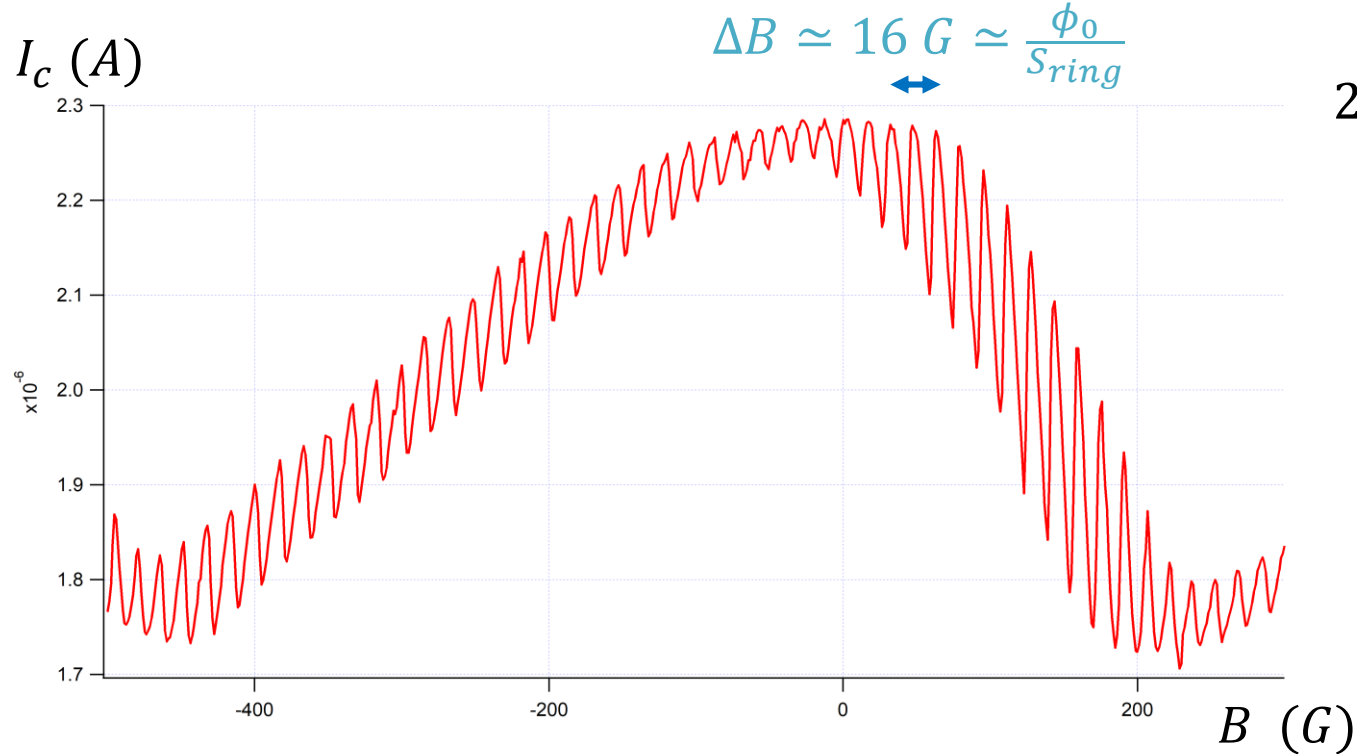
# Supercurrent vs phase: ongoing experiments



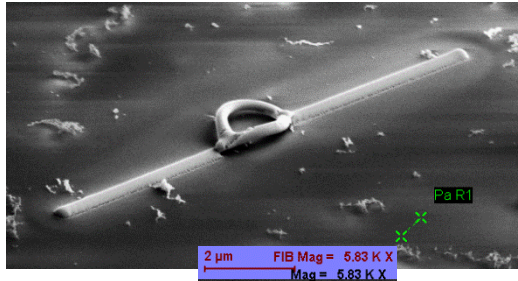
Sawtooth oscillations

=> more like an **build-in asymmetric SQUID** with phase controlled by the flux inside the ring

=> supercurrent vs phase relation of a long ballistic junction



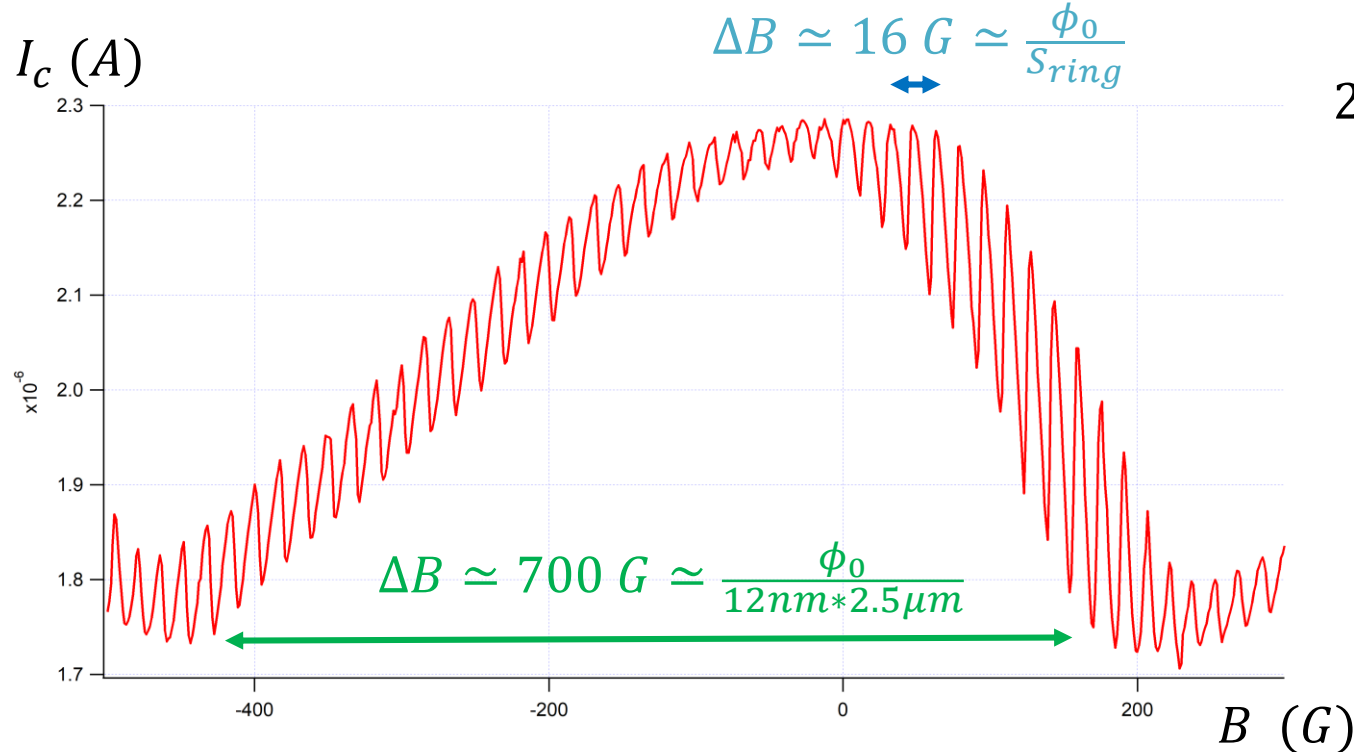
# Supercurrent vs phase: ongoing experiments



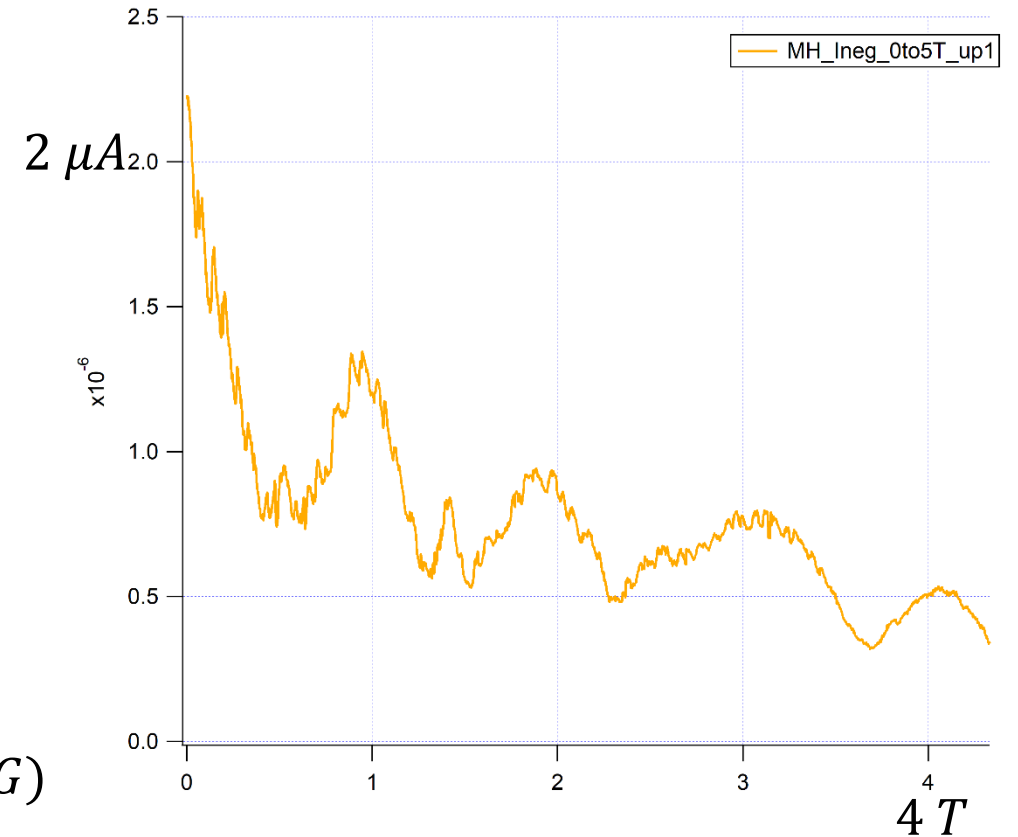
Sawtooth oscillations

=> more like an **build-in asymmetric SQUID** with phase controlled by the flux inside the ring

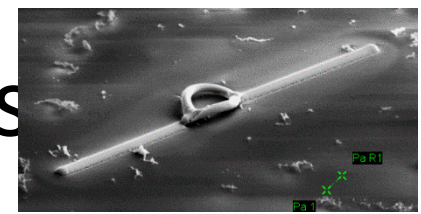
=> supercurrent vs phase relation of a long ballistic junction



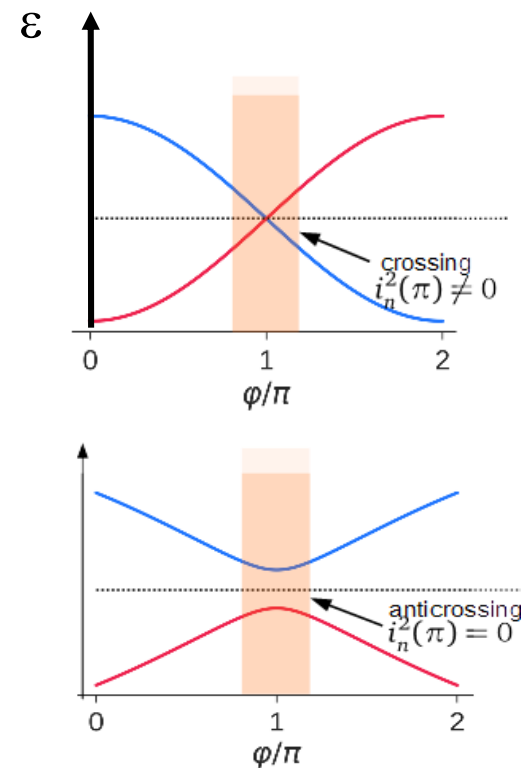
Interferences of  $< 1nm$  wide paths,  
 $\approx 12nm$  apart, in the same branch



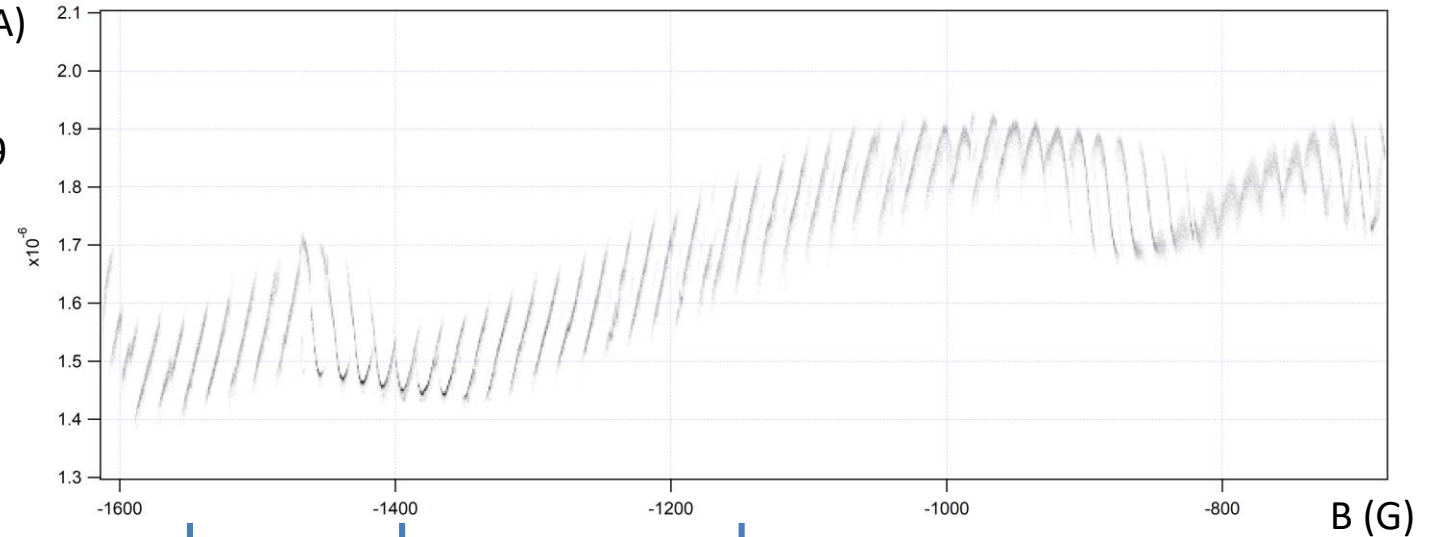
# Supercurrent vs phase: ongoing experiments



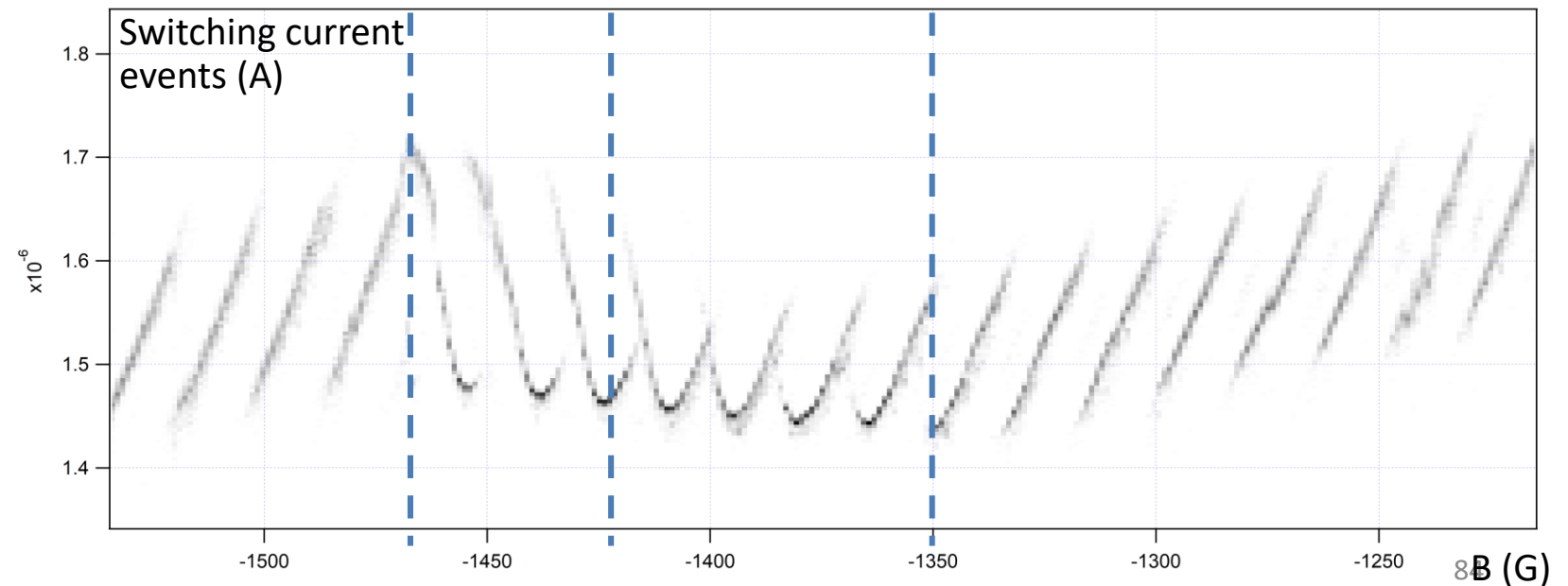
See Peng et al., PRB 2016  
related to current fluctuations, see Fu and Kane PRB 2009  
related to dissipation, see Murani et al. PRL 2019



Switching current events (A)

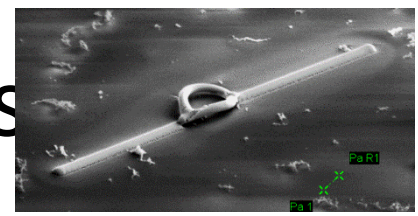


Switching current events (A)

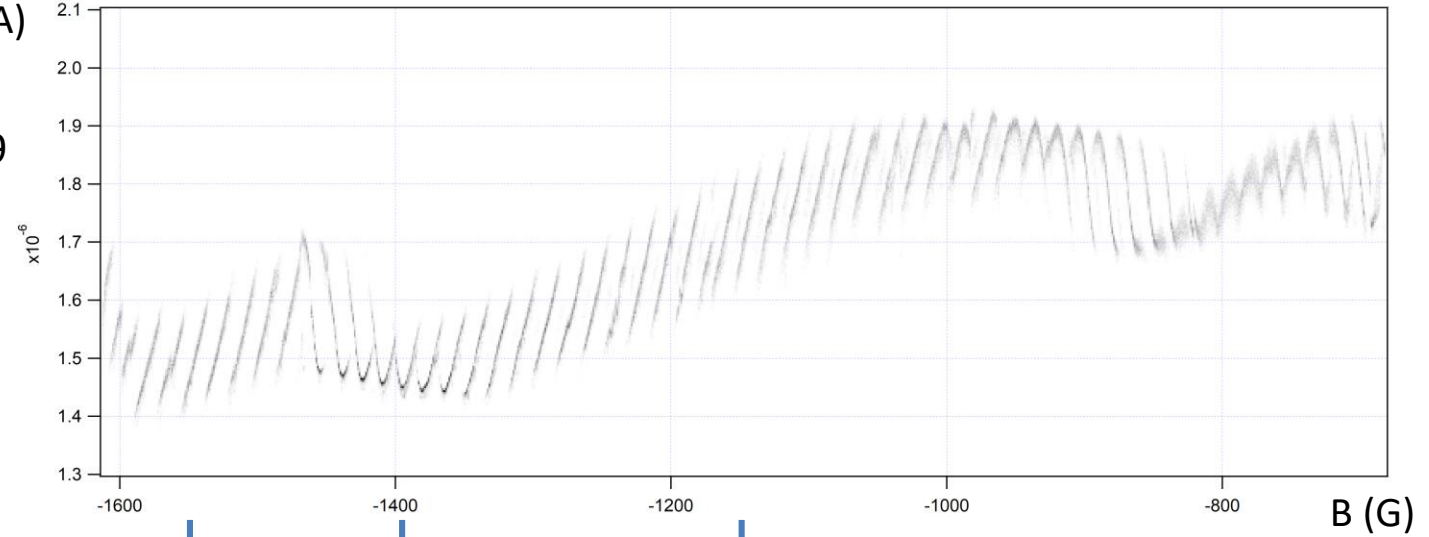




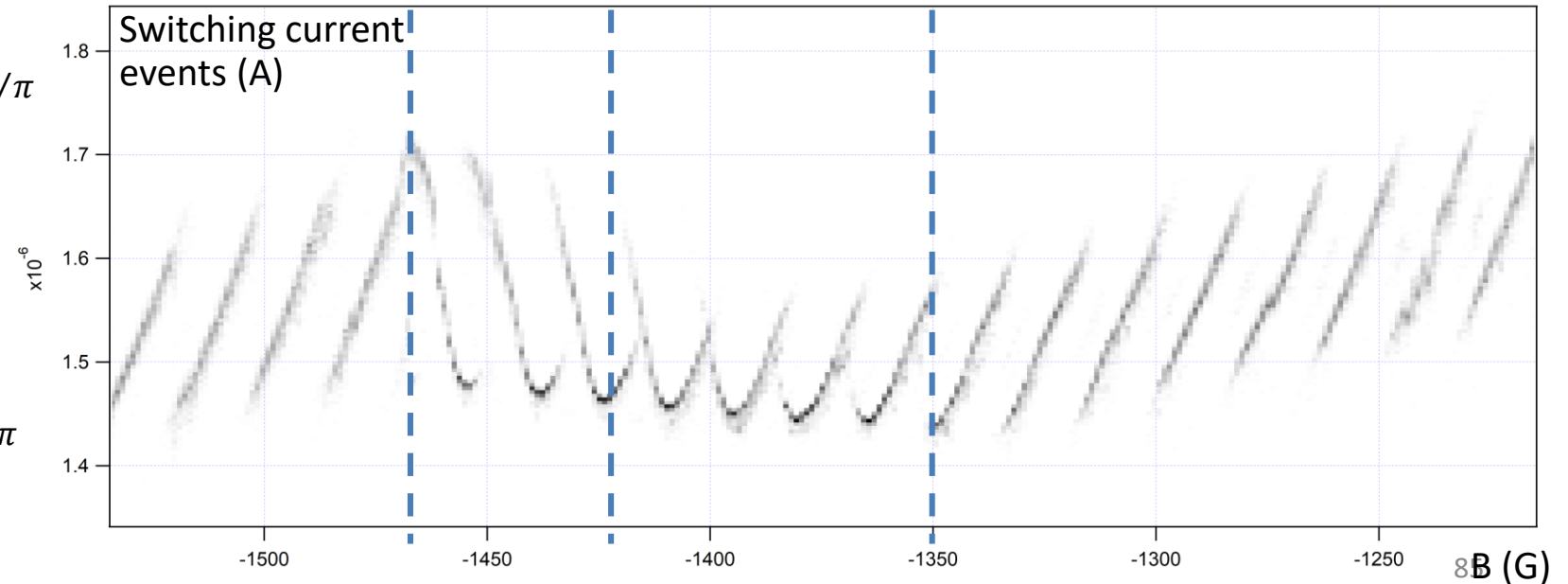
# Supercurrent vs phase: ongoing experiments



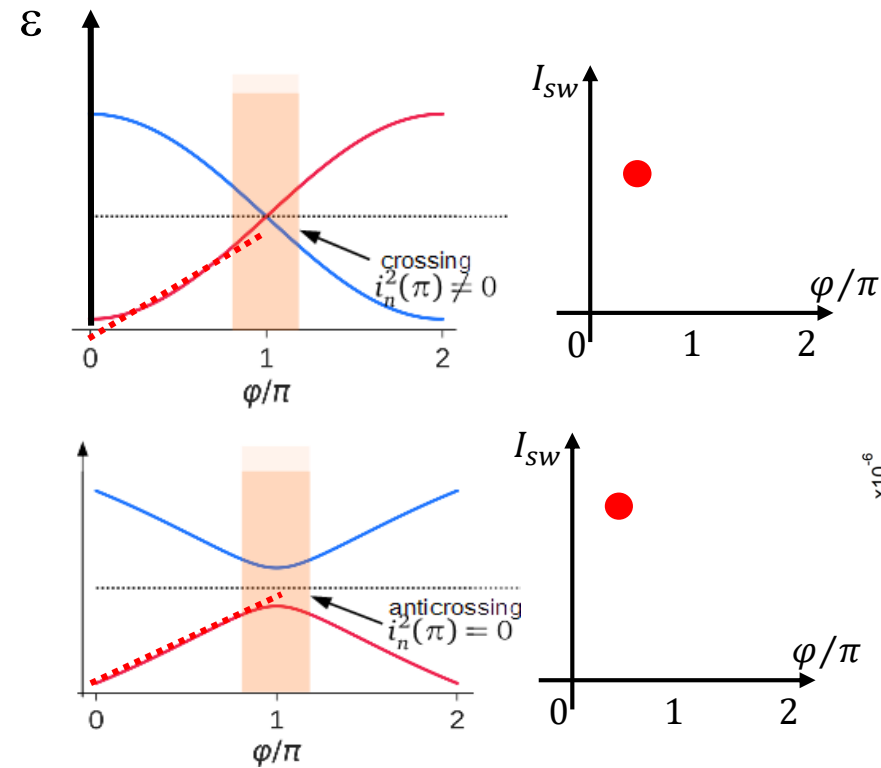
Switching current events (A)



Switching current events (A)

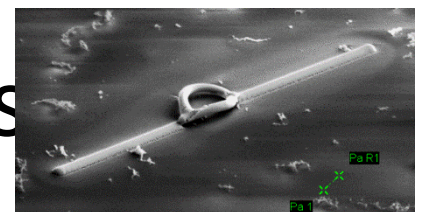


See Peng et al., PRB 2016  
related to current fluctuations, see Fu and Kane PRB 2009  
related to dissipation, see Murani et al. PRL 2019

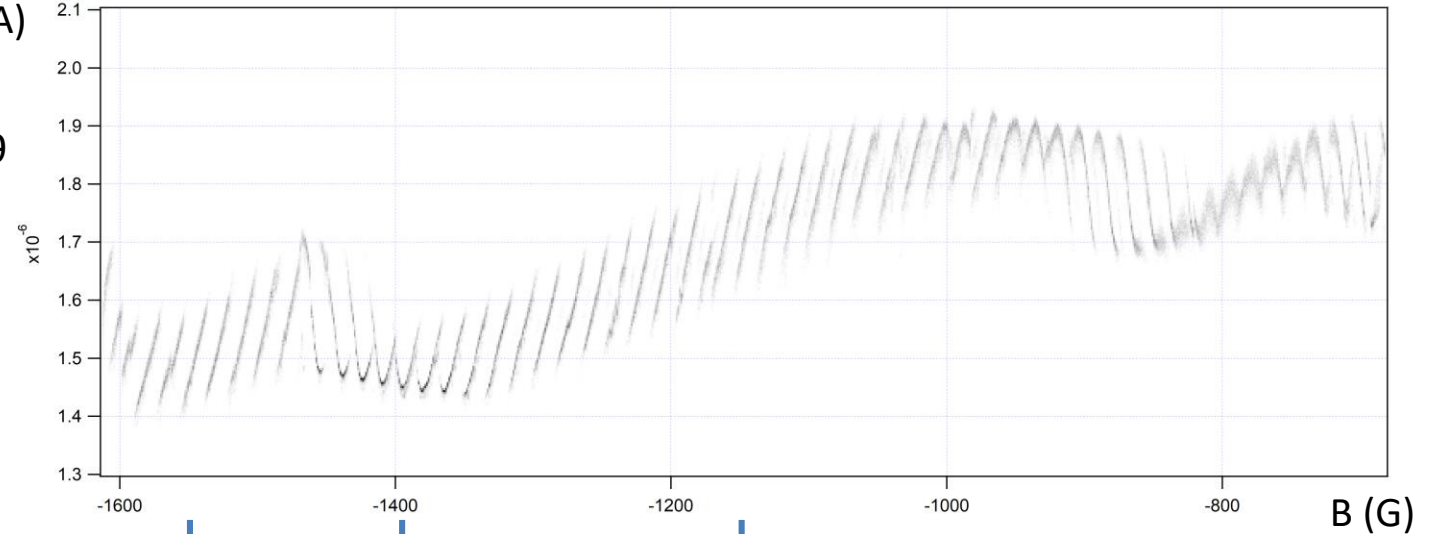




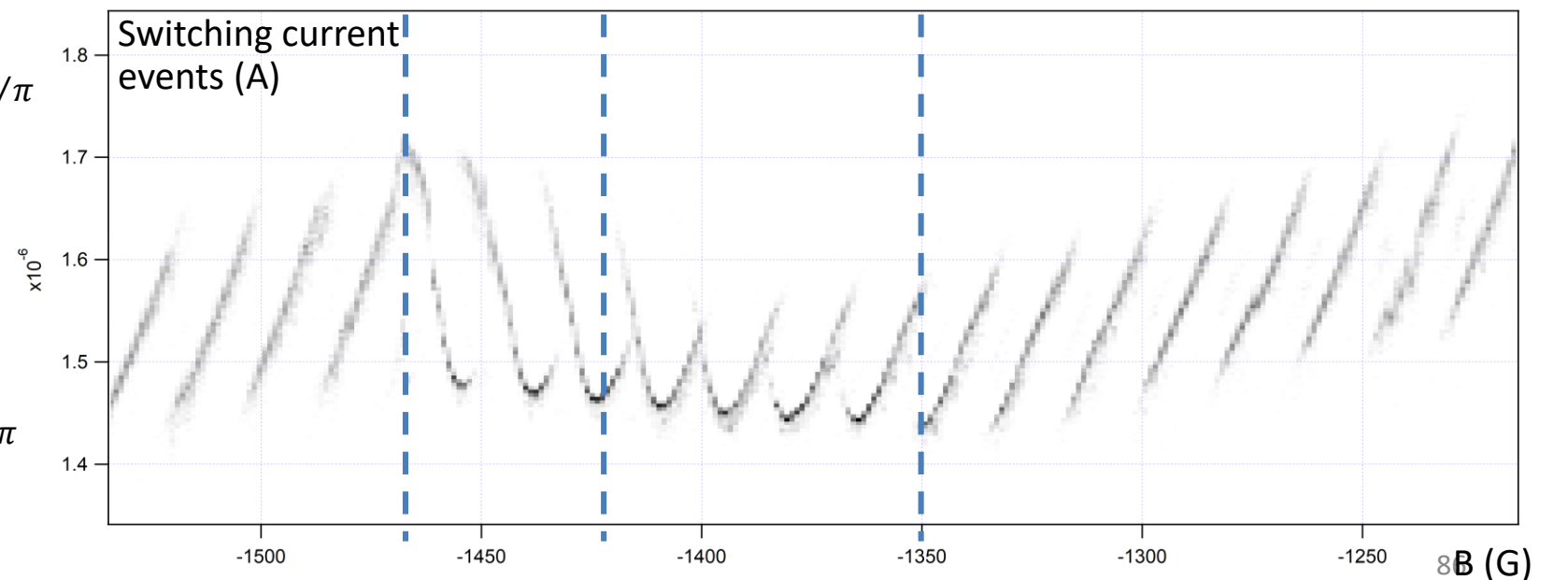
# Supercurrent vs phase: ongoing experiments



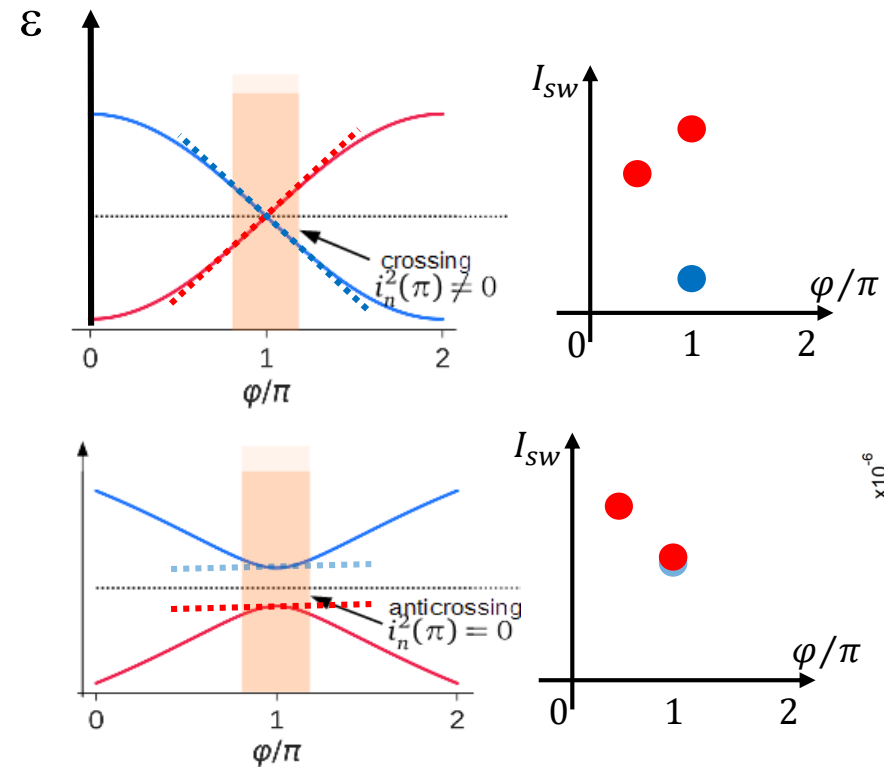
Switching current events (A)



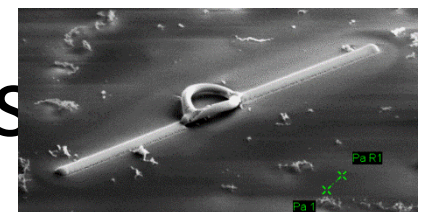
Switching current events (A)



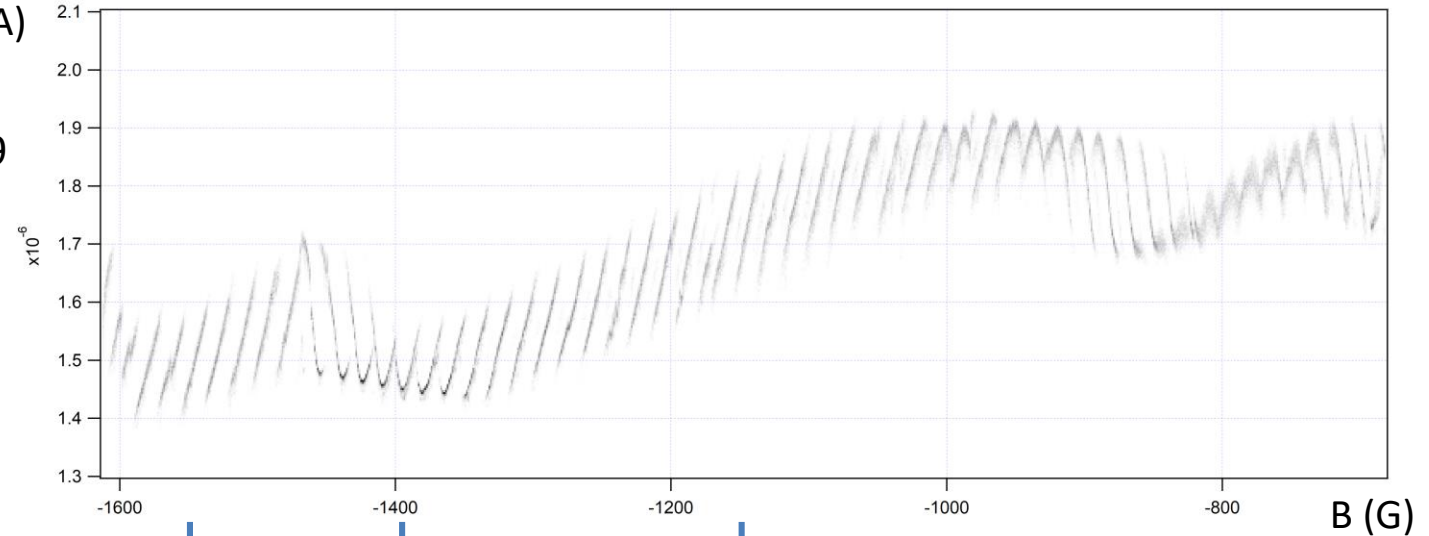
See Peng et al., PRB 2016  
related to current fluctuations, see Fu and Kane PRB 2009  
related to dissipation, see Murani et al. PRL 2019



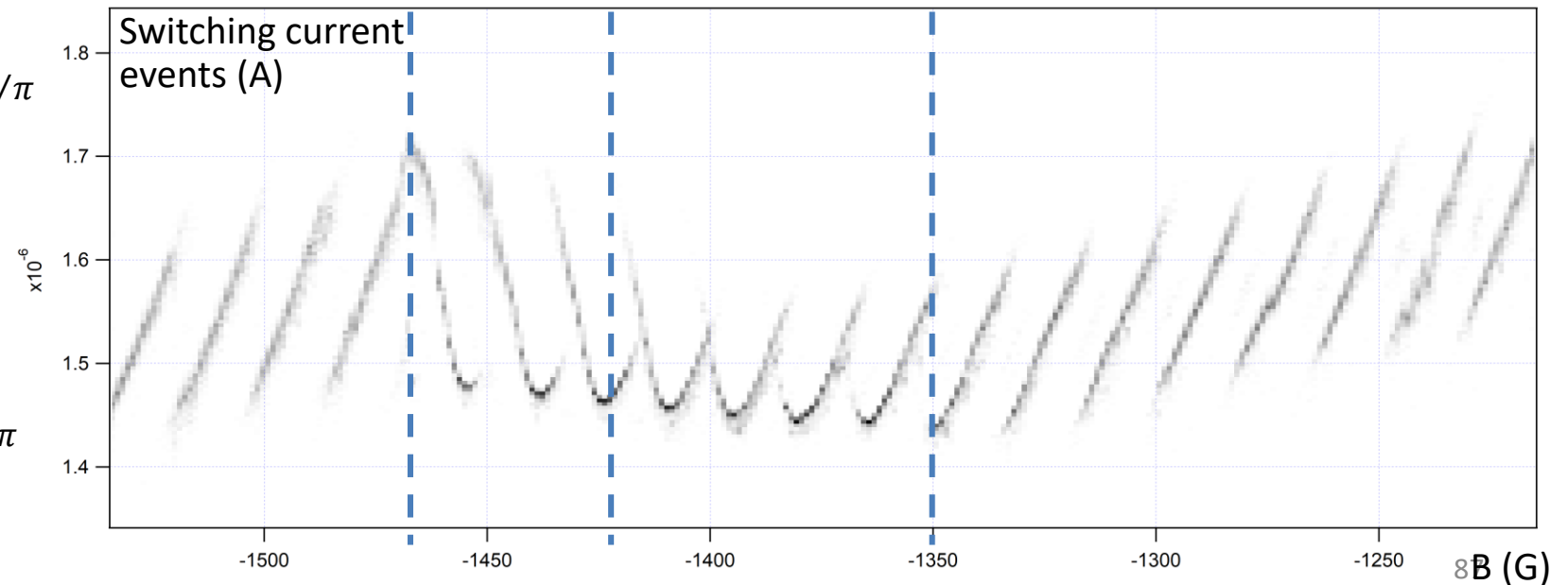
# Supercurrent vs phase: ongoing experiments



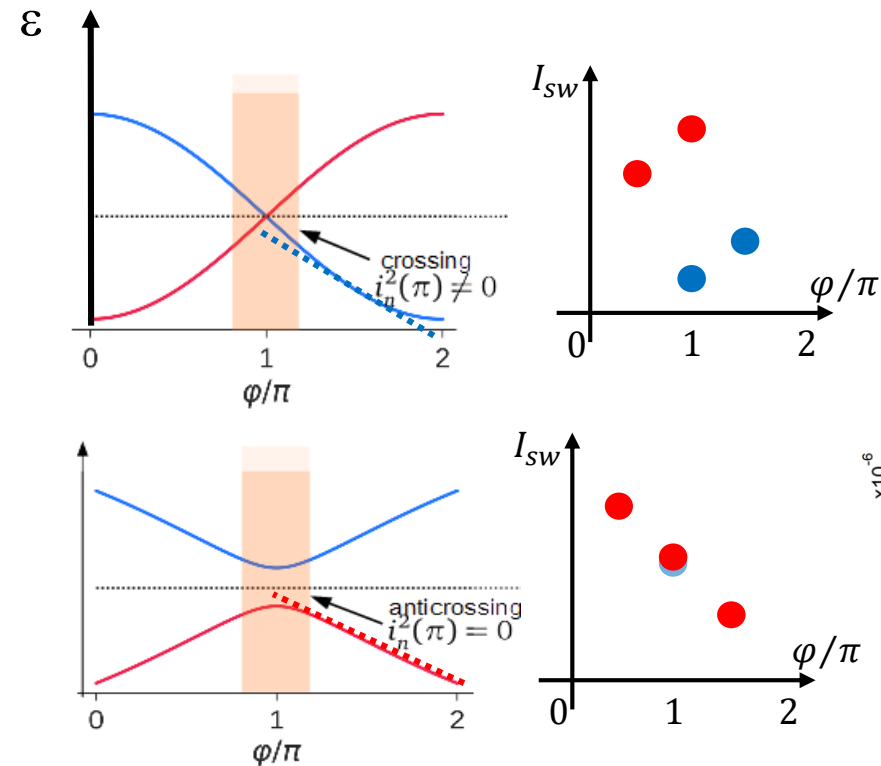
Switching current events (A)



Switching current events (A)

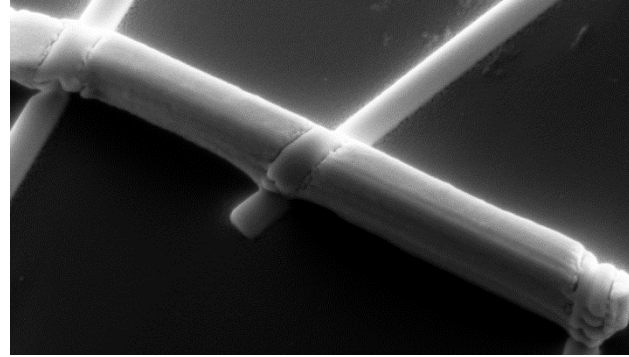


See Peng et al., PRB 2016  
related to current fluctuations, see Fu and Kane PRB 2009  
related to dissipation, see Murani et al. PRL 2019

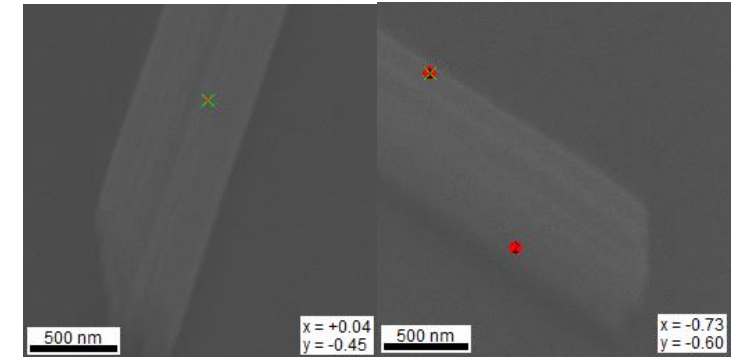


# Open questions

Can a big supercurrent be supported by many hinge states arranged in steps ?

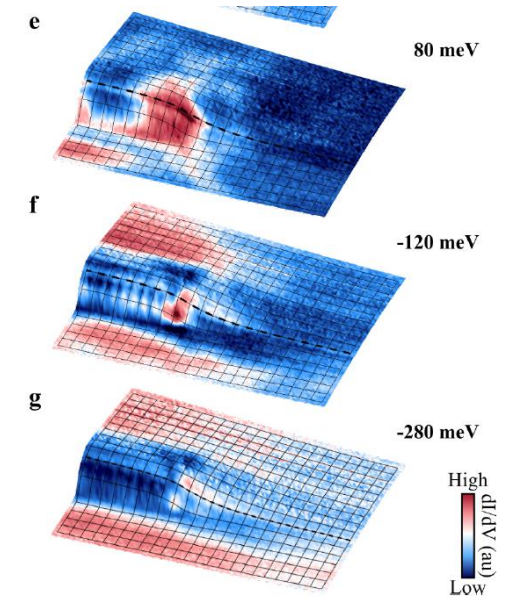
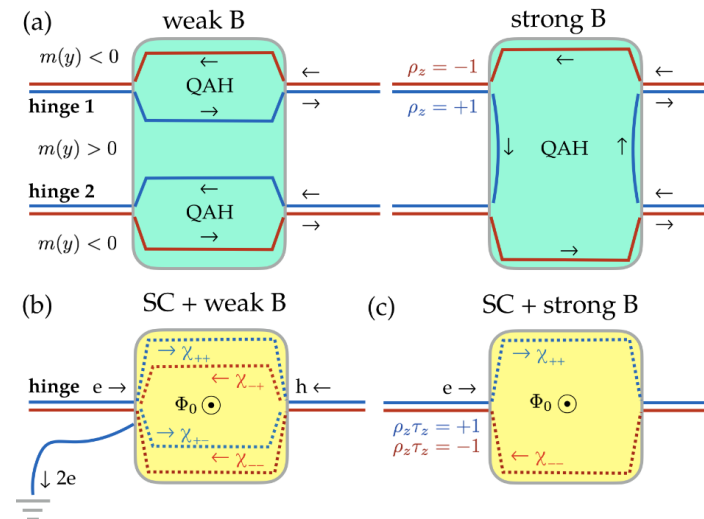


Ishibashi's group, RIKEN



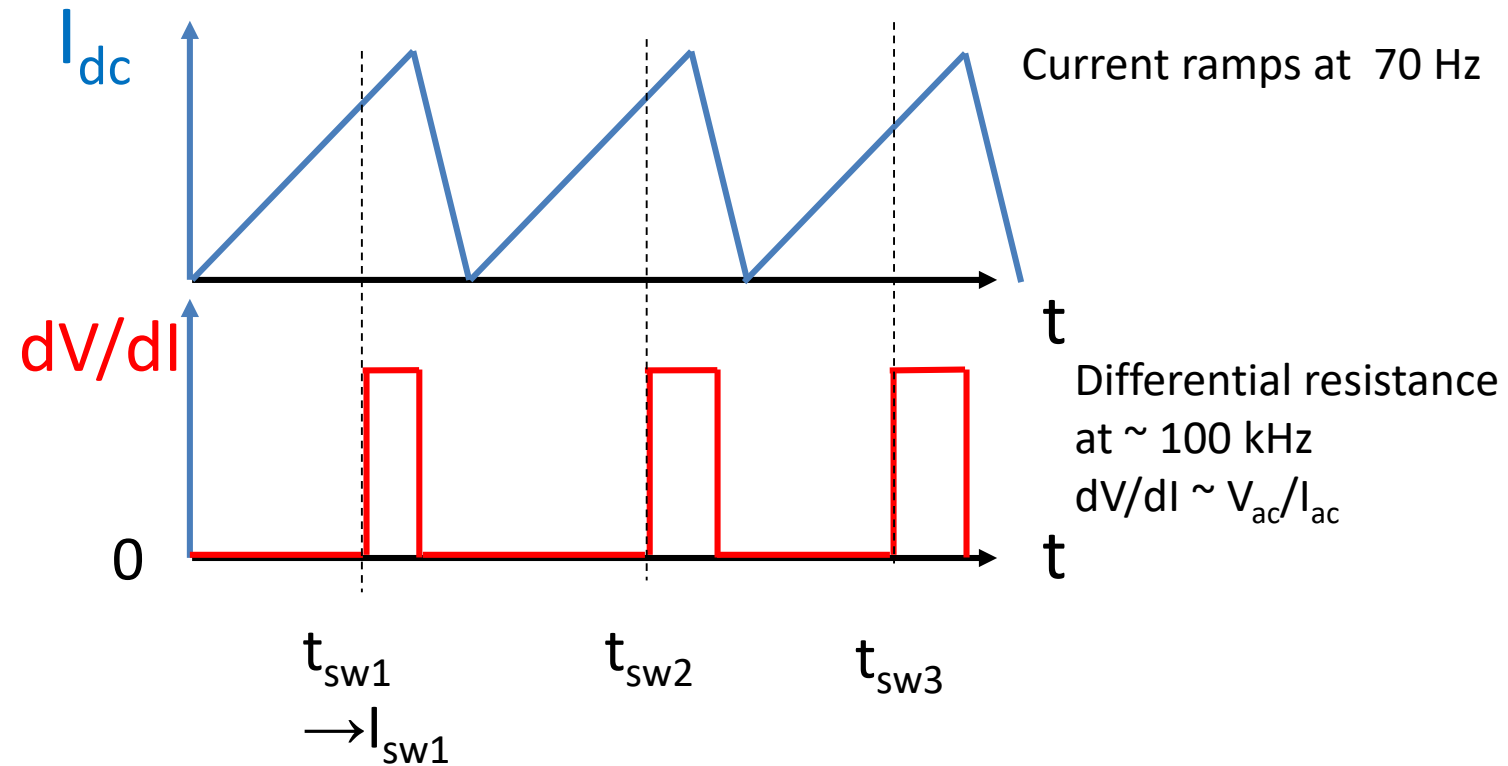
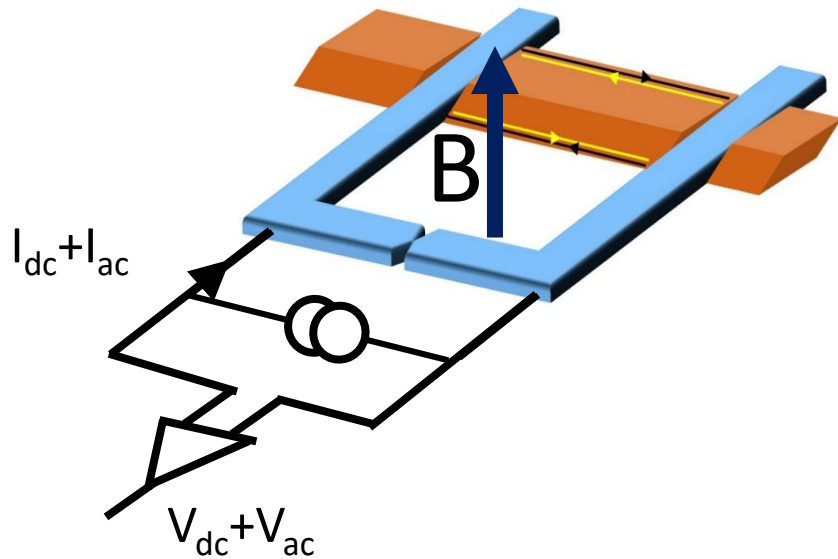
What is the effect of defects on the surface of Bi ?  
 What about strain ?  
 Revealing topological nature with screw dislocations ?  
 (Nayak et al., Cond. Mat. 2019)

What happens at high magnetic field ?  
 (Queiroz and Stern, Cond. Mat. 2019)





# Switching current measurement



Measure  $\langle I_{sw} \rangle$ , averaged over 100 to 400 times, histogram as well